ALMA MATER STUDIORUM - UNIVERSITÀ DI BOLOGNA

SCUOLA DI INGEGNERIA E ARCHITETTURA

DIPARTIMENTO DI INGEGNERIA INDUSTRIALE
DIN

CORSO DI LAUREA IN INGEGNERIA ENERGETICA E NUCLEARE

TESI DI LAUREA

in
TRASMISSIONE DEL CALORE E TERMOFLUIDODINAMICA
APPLICATA M

CHARACTERIZATION OF THERMOELECTRIC COMMERCIAL MODULES FOR POWER GENERATION USING A MODULE TEST SYSTEM

CANDIDATO:

MATTEO URBANI

RELATORE:

Chiar.mo Prof. ANTONIO BARLETTA

CORRELATORI:

Dr. RASMUS BJØRK
Ing. DAN ERIKSEN

Anno Accademico 2012/13

Sessione II

Abstract

Il presente lavoro di tesi è stato svolto presso la DTU, Technical University of Denmark, nel Department of Energy Conversion and Storage, Riso Campus. Lo scopo del periodo di soggiorno estero è stato quello di caratterizzare appropriati moduli termoelettrici forniti da aziende del settore, utilizzando un opportuno apparato di caratterizzazione. Quest'ultimo è noto come *"module test system"* e, nello specifico, è stato fornito dalla PANCO GmbH, azienda anch'essa attiva nel campo delle tecnologie termoelettriche. Partendo da uno studio teorico dei fenomeni fisici interessati (effetto Seebeck per la produzione di potenza termoelettrica), si è cercato in seguito di analizzare le principali caratteristiche, ed elementi, del *"module test system"*. Successivamente a questa prima fase di analisi, sono stati condotti esperimenti che, con l'aiuto di modelli computazionali implementati attraverso il software Comsol Multiphysics, hanno permesso di studiare l'affidabilità del sistema di caratterizzazione. Infine, una volta acquisite le basi necessarie ad una corretta comprensione dei fenomeni fisici e delle caratteristiche relative alla strumentazione, sono stati analizzati moduli termoelettrici di tipo commerciale. In particolare, sono stati estrapolati dati quali correnti, tensioni, gradienti di temperatura, che hanno permesso di ricavare flussi termici, efficienze, e potenze che caratterizzano il modulo in questione durante le condizioni di funzionamento. I risultati ottenuti sono stati successivamente comparati con dati forniti dal produttore, presenti sul catalogo.

Index

Introduction

The modern technologies based on the thermoelectric phenomena have had an important growth in the recent years, especially those related to the power generation.

In the present thesis work the principal aim is to show what is the process and what are the elements needed in order to characterize thermoelectric converters for power generation. It is thus important to achieve a grade of reliability and reproducibility that allows to study TEGs (thermoelectric module generators) performances starting from their output parameters under working conditions.

Although the theory behind thermoelectric effects has been enriched year by year for a period that goes throughout the XX century, the technologies related can be considered a new field of studies. Therefore it becomes relevant the necessity of using module test systems that can provide a good representation of what the TEGs are able to perform and what, in prospective, they could potentially reach in the modern thermoelectric market.

The characterization of a commercial thermoelectric module taken as a sample, were conducted in the Department of Energy Conversion and Storage of DTU, Technical University of Denmark. In this department is available a module test system that is implemented in order to extrapolate output values of temperatures, currents and voltages out of thermoelectric converters for power generation.

The process that will be followed in the thesis work involves various steps that constitute a support for the characterization part, that is intended as the final part of all the experimental process. Characterization has to rely on the thermodynamic behavior of the elements that compose the module test system. This is why a first step of hardware and software configuration study is required in order to understand what are the factors that have to be adjusted or that can affect the TEG behavior. Considering this important aspect of being introduced to a system that can be affected by different errors, a numerical model will be also implemented with the software Comsol Multiphysics. Using a computational simulation will provide us a mirror were the results from the experimental analysis can be compared to an expected theoretical behavior. In this way it will be possible to setup the system in an optimized way before beginning the characterization process.

Mixing the simulation results with a previous understanding of the thermodynamic behavior of the elements that are part of the system, the last part of characterization will be developed through the use of a thermoelectric commercial module provided by Marlow company. It is interesting to observe that, in addition to the validation process provided by the Comsol models, a further validation of the results can be given by a reference datasheet that depicts the results achieved by the company for the mentioned module.

An experience that includes different factors such as theoretical studies, practical and simulation works is thus required and was carried forward during all the evolution of this thesis work.

1

Overview, General Aspects and Basic Principles of Thermoelectric Generation

1.1 Introduction

This chapter is an overview of the thermoelectric technologies that have been developed since the discover of the physical phenomena related to the thermoelectric power generation and thermoelectric cooling, respectively Seebeck and Peltier effects. During the past decades we assisted to a fast rising of the thermoelectric research followed by alternate periods of poor improvements until the recent years where, due to different technological, social and environmental factors, the demands for new ways of energy management and production begun to rise faster and faster. Starting from the historical contest as a background to understand the potential of the thermoelectric technologies, this chapter will introduce then the principal physical elements and equations that support the thermoelectric phenomena. In this way it is important to understand which properties are the most effective in the optimization and improvements of new modules and what are the factors and the potential limits that could affect the development of the future ones. Eventually there will be introduced a general description of the current thermoelectric market, with particular emphasis on the past diffusion of thermoelectric systems, nowadays technologies and possible future applications.

1.2 Thermoelectric Technology History, a Brief Overview

The first of the thermoelectric effects was discovered, in 1821, by T. J. Seebeck. He showed that an electromotive force could be produced by heating the junction between two different electrical conductors. The Seebeck effect can be demonstrated by making a connection between wires of different materials. The other end of the wires should be applied to the terminals of a galvanometer or sensitive voltmeter. If the junction between the wires is heated, it is found that the meter records a small voltage.

Thirteen years after Seebeck made his discovery, J. Peltier, a French watchmaker, observed the second of the thermoelectric effects. He found that the passage of an electric current through a thermocouple produces a small heating or cooling effect depending on its direction. The Peltier effect is quite difficult to demonstrate using metallic thermocouples since it is always accompanied by the Joule heating effect.

Even if it was not immediately realized that the Seebeck and Peltier phenomena are dependent on one another, this interdependency was recognized by W. Thomson (who later became Lord Kelvin), in 1885. By applying the theory of thermodynamics to the problem, he was able to establish a relationship between the coefficients that describe the Seebeck and Peltier effects. His theory also showed that there must be a third thermoelectric effect, which exist in a homogenous conductor. This effect, now known as the Thomson effect, consists of reversible heating or cooling when there is both a flow of electric current and a temperature gradient.

The fact that the Seebeck and Peltier effects occur only at junctions between dissimilar conductors might suggest that they are interfacial phenomena but they are really dependent on the bulk properties of the materials involved. Nowadays, we understand that electric current is carried through a conductor by means of electrons that can possess different energies in different materials. When a current passes from one material to another, the energy transported by electrons is altered, the difference appearing as heating or cooling at the junction, that is as the Peltier effect. Likewise, when the junction is heated, the electrons are enabled to pass from the material in which the electrons have the lower energy into that in which their energy is higher, giving rise to an electromotive force.

Thomson’s work showed that a thermoelectric couple is a type of heat engine and that it might, in principle, be used either as a device for generating electricity from heat or, alternatively, as a heat pump or refrigerator. However, because the reversible thermoelectric effects are always accompanied by the irreversible phenomena of Joule heating and thermal conduction, thermocouples are generally rather inefficient.

The problem of energy conversion using thermocouples was analyzed by Altenkirch, in 1911. He showed that the performance of a thermocouple could be improved by increasing the magnitude of the differential Seebeck coefficient, by increasing the electrical conductivities of the two branches and by reducing their thermal conductivities. Unfortunately, at that time, there were no thermocouples available in which the combination of properties was good enough for reasonably efficient energy conversion, although the

Seebeck effect has long been used for the measurements of temperature and for the detection of thermal radiation. It was only in the 1950's that the introduction of semiconductors as thermoelectric materials allowed practical Peltier refrigerators to be made. Work on semiconductor thermocouples also led to the construction of thermoelectric generators with a high enough efficiency for special applications. Nevertheless, the performance of thermoelectric energy convertors has always remained inferior to that of the best conventional machines.

Thermoelectric technology has undergone stages of significant interest, research and development, along with periods of inactivity and decline. The technology developed slowly until the 1930's, when rapid improvements in all areas of thermoelectric occurred and by the mid 1960's, practical thermoelectric devices emerged for niche applications in aerospace cooling and space-craft power. Progress in efficiency improvement slowed and research peaked by about 1963, followed by a decline in activity that was to continue for nearly three decades. In *Figure 1.1* it is showed the open literature publications in the Web of Science database as a percentage of all publications in the database for each year from 1955 to 2003.

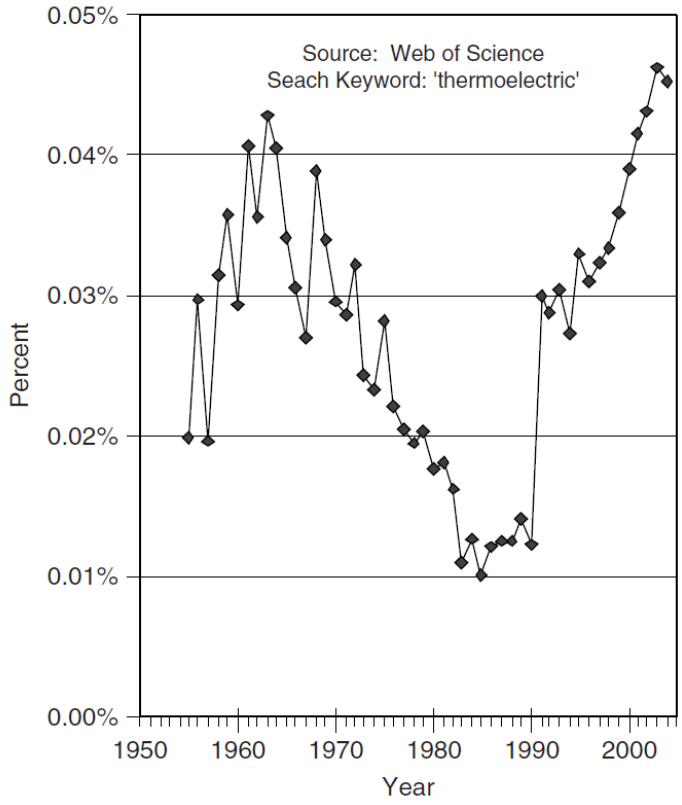

Figure 1.1

It is possible to see from the figure above that between 1963 and 1983, publications in thermoelectrics decreased by a factor of four. During this period, thermoelectric technology

was in fact successfully transitioning from the laboratory to a variety of applications. The marrying of a nuclear heat source to a thermoelectric generator provided long-life power sources for use in inaccessible and hostile environments. Notable were the radioisotope thermoelectric generators (RTGs) providing critical power for NASA missions on the moon and on Mars and for spectacularly successful outer-planetary exploration missions, such as Voyager I and II.

Despite successful use of RTGs, basic thermoelectric science continued to decline. The nascent thermoelectric cooler industry in the U.S. was too small to support significant R&D. The oil crises of the 1970s were just beginning to modify public R&D policy in Japan, but had little lasting effect elsewhere. And during this period, activities in the Soviet Union remained largely unknown in the West. In this inauspicious environment, two men in Texas teamed up in 1970 to organize a series of short courses and conferences which eventually spawned the International Thermoelectric Society (ITS). Initially attendance was quite modest. By 1975, there were more speakers than attendees. Raymond Marlow from Marlow Industries suggested that Professor K.R. Rao, a professor of Electrical Engineering with the University of Texas at Arlington, reorganize as the International Conference on Thermoelectric Energy Conversion (ICOTEC), to be held biannualy. It was at the 1988 meeting (VIIth ICOTEC) that Dr. Charles Wood of NASA/CalTech's Jet Propulsion Laboratory (JPL) and Professor Mike Rowe, Cardiff University, UK, discussed the sensibility of merging the European Conferences on Thermoelectrics with the International Conference on Thermoelectric Energy Conversion. After the formation of a proper committee Dr. Wood was nominated first president of the new society known as "International Thermoelectric Society" (ITS).

In the years following the birth of ITS there was also renewed interest in thermoelectric technology due to a combination of factors , notably environmental concerns regarding refrigerant fluids, alternative refrigeration and interest in cooling electronics. Contemporary interest in the technology is driven by an increasing awareness of the effect of global warming on the planet's environment, a renewed requirement for long-life electrical power sources, and the increasing miniaturization of electronic circuits and sensors.

1.3 Thermoelectric Effects

1.3.1 Seebeck Effect, Peltier Effect, Thomson Effect

The thermoelectric effects which underlie thermoelectric energy conversion can be conveniently discussed to the schematic of a thermocouple shown in *Figure 1.2*.

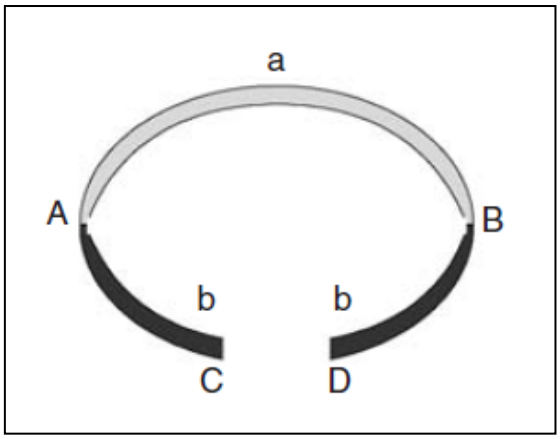

Figure 1.2

It can be considered as a circuit formed from two dissimilar conductors, a and b (referred to in thermoelectrics as thermocouple legs, arms, thermoelements) which are connected electrically in series but thermally in parallel. If the junctions at A and B are maintained at different temperatures T_1 and T_2 and $T_1 > T_2$ an open circuit electromotive force (emf), V is developed between C and D and given by $V = \alpha (T_1 - T_2)$ or $\alpha = V/\Delta T$, which defines the differential Seebeck coefficient α_{ab} between the elements a and b. For small temperature differences the relationship is linear. Although by convention α is the symbol for the Seebeck coefficient, S is also sometimes used and the Seebeck coefficient referred to as the thermal emf or thermopower. The sign of α is positive if the emf causes a current to flow in a clockwise direction around the circuit and is measured in V/K.

The Seebeck effect is related to the migration of the more energetic electrons that move to a lower potential until an electric field is established to impede the further flow of electrons.

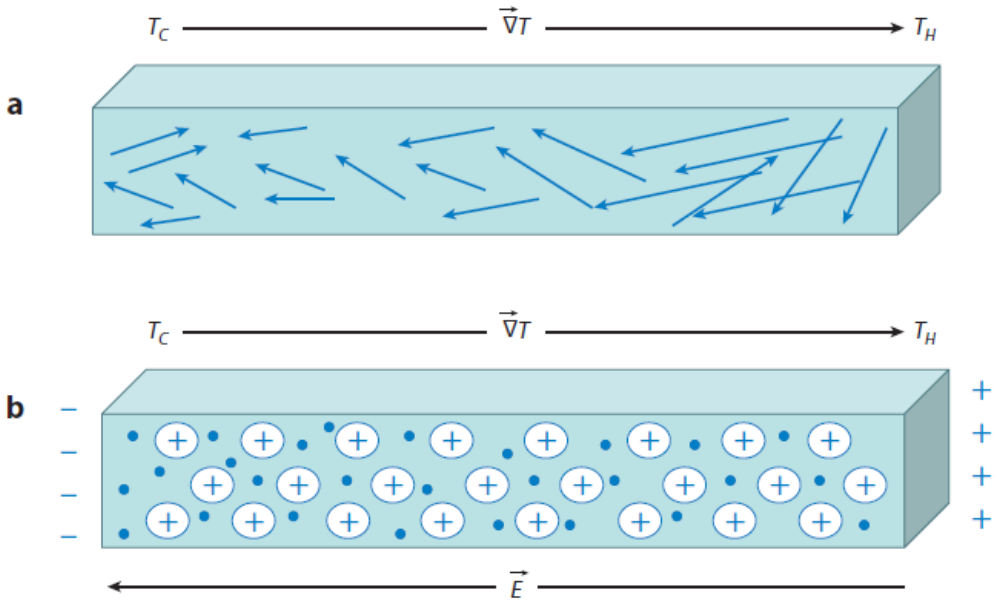

Figure 1.3

In *Figure 1.3* it is shown that the more energetic electrons have a longer mean free path (a). these more energetic electrons (denoted by *blue dots*) then diffuse to the cold side (b) until an electric field (E) is developed to oppose any further diffusion. Because the electrons are negatively charged, the established electric field is the opposite of that of the temperature gradient.

If in *Figure 1.2* the reverse situation is considered with an external emf source applied across C and D and a current I flows in a clockwise sense around the circuit, then a rate of heating q occurs at one junction between a and b and a rate of cooling –q occurs at the other. This effect is known as the Peltier effect and the ratio of I to q defines the Peltier coefficient given by $\pi = I/q$, is positive if A is heated and B is cooled, and is measured in watts per ampere or in volts.

The last of the thermoelectric effects, the Thomson effect, relates to the rate of generation of reversible heat q which results from the passage of a current along a portion of a single conductor along which there is a temperature difference ΔT. Providing the temperature difference is small, $q = \beta I \Delta T$ where β is the Thomson coefficient. The units of β are the same as those of the Seebeck coefficient V/K. Although the Thomson effect is not of primary importance in thermoelectric devices it should not be neglected in detailed calculations.

1.3.2 The Kelvin Relationships

The above three thermoelectric coefficient are related by the Kelvin relationships:

$$\alpha_{ab} = \pi_{ab}/T \quad \text{and} \quad \frac{d\alpha_{ab}}{dT} = \frac{\beta_a - \beta_b}{T}$$

These relationships can be derived using irreversible thermodynamics. Their validity has been demonstrated for many thermoelectric materials and it is assumed that they hold for all materials used in thermoelectric applications.

1.4 Thermoelectric Generation, Description of the Figure-of-Merit and Thermoelectric Performance

A thermoelectric converter is a heat engine and like all heat engines it obeys the laws of thermodynamics. If we first consider the converter operating as an ideal generator in which there are no losses, the efficiency is defined as the ratio of the electrical power delivered to the load to the heat absorbed at the hot junction. Expressions for the important parameters in thermoelectric generation can readily be derived considering the simplest generator

consisting of a single thermocouple with thermoelements fabricated from n- and p-type semiconductors as shown in *Figure 1.4.*

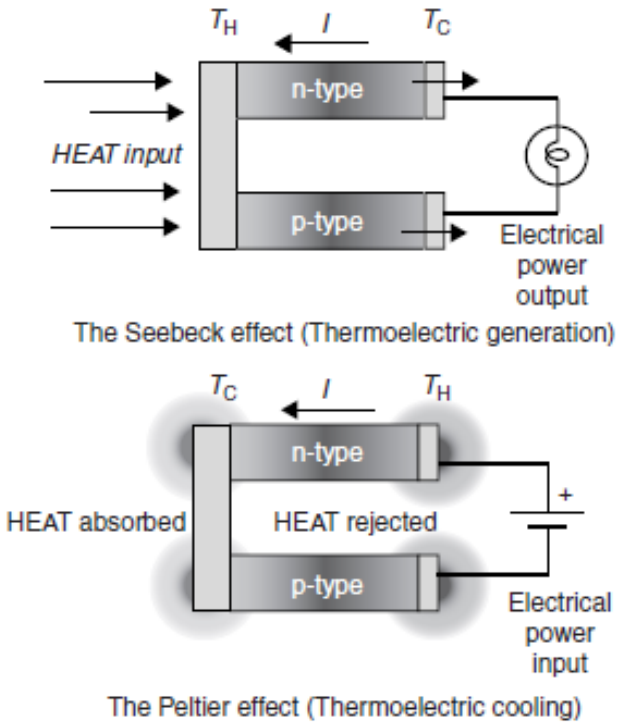

Figure 1.4

The efficiency of the generator is given by

$$\Phi = \frac{energy\ supplied\ to\ the\ load}{heat\ energy\ absorbed\ at\ hot\ junction} = \frac{W}{Q_h}$$

If it is assumed that the electrical conductivities, thermal conductivities, and Seebeck coefficients of a and b are constant within an arm, and that the contact resistances at the hot and cold junctions are negligible compared with the sum of the arm resistance, then the efficiency can be expressed as

$$\Phi = \frac{I^2R}{\alpha_{ab}IT_H = \lambda(T_H - T_C) - \frac{1}{2}I^2R}$$

where λ is the thermal conductance of a and b in parallel and R is the series resistance of a and b. In thermoelectric materials λ and α change with temperature, and in both, generation and refrigeration should be taken into account.

Efficiency is clearly a function of the ratio of the load resistance to the sum of the generator arm resistances, and at maximum power output it can be shown that

$$\Phi_p = \frac{T_H - T_C}{\frac{3T_H}{2} + \frac{T_C}{2} + \frac{4}{Z_C}}$$

while the maximum efficiency

$$\Phi_{max} = \eta_c \gamma$$

where

$$\eta_c = \frac{T_H - T_C}{T_H}$$

$$\gamma = \frac{\sqrt{1 + T_m Z_C} - 1}{\sqrt{1 + T_m Z_C} + \frac{T_C}{T_H}}$$

$$T_m = \frac{T_H + T_C}{2}$$

$$Z_c\ (the\ figure - of - merit\ of\ the\ couple) = \frac{\alpha_{ab}^2}{R\lambda}$$

The maximum efficiency is thus the product of the Carnot efficiency, which is clearly less than unity, and γ, which embodies the parameters of the materials.

If the geometries of a and b are matched to minimize heat absorption, then

$$Z_c = \frac{\alpha_{ab}^2}{\left[\left(\frac{\lambda_a}{\sigma_a}\right)^{\frac{1}{2}} + \left(\frac{\lambda_b}{\sigma_b}\right)^{\frac{1}{2}}\right]^2}$$

In practice, the two arms of the junction have similar constants, in which case the concept of a figure-of-merit for a material is employed and given by

$$Z = \frac{\alpha^2 \sigma}{\lambda}$$

where $\alpha^2\sigma$ is referred to as the electrical power factor.

The above relationships have been derived assuming that the thermoelectric parameters which occur in the figure-of-merit are independent to temperature.

The conversion efficiency as a function of operating temperature difference and for a range of values of the material's figure-of-merit is displayed in *Figure 1.5*.

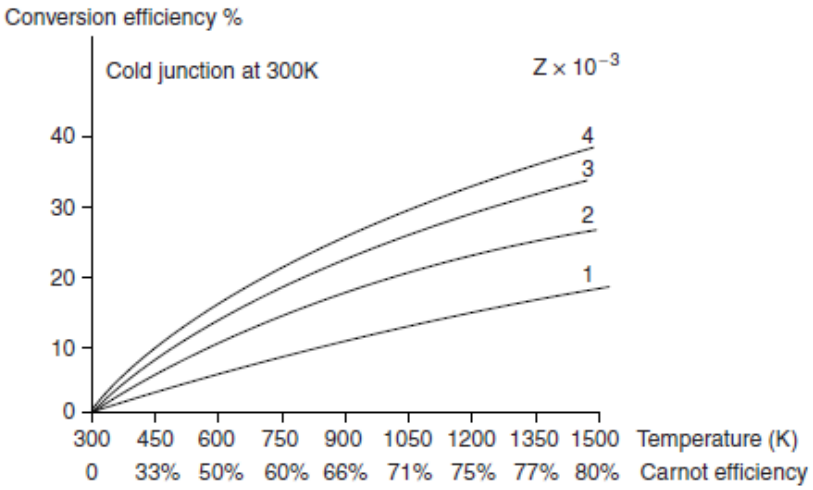

Figure 1.5

Evidently an increase in temperature difference provides a corresponding increase in available heat for conversion as dictated by the Carnot efficiency, so large temperature differences are desirable.

1.5 Thermoelectric Materials

One of the parameters that is used in the classification of materials is the electrical conductivity. Metals have a high electrical conductivity while in insulators the conductivity is very low and under normal conditions is taken as zero with semiconductors occupying an intermediate position between the two. The electrical conductivity is a reflection of the charge carrier concentration and all three parameters which occur in the figure-of merit are functions of carrier concentration as shown in *Figure 1.6*. The Seebeck coefficient decreases with increase in power concentration and the electrical power factor maximizing at a carrier concentration of around 10^{25}/cm. The electronic contribution to the thermal conductivity λ, which in thermoelectric materials is generally around 1/3 of the total thermal conductivity, also increases with carrier concentration. Evidently the figure-of-merit optimizes at carrier

concentrations which corresponds to semiconductors materials. Consequently, semiconductors are the materials most researched for thermoelectric applications.

Thermoelectric phenomena are exhibited in almost all conducting materials (except for superconductors below T_c). Because the figure-of-merit varies with temperature a more meaningful measure of performance is the dimensionless figure-of-merit ZT where T is absolute temperature. However, only those materials which possess a ZT>0,5 are usually regarded as thermoelectric materials.

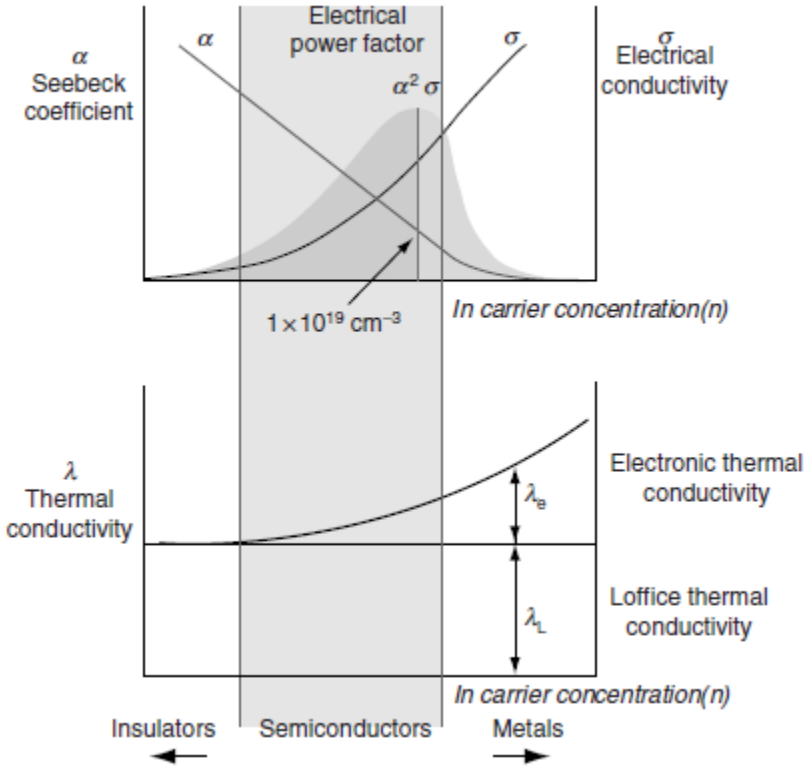

Figure 1.6

1.5.1 Limits to the Dimensionless Figure-of-Merit

Thermodynamics does not place any upper limit on the dimensionless figure-of-merit, ZT, but for many years it was impossible to find values significantly greater than unity. Empirically, one can predict an upper bound by combining the best electronic properties of any known crystalline material with a phonon conductivity that is typical of glass. By this means, one arrives at a highest value of ZT equal to about four. Recently, however, it has been demonstrated that certain low-dimensional structures can have values of the figure-of-merit that exceed those found in bulk materials. This allows us to upgrade our predicted limit for ZT to, perhaps, 20.

Several attempts have been made in the past to estimate the maximum thermoelectric figure-of-merit that will ever be reached. There is no restriction placed on the value of ZT by thermodynamics since, if this quantity ever became infinite, the thermoelectric efficiency would still be no greater than that of the Carnot cycle. At room temperature, the best thermoelectric materials are solid solutions based on bismuth telluride. A value of ZT equal to about one was established for these materials in the late 1950's and has not been improved upon since then. At the present time , the greatest dimensionless figure-of-merit for bulk materials is of the order of unity under ordinary conditions.

If we referred to the dimensionless figure-of-merit expression described in 1.4 section of this chapter we can considerate that the total thermal conductivity is a sum of two different factors, respectively the lattice and the electronic contribution. In this way, ZT may be increased either by decreasing the lattice factor or by increasing either α or σ. However, σ is tied to the electronic contribution of the thermal conductivity through the Wiedemann-Franz relationship, and their ratio is essentially constant at a given temperature for the majority of TE materials. Some of the goals of current research efforts are to find new materials that either increase the current efficiency of TE devices or have the capability of operating in new and broader temperature regimes, especially at lower temperatures (T<250 K) and at high temperatures (T>400 K).

1.6 Thermoelectric Modules

The basic unit of a thermoelectric (TE) generator or refrigerator is a "thermocouple" shown schematically in *Figure 1.7a*.

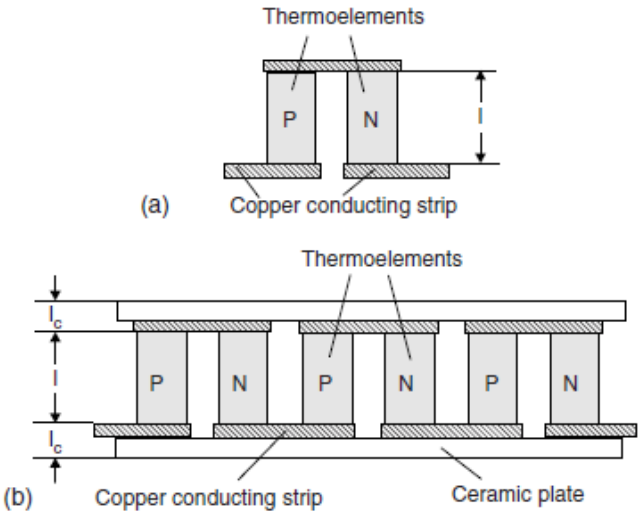

Figure 1.7

It consists of an n-type and a p-type thermoelement connected electrically in series by a conducting strip (usually copper). Although this basic unit can also be employed as the "engineering" building-block for construction of thermoelectric conversion systems, a less complicated approach for system engineers is to employ "thermoelectric module" as the building-block. *Figure 1.7b* show schematically a thermoelectric module, which consist of a number of the basic units connected electrically in series but thermally in parallel and sandwiched between two ceramic plates. A complete configuration of a thermoelectric module (in this case a typical Peltier cooler) can be seen in *Figure 1.8*.

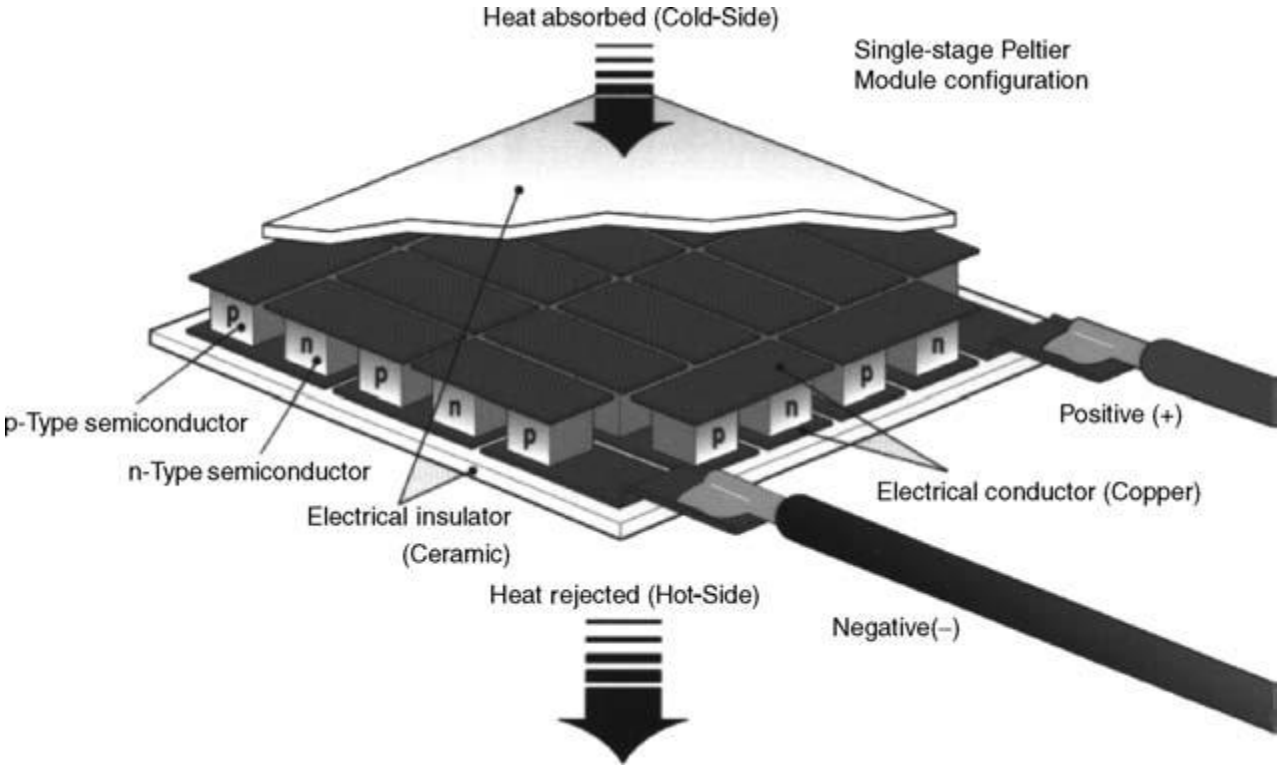

Figure 1.8

The generating performance of a thermoelectric module is caused primarily by the conversion efficiency and power-per-unit-area, while the cooling performance by the coefficient of performance (COP) and heat pumping capacity. These quantities may be estimated using a theory developed by Ioffe based on a simplified model in which the thermal and electrical contact resistances had been neglected. Although this theory has proven to be adequate for analysis of large-dimension thermoelectric modules, it becomes inaccurate for the modules which possess short thermoelement length. Over the past few years, an improved theory has been developed based on a more realistic model which takes into account the thermal and electrical contact resistances of the modules.

The electrical power generated from a module depends upon the numbers of thermocouples in a module, thermoelement configuration, thermoelectric properties of

thermoelement materials, thermal, and electrical properties of contact layers, and the temperature difference across the module. It can be shown then, that when the module operates with a matched load, the output voltage V and current I are given by:

$$V = \frac{N\alpha(T_H - T_C)}{1 + \frac{2rl_c}{l}} \tag{1.1}$$

$$I = \frac{A\alpha(T_H - T_C)}{2\rho(n + l)\left(1 + \frac{2rl_c}{l}\right)} \tag{1.2}$$

where N is the number of thermocouples in a module, α the Seebeck coefficient of the thermoelement material employed, and ρ the electrical resistivity, T_H and T_C are temperatures at the hot and cold sides of the module, respectively, A and *l* are the cross-sectional area and thermoelement length, respectively, l_c is the thickness of the contact layer, $n=2\rho_c/\rho$ and $r=\lambda/\lambda_c$ (where ρ_c is the electrical contact resistivity, λ_c the thermal contact conductivity, and λ the thermal conductivity of thermoelement materials). n and r are usually referred to as electrical and thermal contact parameters, respectively.

1.6.1 Fabrication Cost and Optimization

The parameters appearing in equation *(1.1)* and equation *(1.2)* can be grouped into three categories:

1. *Specifications*: The operating temperatures T_C and T_H, the required output voltage V and current I.
2. *Material parameters*: The thermoelectric properties α, σ, λ and the module contact properties n and r.
3. *Design parameters*: The thermoelement length *l*, the cross-sectional area A, and the number of the thermocouples N.

The specifications are usually provided by customers depending on the requirements of a particular application. The material parameters are restricted by currently available materials and module fabricating technologies. Consequently, the main objective of thermoelectric module design is to determine a set of design parameters which meet the required specifications at minimum cost. The number of the thermocouples N, required in a module can be determined using equation *(1.1)*, while the cross-sectional area, A, can be obtained

from equation *(1.2)*. The determination of N and A for a given thermoelement length is usually a straightforward calculation.

In general, a high conversion efficiency is required if the heat source (fuel) is expensive, while a large power-per-unit-area is required if fabrication cost is to be reduced. In practice, the cost-per-kilowatt-hour is generally used as a yardstick of the economic viability of a generator. The cost-per-kilowatt-hour, c, of electricity generated using a thermoelectric module may be estimated using

$$c = \frac{c_m}{p\Delta t} + \frac{c_f}{\Phi}$$

where c_m is the fabrication cost of a thermoelectric module, c_f the input thermal energy cost per kilowatt hour, Δt the operation period, and p and Φ are the power output and conversion efficiency, respectively, of a thermoelectric module. *Figure 1.9* shows the cost per-kilowatt-hour vs. the conversion efficiency and power-per-unit-area for different fuel costs for ΔT=100 K.

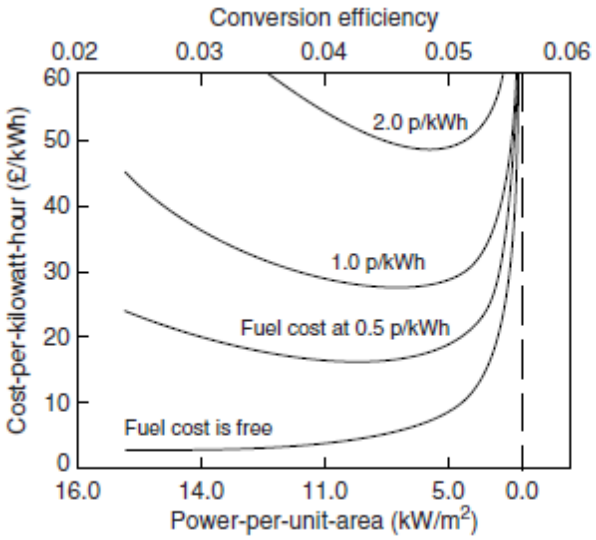

Figure 1.9

It can be seen that a trade-off between the conversion efficiency and power output is dependent on the cost of heat source employed. If the heat source employed is expensive, the module should be designed to obtain large conversion efficiency. However, if the heat source is inexpensive or essentially free, such as in the case of waste heat, increasing the power-per-unit-area will result in a reduction in the cost of electricity generation. This can be achieved by employing thermoelements with shorter legs.

1.7 Thermoelectric Systems Diffusion and Applications

1.7.1 Current Thermoelectric Market

Thermoelectric technology is commercially successful in cooling, refrigeration and space-craft power applications. Estimated sales of thermoelectric modules in 2006 is around $200 million, with the consumer market being the largest sector, accounting for 35% of the total market distribution, followed by telecom at 16% and automotive at 14%. The laboratory, medical and biological market account for 12%, semiconductor processing at 8%, and the Defence and Space sector now accounting for only 6% of the total market.

Historically, the Defence and Space industries used to be at the centre of the industry, with Radioisotope Thermoelectric Generators (RTG's as discussed in the previous paragraphs) having been a genuinely enabling technology for deep space exploration. However, this sector of the market is now flat and is not showing signs of growth. The consumer market is now the largest sector and includes water coolers, cooler boxes and refrigerators. Thermoelectric coolers are widely employed in microelectronics to stabilize the temperature of laser diodes, to cool infrared detectors and charge-coupled devices, computer electronics and individual computer chips. Recent growth can be seen in the automotive market, especially in automotive seat cooling applications.

1.7.2 Future Thermoelectric Market

The consumer market is predicted to continue with water cooler boxes and mini refrigerators remaining an important product application. Besides this success, thermoelectric refrigeration appears to have made little impact on the domestic refrigeration market. The energy efficiency of thermoelectric refrigerators, based on currently available materials and technology, is still lower than its compressor counterparts. However a market thermoelectric refrigerator can be made with an acceptable Coefficient of Performance (COP). The automotive industry is seen as a potential high volume market, and market growth exists for thermoelectric generators, specifically for waste heat recovery and the replacement of batteries in small remote power sources.

The possibility of using thermoelectric technology to convert waste heat into electrical power has been considered for some time. Thermoelectric solutions for self-powered space and water heating have shown that the electricity generated by a thermoelectric power unit is sufficient to power all the electrical components for a residential central heating system. In some areas of the developing world, electric power supply is unreliable and intermittent, and it is common to find wood or diesel fired stoves. Studies have demonstrated acceptable economic performance for stove-top thermoelectric generators, and a domestic wood-stove and thermoelectric generator system can be achieved at a low cost with minimal complexity.

The need for lightning the battery burden in present and future military systems is a focus for implementing thermoelectric technology within the US Army, and a market exists for thermoelectric air-conditioners in submarines.

An interesting problem potentially facing the thermoelectric industry is the availability of raw materials. There are four main raw materials used in thermoelectric elements, Te, Bi, Sb, Se. These materials are regarded as rare materials and their supply may be limited in the future, highlighting the need to develop other types of materials.

Contemporary problems surrounding climate change will act as a stimulus for the development of thermoelectrics, with the International Thermoelectric Society having recently adopted as their primary goal "To promote an understanding of the role thermoelectric technology may play in environmental impact and mitigating global climate change".

1.8 Advantages and Disadvantages of Thermoelectric Technology

Thermoelectric technology is considered to have several advantages, notably it has no moving parts, an ability to function in harsh environments, and substantially less maintenance requirements than comparable technologies. For cooling or refrigeration applications, no chlorofluorocarbons or other materials that require periodic replenishment are necessary, providing a potential environment benefit, with precise temperature control. The modules are relatively small in size and weight, and can be mounted in any orientation as they are not position dependent. Furthermore, thermoelectric devices are electrically quiet in operation and can be considered an environmentally friendly technology.

The main disadvantage of thermoelectrics is the relatively low conversion efficiency and figure-of-merit (ZT) compared with other technologies. For thermoelectric power generation, current thermoelectric efficiencies are between 5%-10%. Until recently, thermoelectric applications have been confined to niche applications because of this low conversion efficiency. There is significant research into synthesizing new materials and fabricating material structures with improved thermoelectric performance, in an attempt to improve the thermoelectric figure-of-merit by reducing the lattice thermal conductivity. However, in some parasitic applications this low conversion efficiency can also be viewed as a distinct advantage. Furthermore, it has been acknowledged that in situations where the supply of heat is cheap or free, as in the case of waste heat or solar energy, efficiency of the thermoelectric generation system is not an overriding consideration.

2

Module Test System

2.1 Introduction

This chapter introduces the importance and the different ways of using a module test system in order to gain the most reliable parameters from an operating thermoelectric module.

Nowadays the research about thermoelectrics (both for refrigeration and power generation) is focusing on new ways of improvements related to the study of new materials, figure-of-merit optimization, development of future applications, reduction of the most influential physical factors that inhibit the achievement of higher efficiencies and many other aspects that are relevant for a faster growth of the thermoelectric market. With this optic of reaching new goals in this field of thermodynamics it become more and more relevant to acquire and promote the most effective testing systems in order to verify the real potentials of the modern and future thermoelectric modules.

In the next pages there will be shown different ways actually used to test TEGs (thermoelectric module generators) and Peltier cooling modules and how they can be effectively realistic about the output parameters. Different researches have been developed during the recent years in order to achieve a method as close as possible to a standardization of the thermoelectric module testing, in this chapter few of them there will be introduced.

Following the pattern outlined by the actual utilization of different module test systems, eventually there will be described and introduced the system used to characterize the commercial modules that form the main body of this thesis work. There will be described its technical and logical characteristics and how an operator that interfaces with the system has to set up all the different elements that contributes to the extrapolation of the parameters

from a module under work conditions. Therefore if it is important to comprehend and analyze all the criteria that drive the development of the thermoelectric modules physical aspects, it's even more important to obtain the most accurate results in terms of output parameters , especially when it can affect the growth of a recent technology.

2.2 The Importance of Characterization

In the field of thermoelectrics there are several factors that influence the optimization and the commercial success of new modules. Beneath all the steps that contributes to the understanding of how these factors can affect or not a thermoelectric module, there is the validation process that leads to the connection between what has been improved to get the final product and how the product itself relates to the actual thermoelectric standards.

Considering a thermoelectric module generator (TEG), it is possible to follow its timeline growth from the theoretical considerations about its physical behavior to the effective assembly of the thermocouple to form a single module. It is important to understand that all the research and work beneath this process would not be validate if at the end of the timeline a good characterization method is not supporting the results that it is possible to achieve using a TEG.

The important aspects that we have to consider about the characterization of TEG, are essentially the output parameters that helps to compare different modules in order to understand their real potentials. A module test system provides, usually with fast and reliable operations, the best way to collect output parameters such as voltages, currents, heat fluxes across the TEG and temperature fields, that allows later to get power and efficiency values characterizing the single module. Once is possible to have the full range of plots regarding the different reactions of the module under different loads of temperature and resistances, it will be easier to understand what can be done for new improvements. In this way it will be also possible to know what has to be done in order to implement new elements, in the module test system configuration, that could be useful to improve the way and the precision of the data collection.

Comparing to the other ways of using a module test system that are presented in literature (few of them there will be shown in the next paragraphs), this thesis work focuses on a system that will also have the help of an computational model that will be used as a mirror where the results gained from the working conditions will be validated.

It is also important to understand that the optimization of the physical parameters that affect a thermoelectric module is also strictly related to the characterization process. This interrelation is due to the fact that most of these parameters are evaluated through methods that not considers the module in its effective load working conditions. Besides, parameters such as α, ρ, κ, z change not only with temperature but also with respect to the physical

dimensions of the semiconductor. Furthermore, the fact that the structural and technological factors of a real module are not considered in the calculation renders these methods insufficient. That is why the development of a practical and efficient characterization system is very important both for theory and application.

2.3 Literature Overview on Different Ways of Characterization Approach Using a Module Test System

During the development of the thermoelectric modules in the past years, several methods have been established in order to characterize key properties such as efficiency, current and voltages output values, and heat fluxes throughout the generator. As regarding the efficiency, for example, two main issues have to be underlined as to determine accurate results are the electrical output power and the heat flow. Considering measurement of the electrical output power the usually very low internal resistance of the modules has to be considered, as it has to be possible to apply even lower load resistance to the generator. A greater difficulty and the actual challenge is the measurement of the heat flow that I supplied to the generator. It has been previously proposed by Birkholz *et al.* to use a comparative measurement by employing a reference material in form of a reference block placed next to the generator into the heat conduction path.

This approach, however, is affected by some sources of serious systematic errors like the uncertainty of the reference material's heat conductivity. Another difficulty is to avoid heat losses in the reference blocks by radiation or convection. These heat losses are difficult to estimate and correct, which will lead to systematic errors in the hat flow measurement.

In order to overcome these uncertainties an absolute method for the measurement of the heat flow is presented by L. Rauscher, S. Fujimoto *et al.* work [2005]. It is realized by measuring the power dissipation of an electrical heater, which supplies the thermal energy on the hot side of the module. This avoids the necessity of any thermal conductivity reference and does not require the measurement of small temperature differences. The method, however, depends critically on the avoidance of any parasitic heat flow, and the measuring heater has to be shielded very carefully.

In *Figure 2.1* it is shown the assembled set up as it was used for the test measurements in Rauscher and Fujimoto work. It can be seen that on top of the guardian heater, a massive copper block was attached to provide mechanical support and a heat reservoir, which was used to thermally anchor all wires and the radiation baffles. Carbon sheets were used to ensure good thermal contact between all parts. The cold side heat exchanger is mounted on a lift cylinder to apply a vertical pressure to the system to achieve good thermal contact between the generator and the heaters. A centered steel ball is used to give a flexible and thermally separated support to an upper side support.

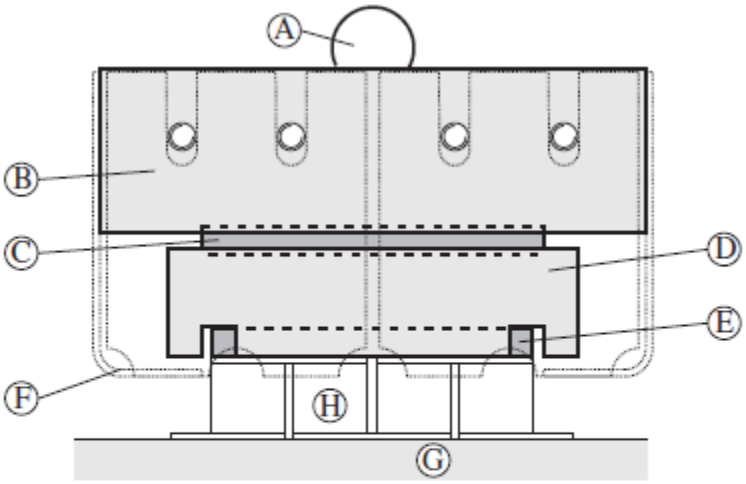

Assembled heaters with (A) abutment steel ball, (B) covering Cu block, (C) guarding heater, (D) isolation block, (E) measuring heater, (F) radiation shield, (G) cold side cooler and (H) thermoelectric generator module.

Figure 2.1

Another characterization method was carried on by R. Bonin, D. Boer *et al.*[2013]. The novelty of this work has to found both in the originality of the proposed device, by considering its whole structure, and the field of application. Moreover, they highlight the peculiarity of the heat source employed since the heat is supplied by a flameless catalytic burner. This kind of heat source is more competitive and reliable with respect to flame burner when it is used for applications where low power and small dimensions are required.

In addition, this study permits to model the thermoelectric generator when different natural heat sources are considered since the employed catalytic burner basically provides a low-temperature heat source, exactly representing what can be obtained by a renewable heat source such as geothermal, ocean thermal energy, and waste heat. A schematic section of the whole device is shown in *Figure 2.2*.

In Bonin and Boer work, in order to properly manage the energy produced by the generator, it is necessary to consider that the system, when switched on, starts to produce energy till the end of the fuel also if no load uses that energy. The best solution is not only to convert this energy to be used with the most part of microprocessors or sensors available on the market, but also to store that part of the energy that is not instantly used. Considering the storage system, it can be divided in two main components based on different technologies:

- Electrostatic storage: most suitable when the external load requires small quantity of energy in short intervals and the generator continuously supplies the average energy required.

- Chemical storage: most suitable when the generator has an intermittent production or the external load requires medium/large quantity of energy with long pause interval also when the generator is switched off.

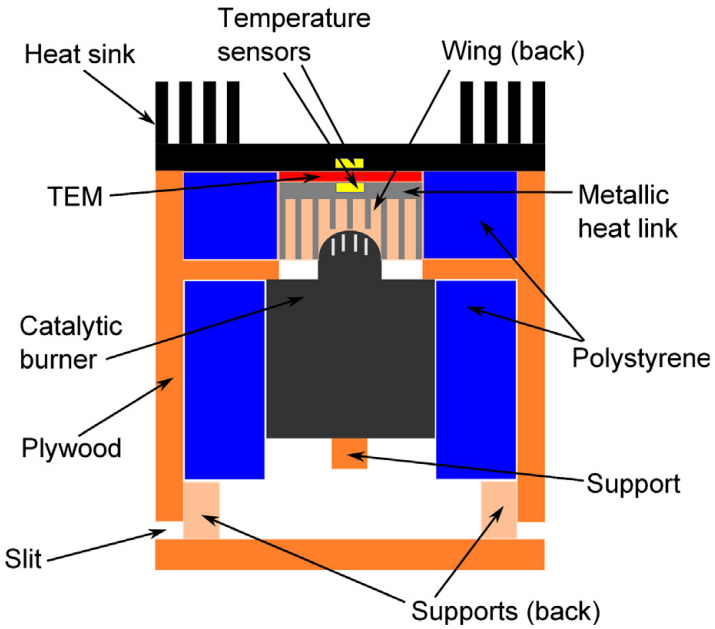

Figure 2.2

A characterization method is also proposed by R. Aishka and S. Dislitas work [2010]. Their developed system consists of three sections: TE module mechanism, Cooling System, and Heating System. The main structure can be seen in *Figure 2.3*.

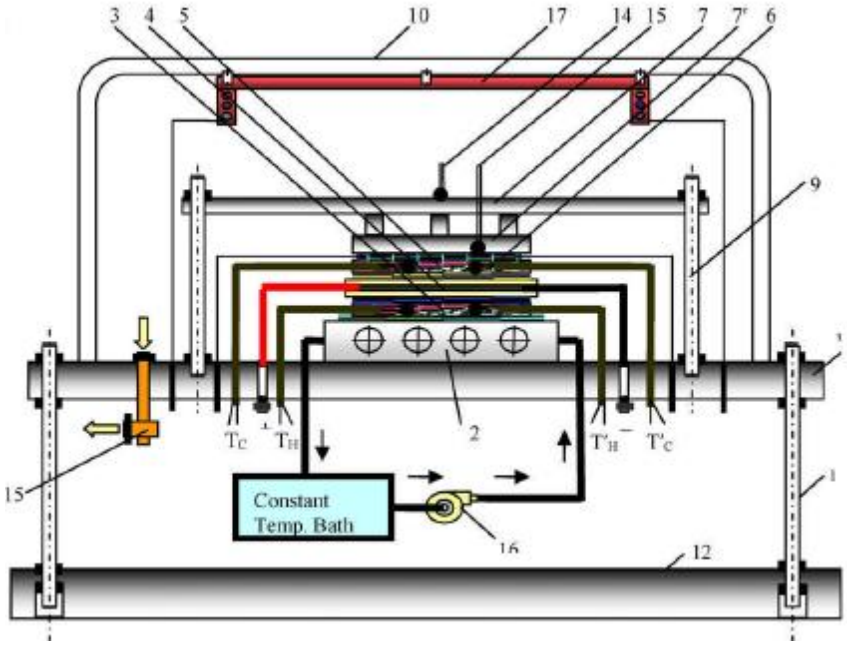

Figure 2.3

We can see that 1- indicates the copper base on which there are two water radiators, 2- indicates the water radiators, and 3- is the plate of 2.5 mm width providing a thermal balance. In the figure, 4- is the thermoelectric module, 5- is the second plate providing thermal balance and 6- is the heater. Cold side of the module 4-, thermal balance plate 5-, and the heater 6-, are isolated by cylindrical foam indicated as 7-. The cylindrical foam, 7-, also covers top surface of the heater 6-. This entire sandwich is assembled to the base, 1-, with screws, 9-, and this block is closed with a cover, 10-. In order to ease the usage of the set, this block is assembled to the base, 12-, with screws, 11-, also. Electric supply cables of the thermoelectric module and the heater, and the free ends of the thermocouples T_1-T_4 are intentionally extracted out of the structure. As to measure the temperatures of the cold and the hot side of the module as precisely as possible, thermal balancer plates 3- and 5- are made of red copper and thermocouples are placed into thin holes of diameter 1.5 mm, drilled 15 mm to the center of these plates. All contact surfaces around the block are covered with thermally conductive silicon coating. There is also a loop thermoelectric cooling system, consisting of a pump, 16-, fan and a radiator, which keeps temperature T_H constant and remove the thermal load out of the hot surface.

In the literature it is also possible to find different configurations in which thermoelectric modules are tested. It is interesting, for example, to consider the work proposed by Gaowei Liang, Jiemin Zhou *et al.* [2011]. In their work they show that as the output power of the TEG composed of only one TE module is very small, to obtain higher output power, it is possible to make a TEG by multiple TE modules in series connection or parallel connection. The results showed that when all the modules had the same parameters, and worked in the same condition, the series-parallel properties of the TEG where the same as the series-parallel properties of common DC power. However, to a multiple modules TEG, it is hard to guarantee every TE module works in the same conditions. Therefore, there are more components in the multiple modules TEG, and its performance analysis is more complex than the one module TEG. In the research carried forward by Liang and Zhou, the output performance of parallel TEG is studied and an analytical model of parallel TEG is proposed based on thermodynamic theory, semiconductor thermoelectric theory, and law of conservation of energy. The model can also be used to analyze the output performance of parallel TEG when all TE modules work in different conditions.

In order to verify their parallel model established in the research, Liang and Zhou developed a parallel TEG experimental system, which schematic representation is shown in *Figure 2.4*. The parallel TEG consists of two TE modules which are numbered as TE-1 and TE-2, respectively. The heat source of each TE module is a heating plate made of aluminum, its temperature can be adjusted by the voltage on the electric heating tube. The heat sink of each TE module is a water cooling plate made of copper, its temperature can be adjusted by the flow and temperature of cooling water. Some U-shaped slots are cut on the heating plates surface and water cooling plates surface which contact with the TE modules.

To reduce the thermal contact resistance, the interfaces of the heat source and the TE module, the TE module and heat sink are all coated with heat conductive silicone grease, it can be thought that all the interfaces have good contact addition.

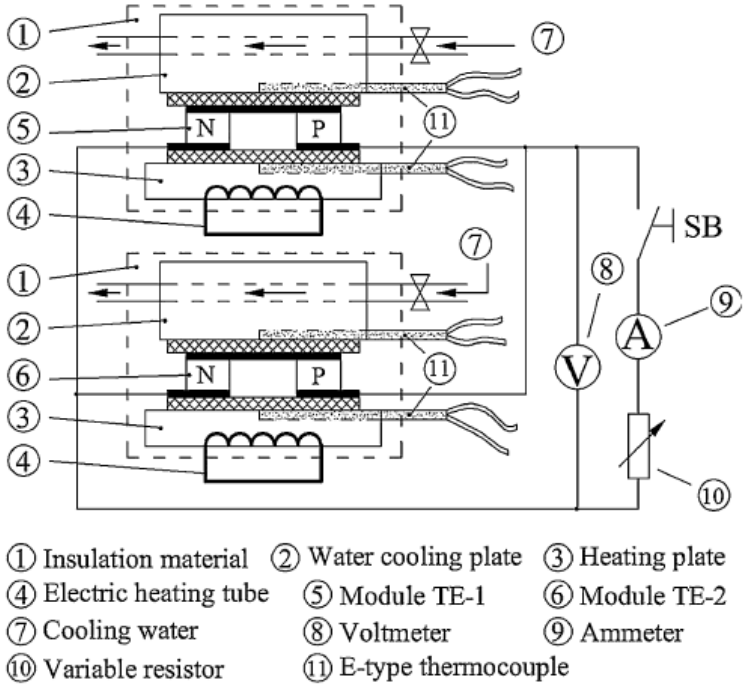

Figure 2.4

The last characterization method presented in this review has been developed by Bunyamin Ciylan and Sezayi Yilmaz [2006]. Their thermoelectric module test system consists of 3 main blocks; power supply cooling system, an electronic control and data acquisition. Power supply is a switched mode type and cooling system is a water circulation type heat exchanger. Temperature measurements are taken via a K-type thermocouple and current is sampled by a Hall-effect sensor. The front end for temperature measurements is also suitable for T-type thermocouples.

A schematic diagram of the mechanical structure of the test system is shown in *Figure 2.5*. Hot side of the thermoelectric module is cooled by water circulating cooling system. There is a thin layer of copper sheet between the brass cooling plate and hot side of the thermoelectric module. Its purpose is to provide a thermally conductive means in which the thermocouples can be attached freely to measure the hot and cold side temperatures and also this layer serves to distribute the heat uniformly all over the surface of the contact area with the aid of a thermally conductive paste. There is a heater plate made form brass between the cold sides of two thermoelectric modules. One of the thermoelectric modules is the device under test, while the other one, which is identical with the module under investigation, is used to distribute the heat load posed by the heater equally between its two sides. All the

test apparatus is covered by a 5 cm polyurethane coating to minimize the external heat load and the internal heat losses.

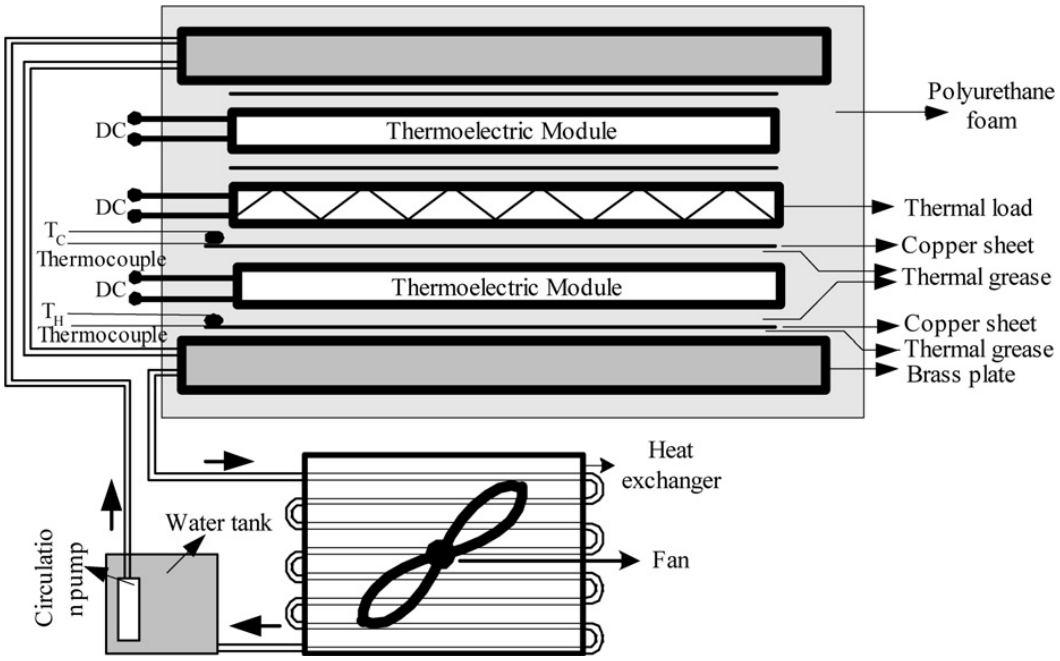

Figure 2.5

2.4 Module Test System for Characterization of Commercial TEGs Used in the Development of the Thesis Work

2.4.1 Introduction to Panco *TEGeta*

The current thesis work is about the extrapolation of output parameters from commercial TEGs modules during their load conditions. A thermoelectric power generation module needs a series of devices that helps to conduct the experiments in a reliable and fast procedure that comprehend different issues, such as a mechanical and electrical set-up, good connections, suitable movable elements, data acquisition process and manageability.

The experiments were carried on in the Department of Energy Conversion and Storage of DTU, Technical University of Denmark, Riso Campus. In this Department is available a system developed by PANCO GmbH - Physics Technology, Development and Consulting, a company involved in the development and application of measurements techniques and thermoelectrics.

The equipment developed by PANCO is known as "*TEGeta: Measurement of efficiency and specifications of Thermoelectric Power Generators"*. As can be understood from the abovementioned description, the system main purpose is the measurement of the efficiency

through the elaboration of current and voltages values that occur during the working conditions of a thermoelectric module.

Considering an overlook that synthesize the principal features of the *TEGeta*, we can say that the thermoelectric module is placed between a heating and a cooling plate in order to establish a temperature gradient. In this way, using different load resistors that can be applied to match the load, currents and voltages of the TEG are measured.

2.4.2 Specifications and System Hardware Characteristics

The facility consists mainly of a measurement pillar, data logger and PC for data acquisition.

The measurement pillar is a cooling plate that is cooled. In between two reference blocks are placed to measure the temperature gradient inside the blocks and thus the heat flow. Moreover, in between these reference blocks the TEG is placed. A thermal insulation is used to minimizes the heat losses.

The measurement equipment consists of temperature sensors (for heater, cooling plate and reference blocks) and the connections for voltage and current of the TEG as well as a data logger and electronics to control the load resistance. In addition a vacuum chamber allows measurements under vacuum conditions or in protective gas atmosphere. Generally the equipment can be used in air up to 900°C/1000°C.

The data are acquired by a data logger and saved into a PC. Furthermore the measurement software allows for the control of the devices, temperature settings for the heater, temperature steps for the measurement and control of the load resistors. The data can be saved into .txt format or Excel format (.xls) for further process.

We can consider a list of the principal specifications:

- References blocks (2 pieces), with dimensions changing with the TEG module used
- Cooling plate
- Heater with PID controller
- Thermal insulation
- Connectors for thermal sensors, electrical connections for heater and TEG
- Thermal sensors (type K)
- Load resistors
- Data logger Keithley 2770
- Multiplexer card Keithley 7710
- GPIB-USB connector
- PC with measurement software
- Measurement range temperature: room temperature up to 1000°C
- Measurement range voltage: 0-60 V (accuracy ±1%)
- Measurement range current: 0-30 A

In the following *Figure 2.6*, *Figure 2.7* and *Figure 2.8* is shown a schematic representation of the system and some pictures of the hardware configuration before starting the experiments.

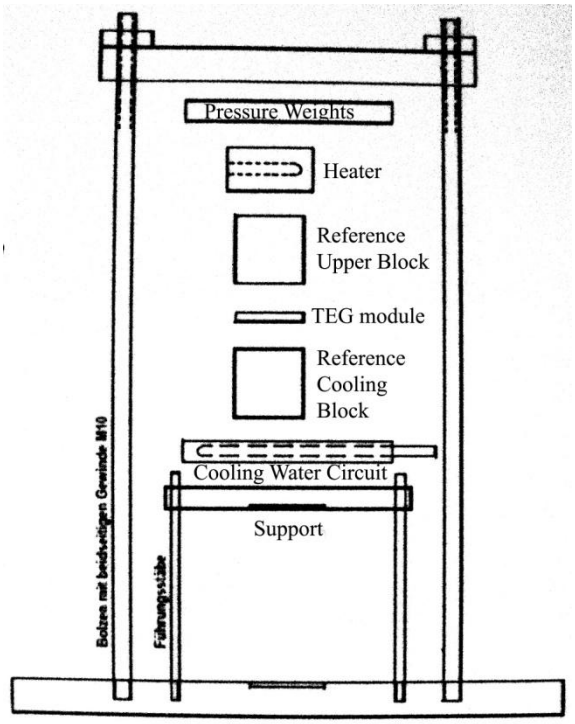

Figure 2.6

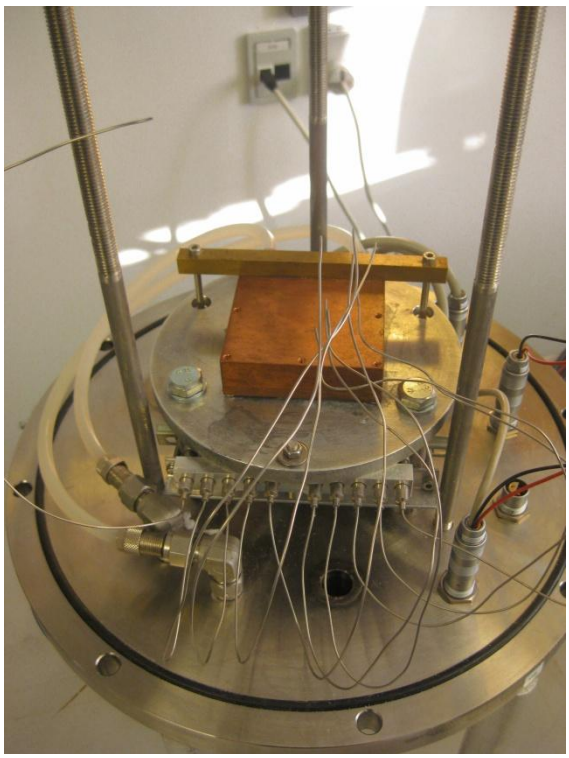

Figure 2.7

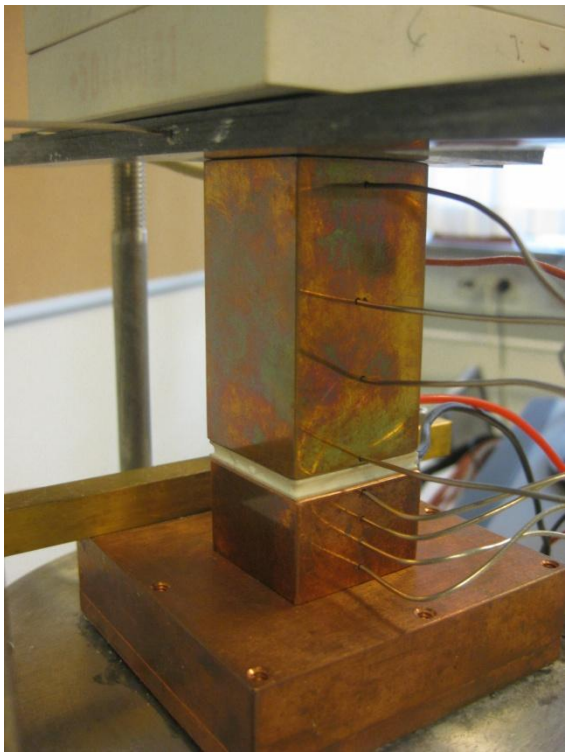

Figure 2.8

2.4.3 Hardware Preparation Before Starting Measurements

In *Figure 2.7* and *Figure 2.6* it is possible to see the mechanical support and the cooling water element that constitutes the basis of the measurement pillar. After positioning the reference cooling block, that has been chosen considering thermoelectric module dimensions, on the cooling plate, it is possible to insert the TEG module sandwiched between the upper reference block and the cooling block. This operation has to be accurate in order to line up all the different elements between each other. It is an important step of the hardware configuration since the TEG has to be totally covered by the blocks without any visible part of its surfaces in order to avoid heat flux dispersions and a temperature gradient collapse.

Once that the first three elements are placed (cooling block, TEG module and upper block) it is possible to place on the top of the pillar the heater and the weight that is needed to assure a good surface contact between the different element of the pillar. The heater element it is shown in *Figure 2.9* and *Figure 2.10* where it is possible to see the wires connections through which the PID controller set the temperature and the hole where the thermocouple is placed.

Figure 2.9

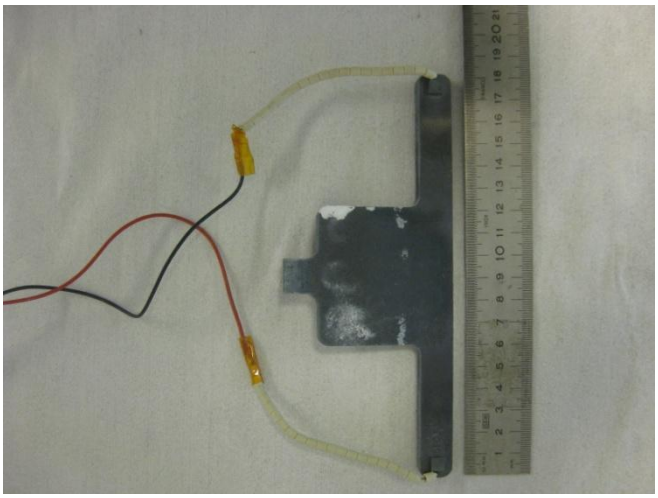

Figure 2.10

During the preparation of the pillar graphite sheets, with the same dimensions of the blocks and the TEG module, are placed in between the different elements surfaces in order to improve the contact between the blocks, the TEG module and the heater. Furthermore graphite is a good conductor that is able to inhibit the thermal resistance that opposes to the heat flow.

The following step after the pillar is formed is to place the thermocouples. Thermocouples are needed in order to control the temperature gradient along the pillar/blocks and to study the heat flow across the module. It is also very important to know the temperatures related

to the hot side and cold side of the TEG module to have an accurate measurement of the heat flow during the different steps of temperature distribution to which the module is subjected. Thermocouples are slightly thinner than the holes drilled in the blocks so it is easy to place them before the experiments and remove them when the data acquisition process is over. In *Figure 2.8* it is possible to notice that there is the same number of holes in both the upper and the cooling block and a respective equal number of thermocouples. There are also different types of commercial thermocouples that could be used in these kind of experiments, in our case we are using a K-type thermocouple that guarantees a wide range of supportable temperatures during its working conditions.

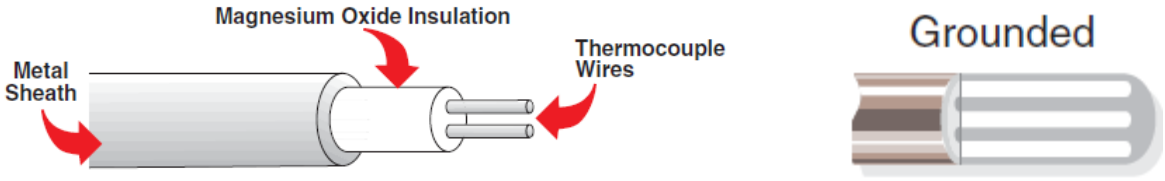

Figure 2.11

In *Figure 2.11* it is possible to see the internal configuration of a thermocouple, made by two thermocouple wires grounded by a magnesium oxide insulation and a metal sheath. In the *Table 1* below it is showed the comparison between type K thermocouples and other different types.

T/C Type	Wire Size						
	8 AWG 0.128"	14 AWG 0.064"	20 AWG 0.032"	24 AWG 0.020"	28 AWG 0.013"	30 AWG 0.010"	36 AWG 0.005"
J	760 (1400)	590 (1100)	480 (900)	370 (700)	370 (700)	320 (600)	315 (590)
K	1260 (2300)	1090 (2000)	980 (1800)	870 (1600)	870 (1600)	760 (1400)	590 (1100)
E	870 (1600)	650 (1200)	540 (1000)	430 (800)	430 (800)	370 (700)	320 (600)
T	370 (700)	370 (700)	260 (500)	200 (400)	200 (400)	150 (300)	
RX/SX	200 (400)	200 (400)	200 (400)	200 (400)	200 (400)	150 (300)	
N	1260 (2300)	1090 (2000)	980 (1800)	980 (1800)	980 (1800)	870 (1600)	
CX	472 (800)	472 (800)	472 (800)	472 (800)	472 (800)	400 (752)	

Table 1

It can be seen from the *Table 1* above how, according to different sizes, K type thermocouples have the most flexible range of tolerated temperatures compared to the other different types.

The last step of the hardware preparation is the switching of the cooling pump in order to let the water begin to circulate in the cooling plate. It is better to make this operation several minutes before the beginning of the experiments in order to get the water to reach a stabilized temperature. The cooling pump, as it is possible to see from *Figure 2.12*, has an adjustable controller that permits to decide at which cooling temperature we want to take the measurements.

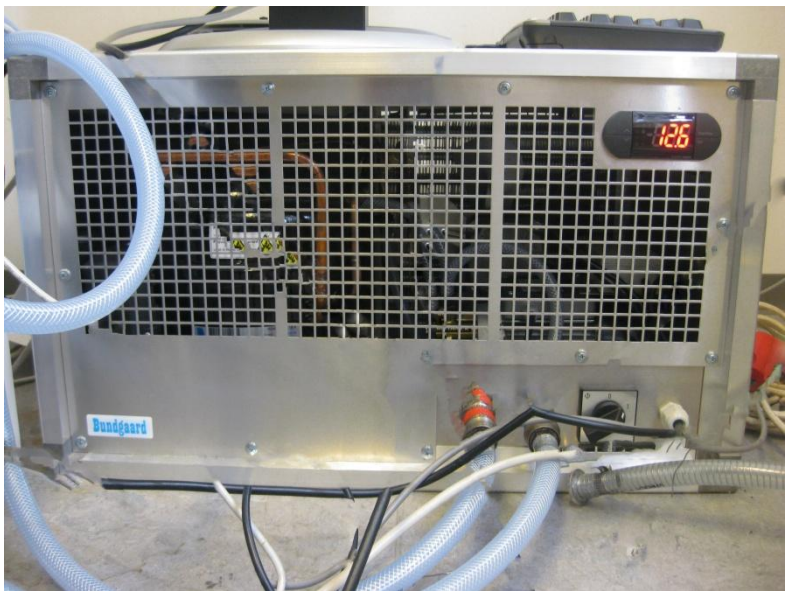

Figure 2.12

2.4.4 Software Configuration

Once the hardware configuration has been set, it is possible to proceed with the software starting. Basically the main features of the software are the temperature control and the data acquisition related to the output voltages and currents. The TEG module is connected through electrical wires to the data acquisition system where load resistors can be adjusted in order to get the matched load (the maximum power output is reached when the internal resistance of the module is equal to resistance load, as explained in the first chapter).

Since a wide range of resistance loads have to be adjusted during the experiment tests, the electrical circuit that provides the load for the current output of the TEG module, is composed by a series of relais which can be configured in order to operate with the desired resistance load. In the *Figure 2.13* it is shown how the relais are combined with the load resistors.

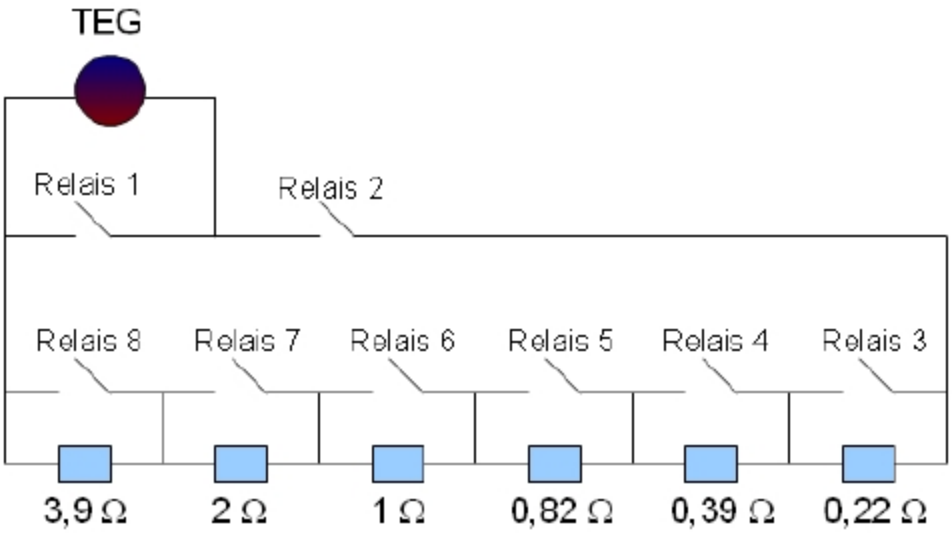

Figure 2.13

Relais 1 is closed for current measurement (short circuit current), while relais 2 is open for the measurement of the Seebeck voltage without any resistance (open circuit voltage), when using the load resistors relais 2 must be closed. The combination of open and closed relais 3 to 8 will adjust the desired load resistors.

In order to set the software for the configuration, the system has to be programmed following the procedure that is shown below in *Figure 2.14*.

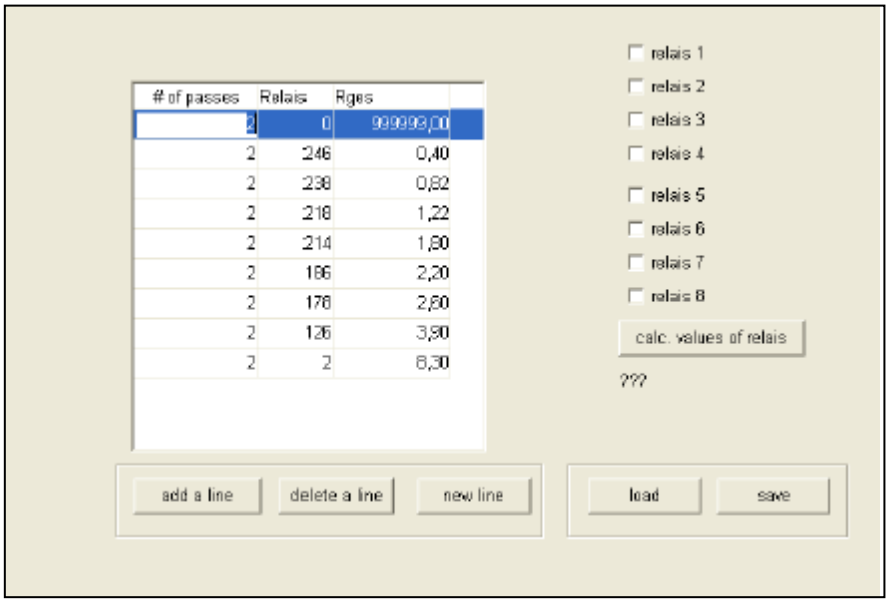

Figure 2.14

It is possible to notice that the command *# of passes* sets the number of measurement runs for each load resistor combination. Relais means the value which is send to a controller to

switch the relais. This number can be calculated with *#calc. values of relais* and will be shown at the question mark's position. In *Rges* the real value of this relais-resistors combination has to be set, this number will appear in the data. With *add a line, delete a line* or *new line* new combinations can be set or withdrawn.

The data acquisition system is powered by a Keithley 2700 and it is integrated with a PC that elaborates the data acquired from the TEG module. It is possible to see the integrated system in the *Figure 2.15* below.

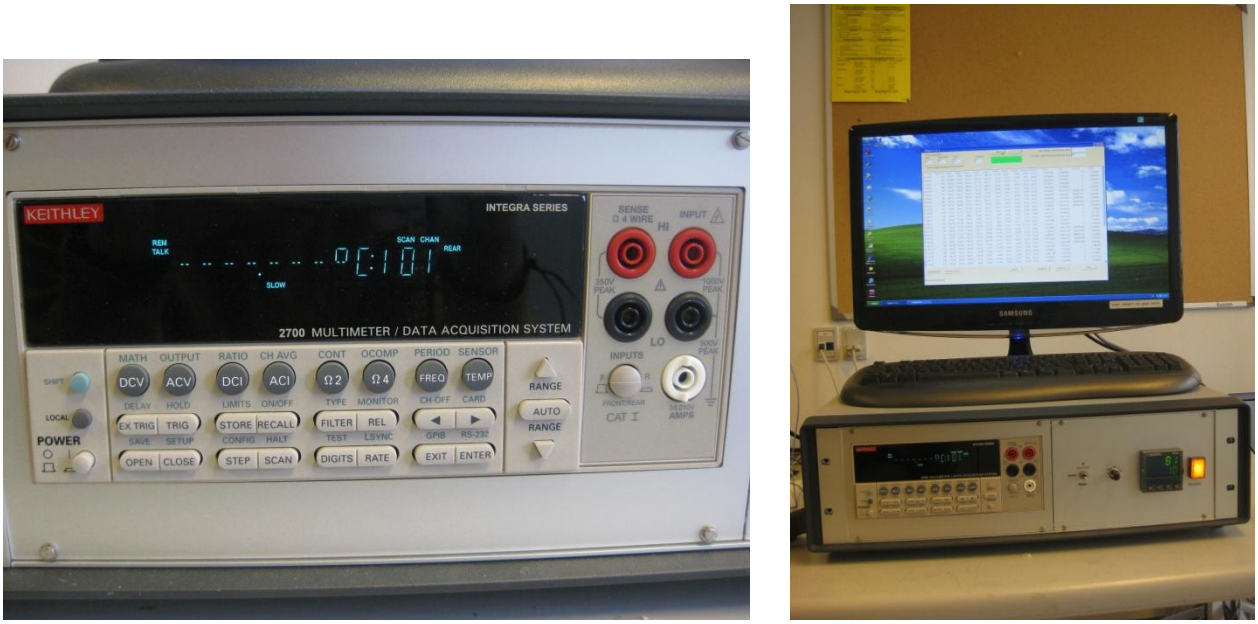

Figure 2.15

The last step of the software configuration is the setting of the temperature steps that are needed to apply to the TEG in order to acquire the data and the range of time that is necessary in order to have a good stabilization of the system. We can refer to the *Figure 2.16* where it is possible to divide the screen in ten parts:

1. Temperature settings
2. Start button
3. Stop button
4. Configuration
5. Machine test
6. Time between measurements
7. Time after set-point temperature reached
8. Measurement data
9. Save button
10. Graphs for direct view of power

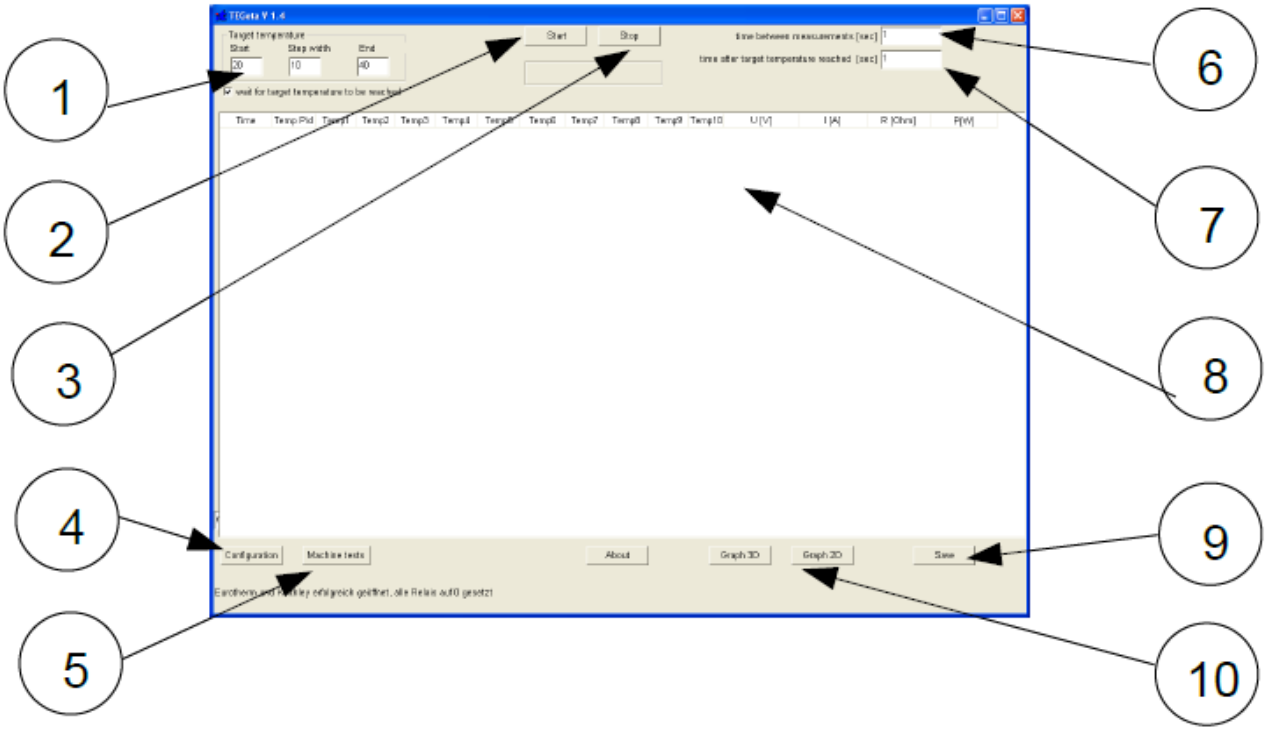

Figure 2.16

With *button 1* the set point temperature can be adjusted. The start temperature is the first temperature to which the PID controller is set. After the measurements at this temperature, the PID controller goes on with the stepwidth further until the end temperature has been reached. The number of steps is thus given.

Field 6 contains the time in seconds that will be waited after each measurement round, while field 7 is the waiting time after the heater has reached the set-point temperature. This time should not be too short, since an equilibrium in the reference blocks and the TEG should be reached.

Field 4 refers to the configuration of the relais-resistors system, as it has been described previously.

As regarding field 5, it opens a new window for a machine test. It means that independently from the main program the temperatures and voltages can be measured and relais combinations can be set. Machine test window is shown in *Figure 2.17*. This is an important part of the command part of the software since it help to check the parameters involved in the process before starting the measurements. Therefore it is possible to control at the same time the heater temperature and the relais configuration in order to get in real time how they affect the TEG module behavior. Using this procedure the operator that is facing the experiments can adjust in the best way possible all the parameters that are needed during the following start of the measurement process.

After setting all the parameters the *button 2* Start can be pressed. During the measurement a red bar appears as it can be seen in *Figure 2.18* below.

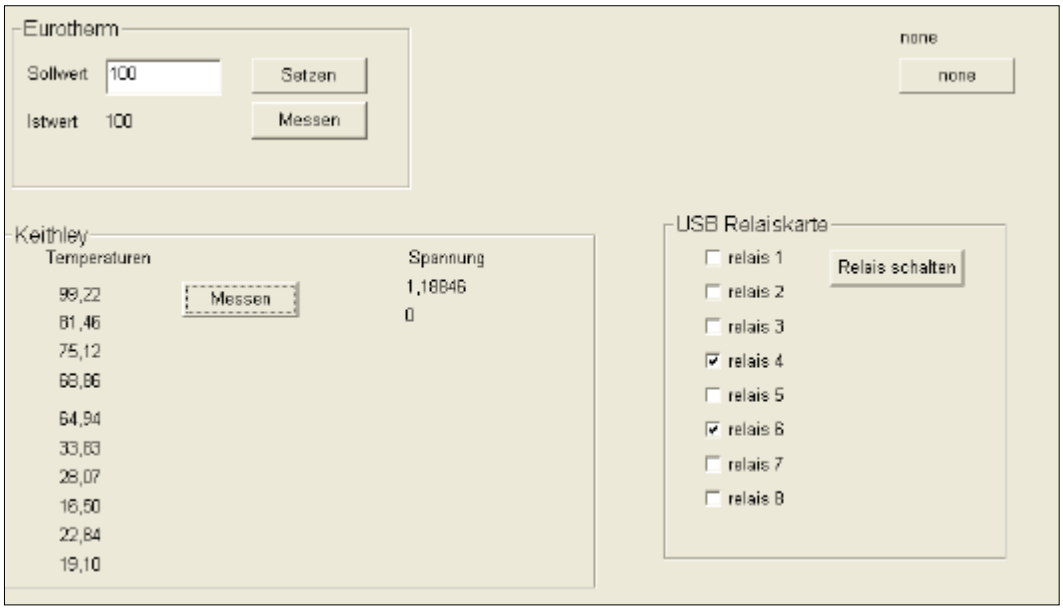

Figure 2.17

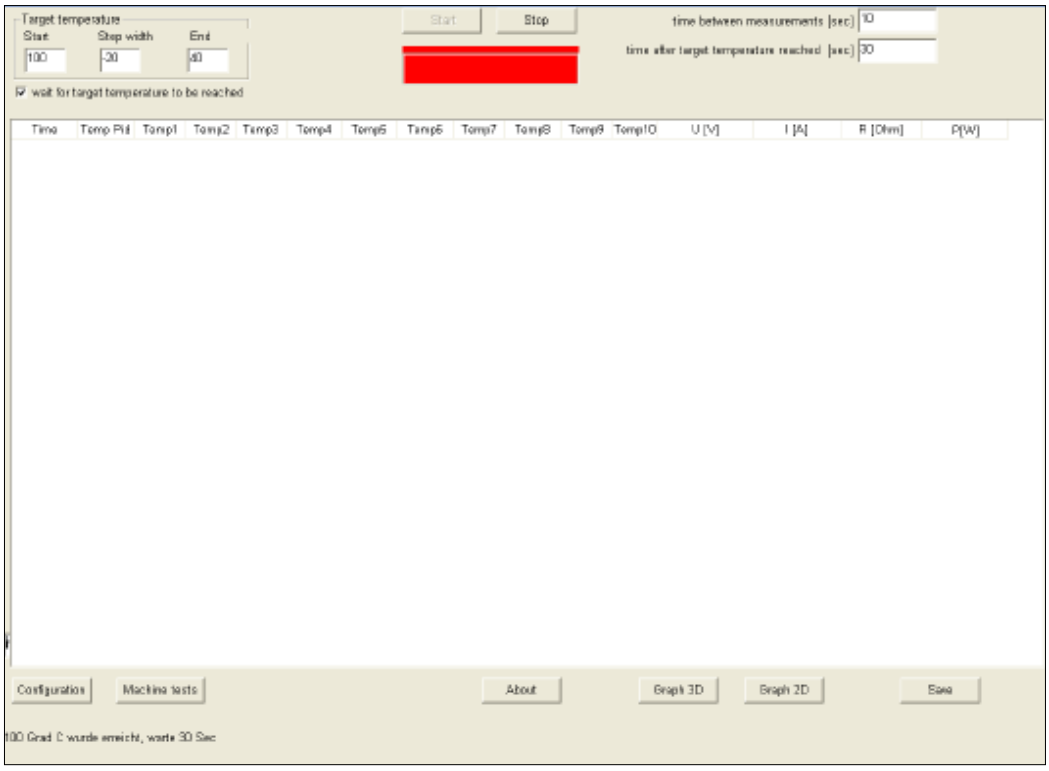

Figure 2.18

The measurement will stop automatically after the last temperature, but it is also possible to stop all the process using the *button 3* Stop.

During the data collection, we can see that, from *Figure 2.18*, all the results are listed in a panel where labels referred to the different parameters are present. It is possible to check, while the experiments are carried on, the different time steps, heater temperature, thermocouples temperature (in the system a total number of ten thermocouples is used), current output, voltage output and resistance load applied respectively for each step of temperature.

Eventually, all the data collected at the end of the experiment can be saved using *button 9*. By using *button 10* it is also possible to plot a graph showing the power output vs the resistance load, but, as will be shown in the next chapter, these kind of graph will be obtained through Microsoft Office Excel when all the data of the singles TEG wil be collected.

3

Temperatures and Heat Fluxes Distribution

3.1 Introduction

This chapter describes the first part of the experimental process that led to the data acquisition on the thermoelectric commercial modules.

As described in the previous chapter the combination between the hardware configuration and the software one is very important in order to get accurate results. This is why, once the system has been prepared to start getting the data, a good calibration is required. In the following paragraphs there will be shown which kind of materials have been used to impose a heat flow across the module, what are their physical characteristics, and how a temperature and heat distribution can be extrapolated using the module test system.

In this first part of the experiment, calculations were made without considering the TEG modules. In this way it was able to analyze the different temperature gradients and heat flows along the blocks that constitute the pillar in which the thermoelectric module is inserted.

These results are very important for two main reasons. The first one is to set all the module test system before starting the electric output extrapolations from the TEGs. In fact, knowing how the thermodynamic characteristics are distributed along the test pillar helps to understand if the real acquisition process is reliable or not. Thanks to the use of the thermocouples inserted in the upper and the cooling block, it is possible then to have information that will be later elaborated and showed in appropriate plots. The second reason is the possibility of comparisons between the experimental results and the simulation ones. As will be described in the next chapters a simulation model will be implemented with the

software Comsol Multiphysics in order to have a background pattern that validate or at least can reproduce the results that come out from the module test experiments. Accordingly to this way of procedure it will be possible to establish if the experimental data reflect the theoretic trend values.

Moreover, during the introduction of the materials that constitutes the pillar blocks, there will be a description of the process used in order to get their physical characteristics such as density and thermal conductivities. In particular, in order to extrapolate the real thermal conductivity values, there will be introduced a system known as Laser Flash.

3.2 Heat Conductive Blocks

3.2.1 Copper Blocks Used for the Experiments

The module test system, as it is also possible to see in the 2nd chapter of this thesis work, is composed by different elements that constitutes the pillar in which the TEG module is inserted for the measurements.

In order to improve the thermal contact with the heater and the cooling plate, and to obtain a control of the heat flow such as the temperature gradient, two conductive blocks are thus placed on both sides of the thermoelectric converter. It is possible to see this configuration in *Figure 3.1*.

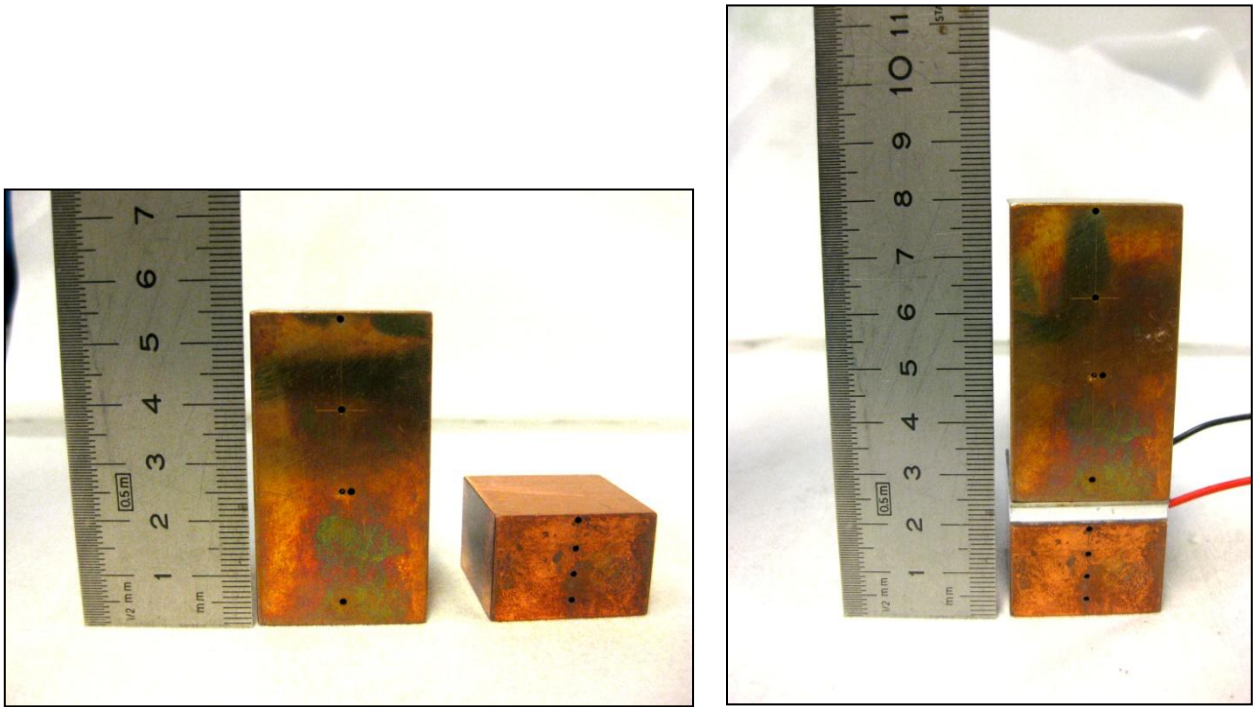

Figure 3.1

In the figure above it is shown the two blocks used in the system configuration and how they are configured in order to place the thermoelectric module. It is important, in this step of the process, to assure that both blocks fit the module without leaving any uncovered part. In fact a bad alignment of these three elements could result in heat flow losses that affect both the data acquisition and the module performances.

In our case we are using two copper blocks which have dimensions *30x30x55 mm* and *30x30x20 mm.* The longer one is placed between the heater and the module hot side, while the shorter one is placed between the cooling plate and the module cold side. Besides, from *Figure 3.1* it is also possible to notice the thermocouples holes. Each hole has been drilled and positioned following the scheme in *Figure 3.2*, where it is shown the hot side block.

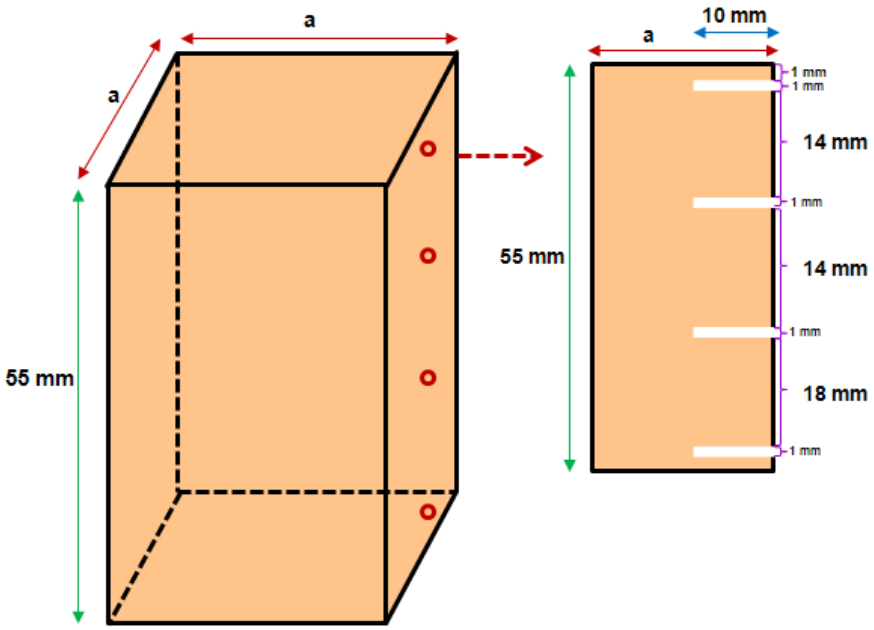

Figure 3.2

The thermocouples holes, as it is possible to see from the figure, are four for each block. It is important to underline that one of the holes has been drilled as close as possible to the surface that is going to be in contact with the module hot side (in our case 1mm above the bottom surface of the block). Using this arrangement the thermocouple that is going to be inserted in this hole would extrapolate a temperature value that is very near to the real temperature value that is present on the TEG hot side.

As regarding the shorter copper block, the configuration is the same of the *Figure 3.2* and the thermocouples are placed from 5mm distance between each other. Also for the shorter

copper block one of the thermocouples holes has been drilled 1mm below the upper surface.

3.2.2 Copper Thermal Conductivity with Laser Flash Method

In order to calculate the heat fluxes that are running across the copper blocks, it is needed a value of the thermal conductivity λ.

Using a sample as a reference for the material used, it is possible to calculate λ using the Laser Flash Method. In principle, this system, helps to extrapolate the thermal diffusivity of a reference sample. Starting from the thermal diffusivity it is later simple to calculate λ knowing the values of specific heat and density of the sample employed as

$$\lambda = \kappa \cdot \rho \cdot c_p$$

While the laser flash equipment is shown in *Figure 3.3 (a)*.

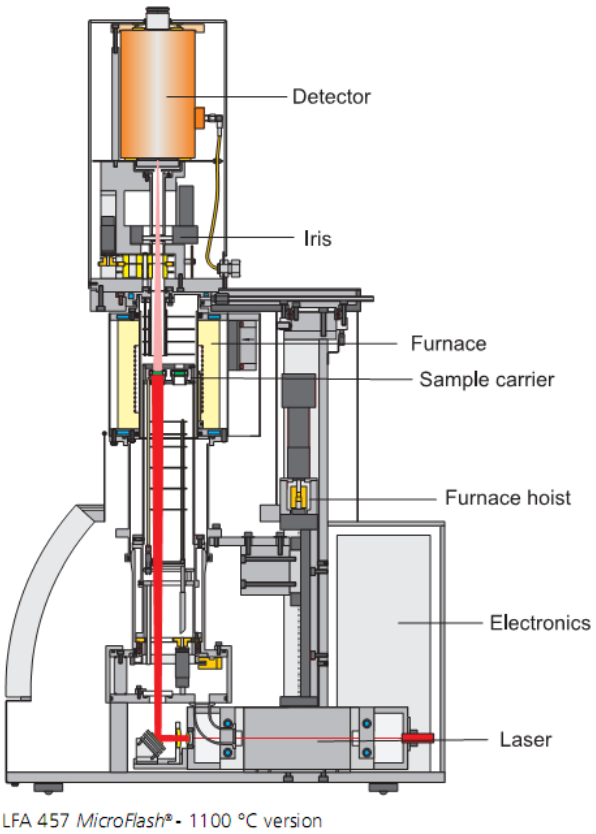

Figure 3.3 (a)

After cutting a specimen from the interested material, it is possible to proceed with the measurements. The specimen is set on a specimen holder inside a vacuum chamber. The

chamber has a vertical cylindrical shape, a pulsed laser beam impinges on the front surface of the specimen through the top window, and an infrared radiation thermometer detects the rear surface of the specimen through the bottom window. The specimen is supported by one ring in order to suppress heat loss to the specimen holder. The laser is used for pulse heating the specimen, while the temperature history curve of the specimen surface is detected using the infrared radiation thermometer. This resulting temperature rise on the back surface of the specimen is measured as a function of time and can be used to derive the thermal diffusivity of the sample. A typical curve of temperature rise v. time is shown in *Figure 3.3 (b)*.

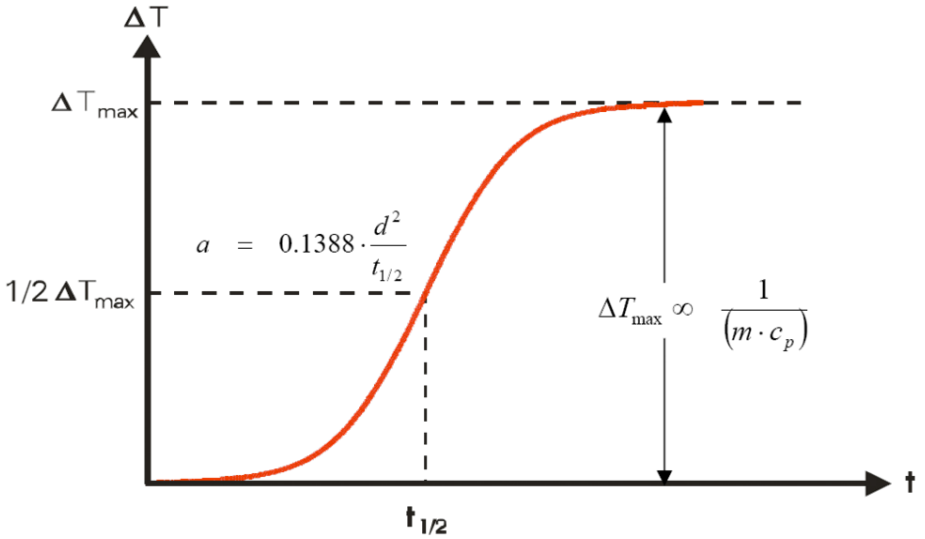

Figure 3.3 (b)

A mathematical analysis of this graph allows for the determination of thermal diffusivity. For ideal, adiabatic conditions, the thermal diffusivity is described by

$$\kappa = 0{,}1388 \cdot \frac{d^2}{t_{1/2}}$$

Additionally, various mathematical models are included in the analysis software to compensate for radiative heat loss from the front and side surfaces of the specimen.

The input values for the laser flash measurements are the sample size and density. Using the simple Archimede principle it is possible to calculate ρ that in our case results to be ρ_{Cu}=0,00895 [g/mm^3].

In *Table 1* there are listed the results extrapolated with the Laser Flash equipment available in the Department of Energy Conversion and Storage of the DTU Technical University of Denmark, Riso Campus.

Using these values of thermal diffusivity in addition to the heat capacity values already available from previous experiments, it was thus possible to calculate the thermal conductivity λ that will be needed in the future measurements of the heat flux. In *Table 2* and *Figure 3.4* are showed all the final data acquired.

Temperature [°C]	Thermal Diffusivity [mm²/s]
31,7	120,793
99,6	118,062
197,6	115,214
297,3	112,645
395,3	108,77
495,1	106,265
593,9	103,357
693,5	98,713
794	95,776
893,3	89,876

Table 1

T [C]	T [K]	Therm cond [W/m*K]
25	298,15	420,8349721
50	323,15	421,1218682
75	348,15	420,4397244
100	373,15	419,6091744
125	398,15	420,1138691
150	423,15	420,5177167
200	473,15	419,4796223
250	523,15	416,8550629
300	573,15	413,9461438
350	623,15	408,6926783
400	673,15	404,572132
450	723,15	404,1956083
500	773,15	403,6854002
550	823,15	402,7608605

Table 2

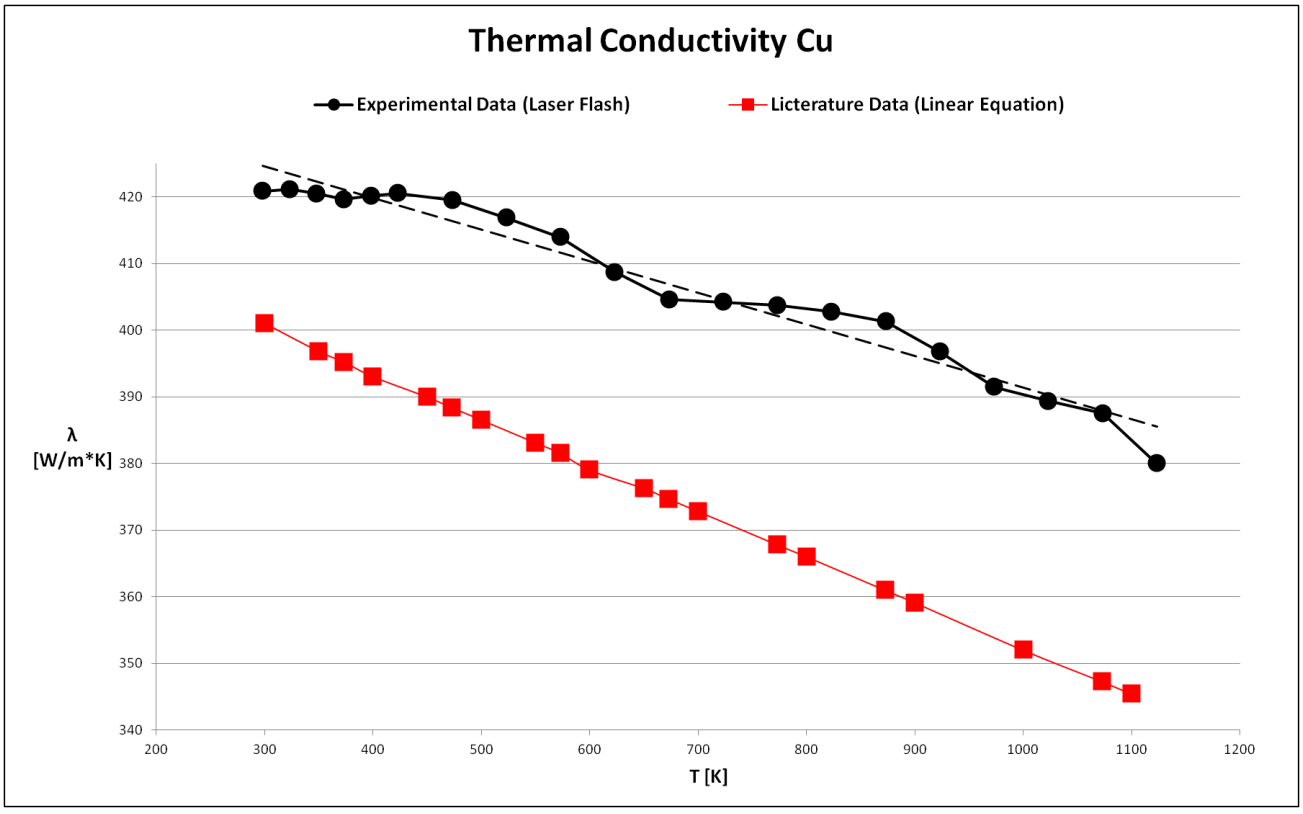

Figure 3.4

In *Figure 3.4* it is shown a comparison between the experimental data acquired from laser flash method and literature ones. It can be seen that they have quite the same progress as the temperature changes.

3.3 Temperature Measurements

The next step that follows the thermal conductivities data acquisition is the measurement of the temperature distribution along the copper blocks. This part of the experimental process is important to characterize the heat fluxes along the pillar and to check if the system setup responds in an accurate way before starting to extrapolate the output parameters form the TEGs.

As underlined also in the previous paragraphs, in this phase there will not be used the thermoelectric module. In fact the two copper blocks are inserted in the module test system in contact with each other. All the surfaces that are supposed to be in contact with the other elements of the pillar are interposed with graphite sheets in order to improve both the thermal conductivities characteristics and the mechanical contacts. Besides, in order to improve the surfaces contact and to guarantee a better heat flow transition along the blocks, it is important to polish the blocks before every operation that they submits in the module test system.

Once the copper blocks are inserted in the pillar, the thermocouples are place in the holes previously drilled along the blocks side surface. Since the holes are slight bigger than the thermocouple size, this operation has to be done carefully as to assure that the thermocouples tips reach the very end of the hole. In fact both the temperature gradient and the heat flow across the blocks will be then compared, as shown in the next chapter, with a numerical model in which we will consider the geometrical center of the pillar as the starting point for the comparison.

Since in the TEGs data acquisition process will be also used an insulation material in order to get higher values of the heat flow inhibiting the heat losses, in this part of the temperature distribution evaluation we are going to consider two cases, one refers to the blocks without insulation while the second one refers to the block surrounded by an insulation material.

The material used as insulator is the vermiculite, a material that guarantees low thermal conductivity and the possibility to work with high temperatures. In *Table 3* there are listed some characteristics of the vermiculite, while in *Figure 3.5* it is showed the actual vermiculite blocks used in the experimental process. Furthermore, since the copper blocks and the insulation material could not have a good contact, favoring heat losses, a more malleable insulation material was interposed between the vermiculite and the copper blocks, the wool glass. In this way, with the use of this configuration, it was possible to analyze the

heat flow both in the case of room environment and in the case of reduced convective and heat radiation losses.

Thermal Properties	Metric
CTE, linear	11.0 µm/m-°C @Temperature 20.0 - 750 °C
Specific Heat Capacity	0.940 J/g-°C
Thermal Conductivity	0.120 W/m-K @Temperature 200 °C
	0.140 W/m-K @Temperature 400 °C
	0.160 W/m-K @Temperature 600 °C
Maximum Service Temperature, Air	1100 °C
Shrinkage	1.0 %

Component Elements Properties	Metric
Al2O3	7.0 %
CaO	2.0 %
Fe2O3	4.0 %
K2O	11 %
MgO	21 %
Na2O	0.50 %
SiO2	47 %
TiO2	0.50 %

Table 3

Figure 3.5

In the software related to the configuration of the module test system, four different steps of temperature have been chosen in order to get the measurements. Accordingly to the software setup, the heater, once the data acquisition started, will thus provide to the blocks a fixed temperature that will be increased after a range of time imposed also by the software. The steps used in these experiments are four, starting from 50°C to 200°C in steps of 50°C. As a time spread between the different temperature steps it has been set up a period of 30 minutes. It is important to choose a period of time that is long enough to let the temperature stabilize along the blocks. In fact, a too short time interval, could not provide a temperature gradient with stationary fluctuations. This is why, during the 30 minutes period chosen, the temperature shows a rising from one step to another followed by a stabilization around the value imposed by the heater. If the waiting period was too short, it may be possible to get temperature measurement while the temperature it's still rising or it has still big oscillations around a determined value.

The first measurement was carried forward with the copper blocks without insulation, while in the second one insulation material was inserted in order to cover the block from the external environment.

Four thermocouples in the upper block and other four in the bottom block were used plus a thermocouple in the heater for a total number of nine thermocouples. The measurement system collected ten temperature values for each thermocouple and for each step of the

temperature range chosen for the experiments. Then, an average value of these ten temperature points was calculated in order to extrapolate the plots. In *Table 4* and *Table 5* there are shown the average results for the case without insulation and with insulation.

	Copper No Insulation							
	T1	T2	T3	T4	T5	T6	T7	T8
200 [°C]	78,629	72,288	67,952	62,265	37,991	36,282	35,044	33,339
150 [°C]	61,111	56,385	53,186	48,966	31,228	29,951	29,019	27,755
100 [°C]	44,008	40,988	38,931	36,197	24,95	24,107	23,466	22,632
50 [°C]	26,417	25,096	24,153	22,885	18,033	17,625	17,274	16,86

Table 4

	Copper With Insulation							
	T1	T2	T3	T4	T5	T6	T7	T8
200 [°C]	110,66	99,165	91,922	84,499	41,472	39,253	36,985	34,939
150 [°C]	85,556	77,245	72,021	66,634	33,816	32,207	30,511	29,087
100 [°C]	60,14	54,909	51,628	48,204	26,609	25,571	24,409	23,573
50 [°C]	33,52	31,361	29,989	28,502	19,399	18,95	18,381	18,097

Table 5

It is possible to notice that the case with insulation refers to a higher temperature distribution compared to the case without insulation. Using the insulator material it is thus possible to increase the temperature gradient thanks to the reduction of the heat losses due to the convection and the radiation contributes.

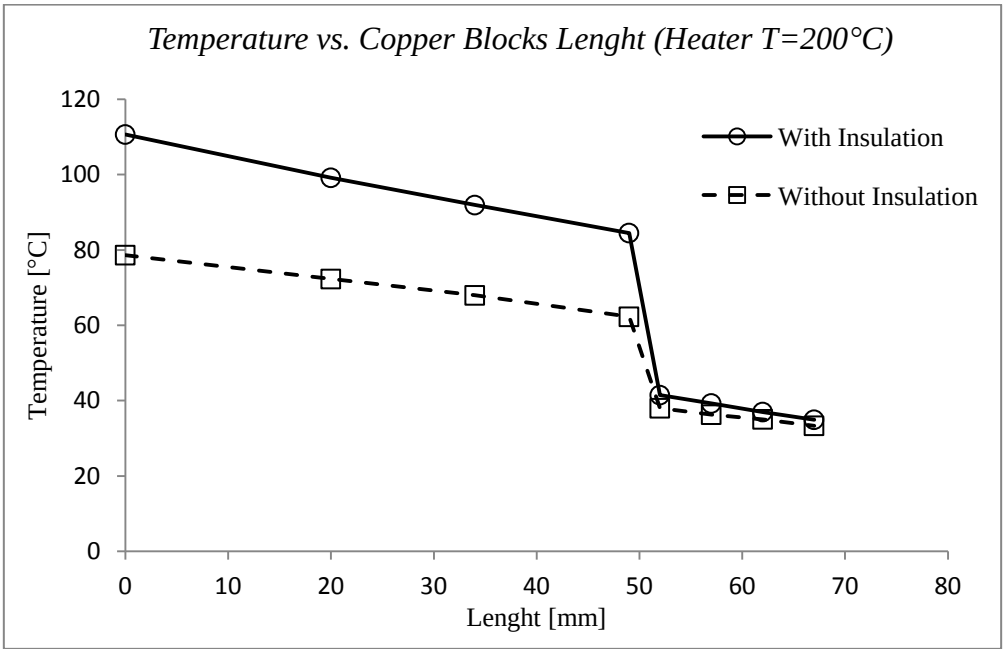

Figure 3.6

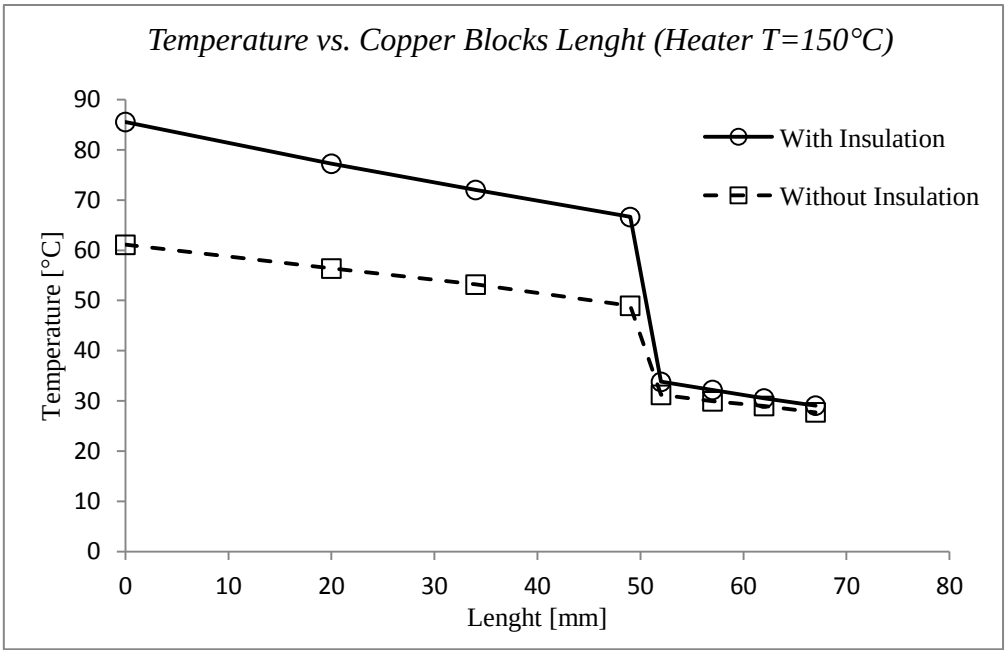

Figure 3.7

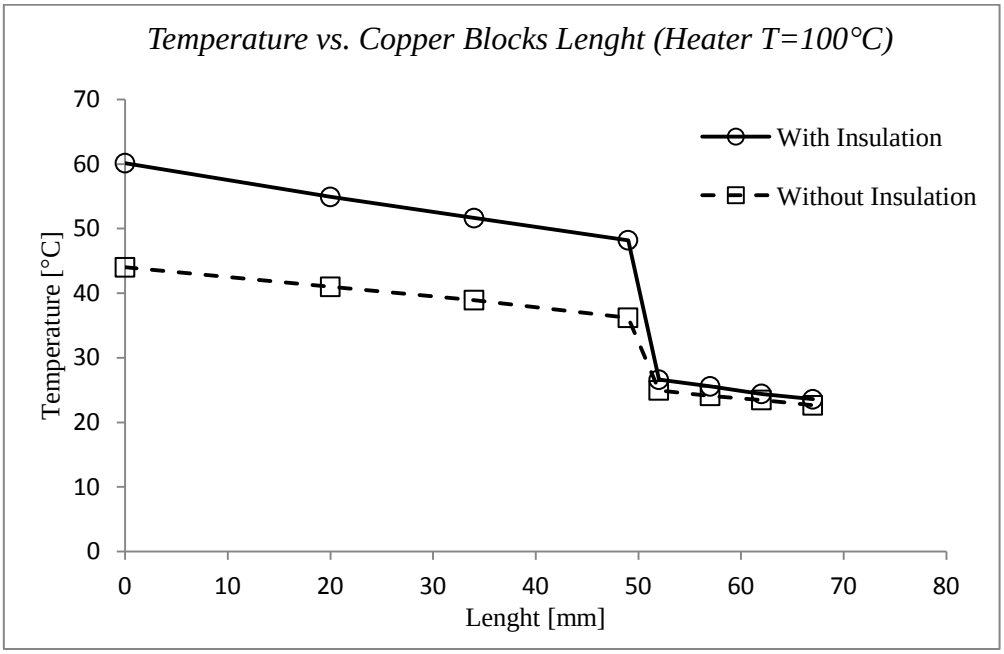

Figure 3.8

As it is possible to see, in the *Table 4* and *Table 5* there are represented the eight thermocouples used in the acquisition process (T1, T2, T3, T4, T5, T6, T7, T8) and the four different steps imposed to the heater (250°C, 150°C, 100°C and 50 °C). Accordingly to the tables, in *Figure 3.6, Figure 3.7* and *Figure 3.8* the difference between the two cases (with and without insulation) is even more noticeable especially considering the upper block.

3.4 Heat Fluxes Calculations

The temperature distribution along the two copper blocks is the starting point from which the heat fluxes are calculated. Knowing the distribution of the heat flux helps both to understand the reliability of the system during the working conditions and to know how the pillar elements react to the different temperatures loads that they undergone.

In this case we are still considering the two measurements with and without insulation and we are going to see the difference between them.

The equation used for the heat fluxes calculation is the simple Fourier law, considering a one dimensional distribution in a steady state analysis.

$$Q = \lambda \cdot \Delta T \cdot \frac{A}{l} \quad [W]$$

Where *A* is the cross sectional area of the block, *l* the distance between the two temperature points while ΔT their temperature difference and λ the thermal conductivity obtained through the laser flash equipment.

The starting point of temperature evaluation is the first thermocouple T1 located below the upper block surface that is in contact with the heater. Considering the other thermocouples, the heat flow has a number of evaluation point equal to the number of thermocouple. Since the distribution is one dimensional, the heat flow is extrapolated along the line that starts from the first thermocouple in the geometrical center of the block and ends to the last thermocouple located in the bottom block. As also discussed in the previous paragraph the TEGs modules are not a part of the pillar while the two copper blocks are in contact with each other. Besides, in the next tables and plots that we are going to show we neglected the thermal resistances between contact surfaces.

However, the accuracy of these measurements relies on the errors that can affect the temperature data acquisition using the thermocouples. Certainly that could be some uncertainties due to the thermal resistances between the thermocouples tips and the holes internal surfaces or even thermocouples calibration could import some error in the following data elaboration. The important aspect to underline is that the experiments showed and the results obtained from now on are the product of a previous understanding of the module test system working conditions. In this way it was possible to say if the data acquired were part of the expected range of results that usually manifests in these kind of experiments. Moreover, to have a more accurate way of comparison a numerical method has been implemented in the following chapter.

In the *Table 6 (a, b, c, d)* and *Table 7(a, b, c, d)* are showed the results calculated using the Fourier law along the temperatures points acquired from the thermocouples, respectively for the not insulated case and the insulated one.

As already seen in the temperature measurement tables, it is possible to notice the difference between the heat fluxes values of the two different cases:

***Table 6*, No Insulation**

Heater Temperature 200 °C	
Lenght [mm]	Heat Flow [W/m²]
20	139811,27
34	138913,23
49	138142,07
56	137103,80
61	136973,41
66	136858,59

a)

Heater Temperature 150 °C	
Lenght [mm]	Heat Flow [W/m²]
20	103916,67
34	103237,50
49	102652,79
56	102479,22
61	102468,86
66	102448,17

b)

Heater Temperature 100 °C	
Lenght [mm]	Heat Flow [W/m²]
20	66952,04
34	66506,95
49	66115,44
56	66097,52
61	66097,52
66	66104,90

c)

Heater Temperature 50 °C	
Lenght [mm]	Heat Flow [W/m²]
20	29577,03
34	29477,63
49	29345,06
56	29316,77
61	29314,81
66	29299,15

d)

***Table 7*, With Insulation**

Heater Temperature 200 °C	
Lenght [mm]	Heat Flow [W/m²]
20	224568,32
34	224046,53
49	223533,62
56	223333,48
61	223383,42
66	223433,37

a)

Heater Temperature 150 °C	
Lenght [mm]	Heat Flow [W/m²]
20	167636,03
34	166574,26
49	166424,82
56	166407,53
61	166426,12
66	166463,30

b)

Heater Temperature 100 °C	
Lenght [mm]	Heat Flow [W/m²]
20	108430,83
34	108397,92
49	108148,56
56	107670,25
61	107682,27
66	107694,29

c)

Heater Temperature 50 °C	
Lenght [mm]	Heat Flow [W/m²]
20	45642,36
34	45652,56
49	45498,01
56	45492,13
61	45497,21
66	45497,21

d)

Before the heat flow calculations, temperature data has been linearized in order to obtain a smoother temperature gradient that is less affected by the thermocouples uncertainties introduced before.

In order to have a better understanding of the difference between the two cases in *Figure 3.9*, *3.10* and *3.11* are plotted the values listed in the *Table 6* and *Table 7*.

The copper blocks are thus affected by the presence of the insulation material. After this step of the module test system set up process, it is eventually possible to place the thermoelectric converter in order to get data about its current and voltage outputs and in different environmental conditions.

As a consequence it will be also possible to see what kind of behavior characterize the heat flow across the pillar elements before and after the introduction of the TEG, and, in case, which are the possible parameters that could affect a correct data acquisition.

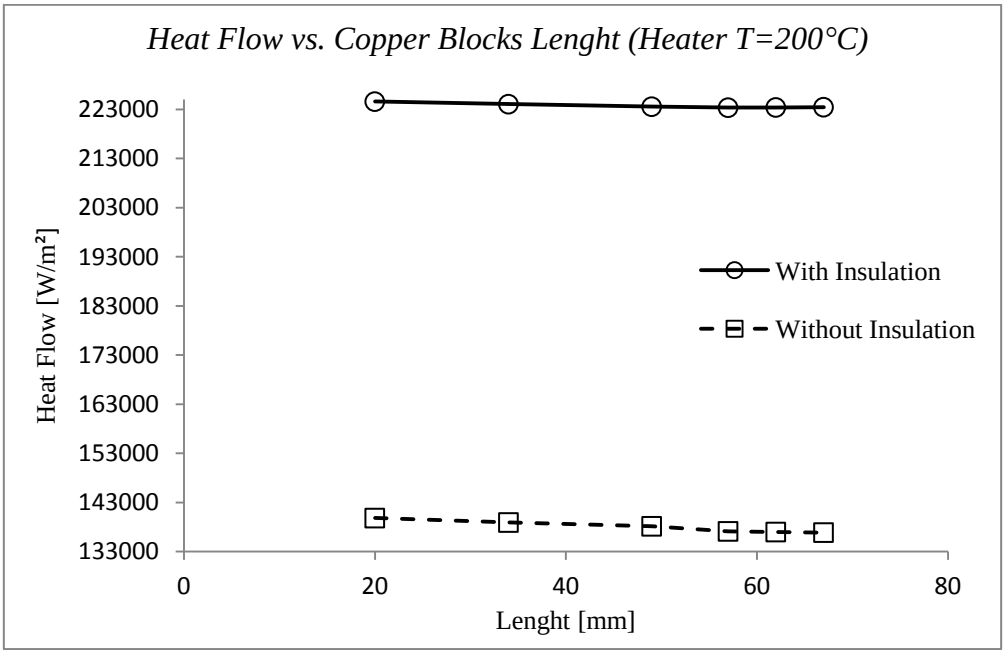

Figure 3.9

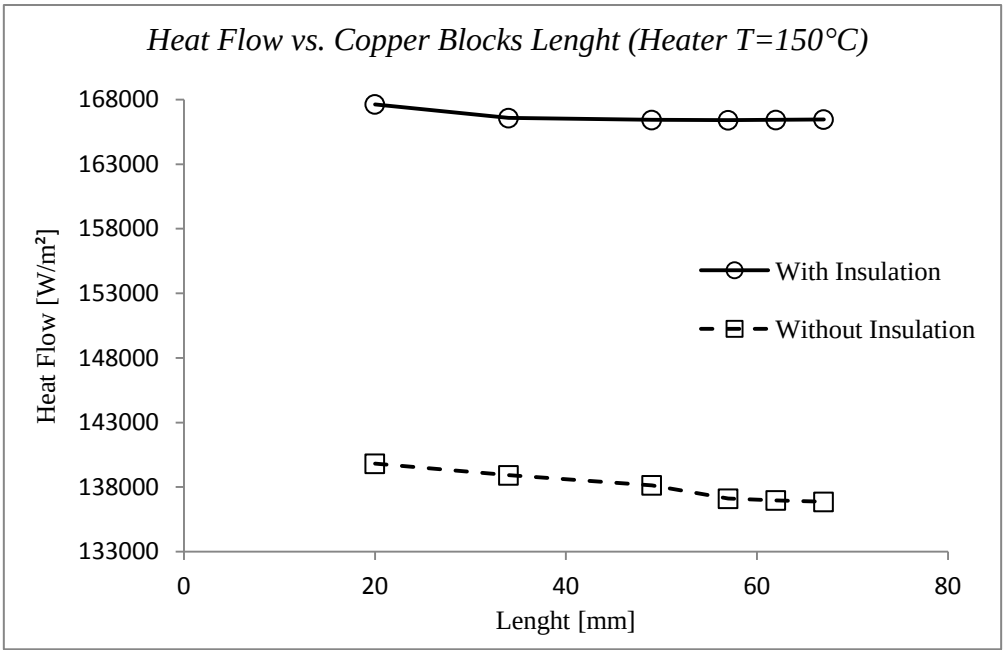

Figure 3.10

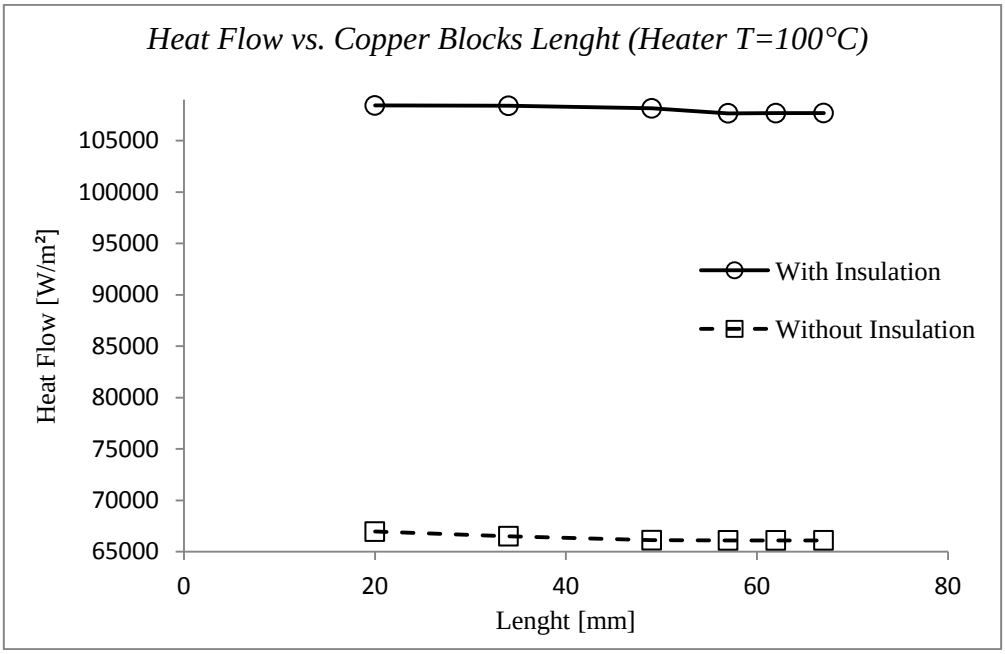

Figure 3.11

4

Numerical Models and Comparisons with Experimental Results

4.1 Introduction

In the following chapter a numerical model will be implemented in order to have a comparison background that validate the experimental results.

In this thesis work the data acquisition process has been carried out by a step-by-step pattern in which each step can be compared to a numerical model that is in charge of the theoretical reliability of the whole process. This model has been implemented on the Comsol Multiphysics software that can provide an excellent understanding of the thermal properties of the materials we are considering for the module test system working operations.

In the case of the copper blocks, as it will be shown in the next paragraphs, all the material properties are available as to be used as an input to the Comsol material section. Starting from this considerations and once a geometrical model that reflects the identical sizes of the pillar elements has been implemented, the software will be able to reproduce what theoretically are the temperature gradients and the heat flows throughout the blocks.

It will be possible to understand how the results acquired in the previous chapter about copper thermodynamic properties differs from the conditions imposed in the numerical analysis. After an introduction about how the Comsol models work and what are the steps involved in their implementation, there will be thus shown the comparisons between the temperature and heat fluxes plots introduced in the 3rd chapter and the ones related to the numerical results.

It is also important to understand that these Comsol models will be also very important in the following steps of the experimental process, where the TEG module will be inserted in the pillar thus changing the temperature field that the thermocouples detected when the copper blocks where in contact with each other.

4.2 Computational Model

4.2.1 Introduction to Comsol Multiphysics

In this thesis work an important aspect of the thermoelectric modules characterization is the possibility to compare the results with a numerical model. The software used for this purpose is Comsol Multiphysics.

There are different physical models that can be used in order to study the phenomena responsible for a determined experiment. In the case of the thermoelectric effects, if we consider the single module, both an electrical and thermal components are involved in a real working condition. However, considering the experimental process we are carrying forward, the physical properties we want to focus on are those referred to the heat conduction.

The module test system, in its main aspect, it's composed by a pillar of elements where the heat conductive blocks behavior affect the TEG output parameters. In this way it is important to implement a numerical model that reflects both geometrically and physically, the behavior of these elements.

Accordingly to this considerations, the physical model chosen for the Comsol models is the one relative to the only heat conduction in a steady-state analysis. Using this model it will be possible to introduce most of the parameters that are involved in a heat conduction process along blocks that are in contact with each other. In fact, since the experimental temperatures, the thermal properties and the environmental conditions of the experiments are already known, properties such as surface emissivities and heat transfer coefficients can be adjusted in order to get the closest results to the experimental analysis.

As regarding the material properties, Comsol Multiphysics provides a materials library were are listed the principal materials that are used for different kind of experimental processes. At the same time it is also possible to introduce a new material and characterize it with the properties that, in our case, have been already calculated, such as the thermal conductivities and the specific heat. Since these properties are a function of the temperature, it is also possible to introduce, in the numerical model, the variables calculated for the material, in our case copper. The same process has been used for the insulation material (vermiculite) which values were taken from reference datasheets.

The software allows also the post processing data evaluation, during which it will be possible to obtain 1D and 2D plots of the temperature distribution and the heat flow rate.

Moreover, the user-friendly configuration that characterize the Comsol models, allow to import changes on the different parameters and geometries in a fast way that helps to understand how much the experimental results differs from the theoretical expected ones.

Since in the previous chapter two different cases has been introduced (the insulated one and the non-insulated one), accordingly two numerical models will be implemented to depict the working conditions of the copper blocks.

4.2.2 Models Preparation

The first step in the models preparation is the choice of the physical conditions that will characterize the working conditions. Comsol software provides us different ways of starting the simulation. In our case we choose "heat transfer in solids" in a steady state analysis as explained in the previous paragraph. A range of the possible options given by the software is showed in *Figure 4.1* below.

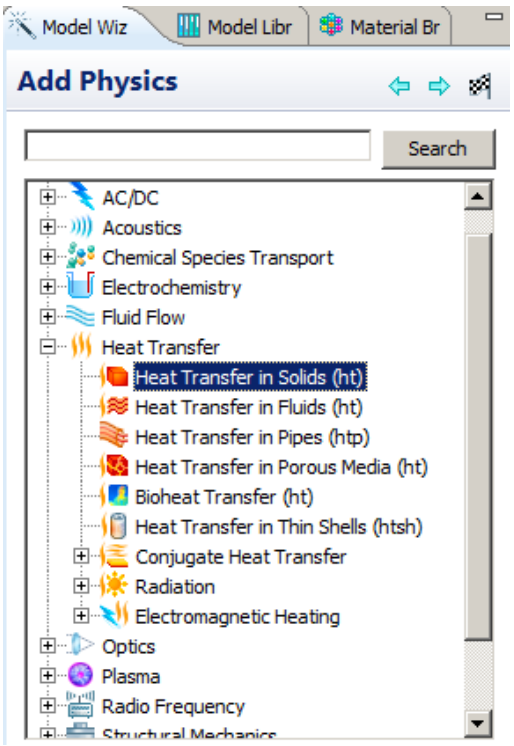

Figure 4.1

After the physical model has been chosen the process involves the 3D modeling of the copper blocks. In our case we already know the geometrical specifications of the two blocks that are *30x30x55 mm* and *30x30x20 mm*. Considering the case without insulation, the

resulting model can be seen in *Figure 4.2*. The two blocks now form the two domain of our numerical model.

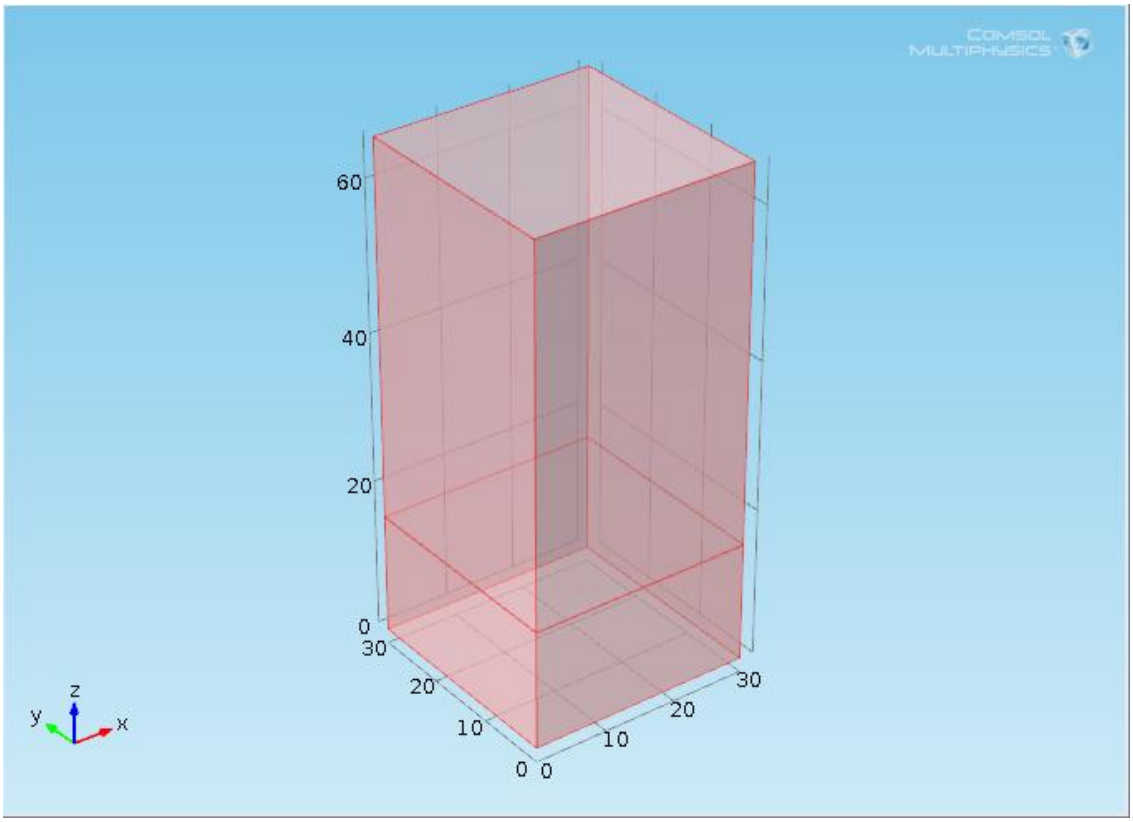

Figure 4.2

It is also possible to notice that the two main blocks are in contact with each other, while in the TEG characterization there will be interposed the thermoelectric converter between them.

However, since the model needs to follow the experimental results, the geometrical dimensions are respected except for the blocks height. In fact we are going to use the temperatures values that the first and the last thermocouples along the blocks detect, as input parameters to start the numerical analysis. This results in a Comsol model shorter than the real one, but both in the experimental part and in the computational one the heat flows and the temperature gradients are calculated along the same length of the blocks. This is why the thermocouples are not placed exactly on the top and the bottom surfaces of the pillar, mainly for hardware characteristics that impose a certain configuration. Besides, the most important parameters we want to study are the hot side and cold side temperature of the TEG, and, in this case, the thermocouples are placed as close as possible to the thermoelectric module surfaces.

Once the geometrical part has been set, the model needs to know which materials are part of the domains. In our case we are considering copper for both the upper block and the

bottom one. After chosing from the material library the copper as a domain material, the software will show a list of properties, adjustable, like the one showed in *Table 1*.

	Property	Name	Value	Unit	Property group
✓	Heat capacity at constant pressure	Cp	cpCu(T)	J/(kg·K)	Basic
✓	Density	rho	8950[kg/m^3]	kg/m³	Basic
✓	Thermal conductivity	k	thermalCond(T)	W/(m·K)	Basic
	Relative permeability	mur	1	1	Basic
	Electrical conductivity	sigma	5.998e7[S/m]	S/m	Basic
	Coefficient of thermal expansion	alpha	17e-6[1/K]	1/K	Basic
	Relative permittivity	epsilonr	1	1	Basic
	Young's modulus	E	110e9[Pa]	Pa	Young's modulus and Poisson's ratio
	Poisson's ratio	nu	0.35	1	Young's modulus and Poisson's ratio
	Reference resistivity	rho0	1.72e-8[ohm...	Ω·m	Linearized resistivity

Table 1

It is possible to notice that the values of thermal conductivity and heat capacity at constant pressure are not expressed as a constant but as a function of the temperature (T). This is why it is possible to introduce in the model the values of the thermal properties previously calculated with the laser flash method (chapter 3).

The last step of the model preparation is the meshing of the domain. This can be done automatically by the software and we can choose which number of elements we want to divide the domain in. The result of the mesh can be seen in *Figure 4.3*.

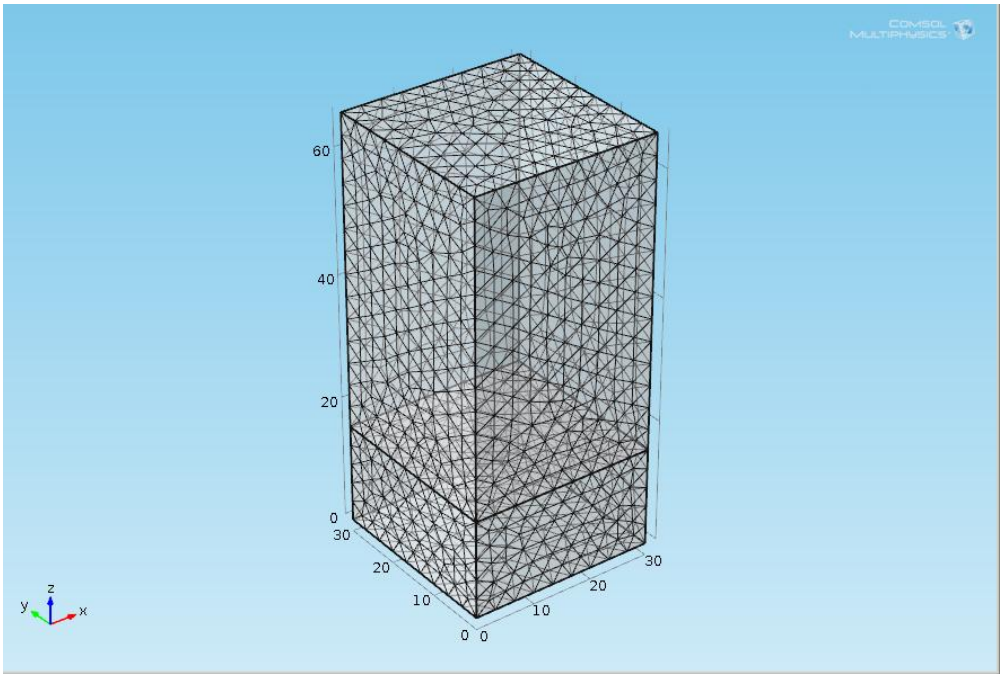

Figure 4.3

The module we implemented in this case is referred to the blocks without insulation material. For the insulated case, the process is the same, but in this case to the previous geometry of the copper blocks we are going to add the insulation material geometry. For the vermiculite (the insulation material) the geometrical dimensions are considered as they fit perfectly the copper blocks ones. Consequently we will have a geometrical block that surrounds the copper blocks with the same height and width previously measured of *26 mm* from the copper block surface. The configuration can be observed in *Figure 4.4*.

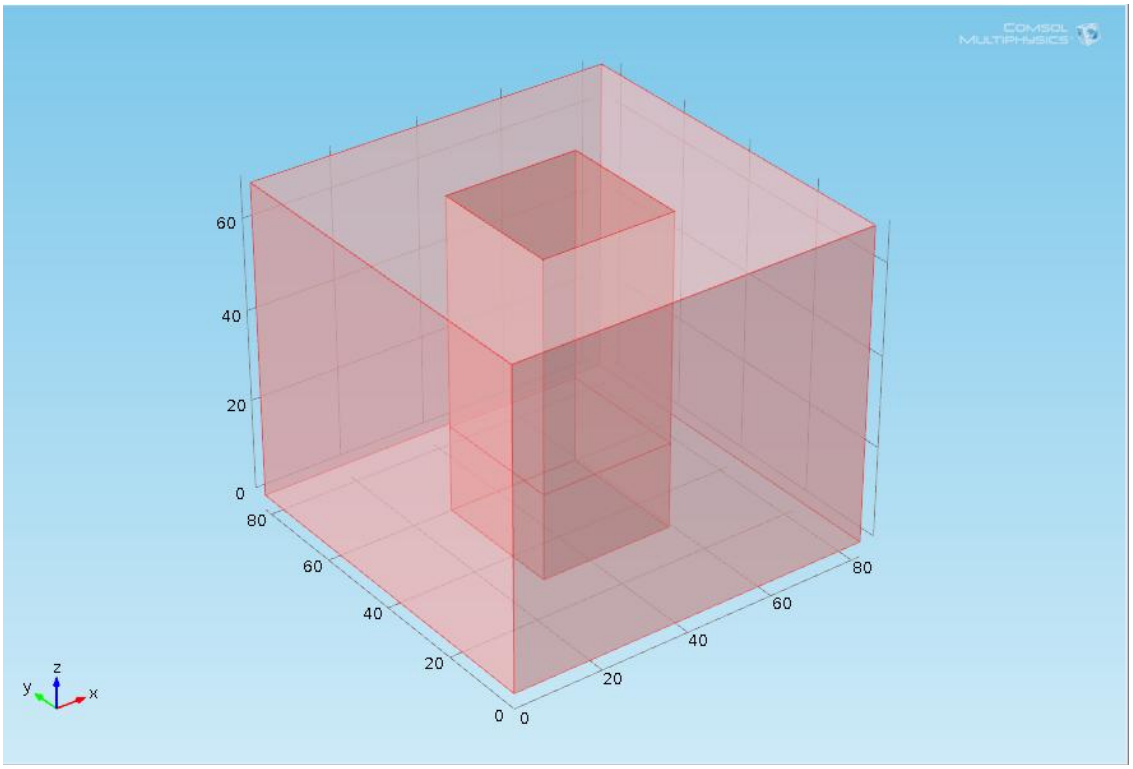

Figure 4.4

The vermiculite is not present in the material library of the software, so a new material window has been introduced with the thermal conductivities data and other values taken from a reference datasheet. The process of meshing is the same considered for the case without insulation.

Once the two modules are ready, the last part to complete before running the simulation is the introduction of the physical conditions that characterize the system domains. In both the simulation model cases we have in fact to specify which are the surfaces subjected to the convective cooling, the emissivity radiation and the temperatures values that, as specified before, refer as an input to the numerical model. The temperatures input is provided by the experimental results and it changes as the heater temperature change. For different steps of temperature, therefore, there will be different temperatures input. In this way, once the model will be run, it will be possible to see how much the heat conduction behavior of the

copper blocks differs from the experimental data. As regarding the convective cooling we have select the surfaces that are in contact with the outside environment (vermiculite external surfaces in case of insulation and external copper blocks surfaces in the case of no insulation), and insert as an input the values of what external fluid is considered (air), at which pressure (environment pressure) and at which temperature (room temperature). Considering the emissivity radiation, we have to introduce the value of the surface emissivity of the external surfaces as well as the external temperature (room temperature). The surface emissivity of both the copper and the vermiculite is taken from reference datasheets.

Another important aspect of the module preparation is the characterization of the thermal contact between the two copper blocks. In our case we will use an option available in the Comsol section of the heat transfer in solids, the thermally resistive layer. This layer is important in our study since the temperature distribution undergoes to a sensible deviation along the surfaces contact point. Therefore it is possible to set the thickness and the thermal conductivity of the layer in order to make the comparison with the experimental results as realistic as the working conditions imposed by the module test system. The thermally resistive layer is also the element most subjected to a change of the thermal properties since, compared to the convective cooling and the radiation losses where their parameters values are fixed as the temperature steps change, it depends on how good is the contact between the surfaces. Accordingly to this considerations, while in the experimental process the contact between the surfaces tends to be influenced by the manual operations, this changes are depicted in the simulation process by the thermally resistive layer.

After the last step of the characterization of the domain physical properties the models are ready to be run. For each step of the heater temperature will be thus given two different values of temperature to be introduced in the model in order to get the simulation results. Obviously all the parameters and the values introduced are adjustable in order to avoid possible not realistic solutions or singularities that can affect the models.

4.3 Temperature Comparisons

The first step involved after the Comsol models set up, is the comparison between the simulation results and the experimental ones. This step is important to understand how much the thermodynamic behavior of the copper blocks differs from a theoretical condition.

As also introduced in the previous paragraph, the input data to insert in the computational model before running the software, are the temperature values of the first and the last thermocouples located on the top and the bottom holes, respectively, along the copper blocks. Once the input data are inserted in the model, it is possible to run the software.

Both for the case without insulation and with insulation, the results that Comsol gives can be studied using different instruments. It is in fact possible to study 3D plots of the temperature distribution that is shown using different colors in relation to its intensity as well as the heat flow. The software also allow to obtain 1D plots and 2D plots after choosing an intersection plane or line.

4.3.1 Temperature Comparisons for Copper Blocks Without Insulation

In this case, as well in the insulated one, we are considering four temperature steps that the heater is going to impose to the pillar. As a consequence we will have four different comparison plots that we can analyze.

The first step of the heater temperature is 200°C and the results obtained from the experimental data, gives us as input temperatures T1=78,63°C (first thermocouple below the heater) and T8=33,34°C (last thermocouple right above the cooler plate). We can use these two values in the Comsol model for the copper blocks without insulation. A 3D plot of the simulation results can be seen in *Figure 4.4.*

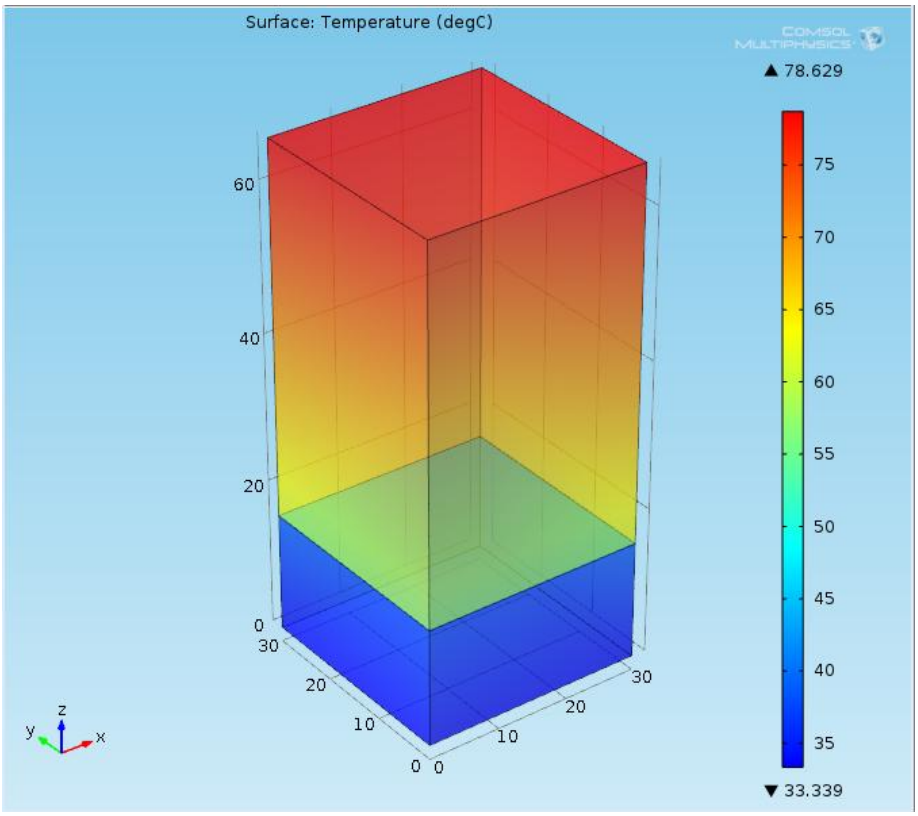

Figure 4.4

The intensity of the temperature, in the figure above, degrades from a red color for higher values, to a blue color for lower ones. The same 3D plots can be obtained for the other

temperatures steps. It is evident how the contact layer between the two blocks has an important role in the temperature distribution, since it divides in a clear way a region with high values of temperature from a region with lower ones. However, even if a complete tridimensional plot can show in a good way the temperature distribution, in this case it is better to analyze the one dimensional plot for an intersection line that cross the geometrical center of the pillar from the top surface to the bottom one.

In *Table 2* (a, b, c, d) are listed the comparison values between the experimental data and the Comsol model ones. These values are considered, for the computational model, in the same position on which the thermocouples detect the temperatures in the module test system (about 15mm inside the block, that can be considered the geometrical center).

Table 2

Heater Temperature 200 °C		
Thermocouples	T exp [°C]	T Comsol [°C]
T1	78,6	78,6
T2	72,3	72,0
T3	68,0	67,2
T4	62,3	62,2
T5	38,0	38,0
T6	36,3	36,3
T7	35,0	34,7
T8	33,3	33,3

a)

Heater Temperature 150 °C		
Thermocouples	T exp [°C]	T Comsol [°C]
T1	61,1	61,1
T2	56,4	56,2
T3	53,2	52,8
T4	49,0	49,1
T5	31,2	31,2
T6	30,0	30,0
T7	29,0	28,8
T8	27,8	27,8

b)

Heater Temperature 100 °C		
Thermocouples	T exp [°C]	T Comsol [°C]
T1	44,0	44,0
T2	41,0	40,9
T3	38,9	38,7
T4	36,2	36,3
T5	25,0	24,8
T6	24,1	24,1
T7	23,5	23,3
T8	22,6	22,6

c)

Heater Temperature 50 °C		
Thermocouples	T exp [°C]	T Comsol [°C]
T1	26,4	26,4
T2	25,1	25,0
T3	24,2	24,1
T4	22,9	23,0
T5	18,0	17,8
T6	17,6	17,5
T7	17,3	17,2
T8	16,9	16,9

d)

From the temperature values showed above it is possible to see that the experimental data are very similar to the theoretical ones related to the Comsol Multiphysics model. Therefore

we can say that the working conditions of the module test system are reliable since they depicts in a good way what has been considered as a theoretical model.

In *Figure 4.5, Figure 4.6, Figure 4.7 and Figure 4.8* it is even more clear the similarity between the experimental and the simulation results.

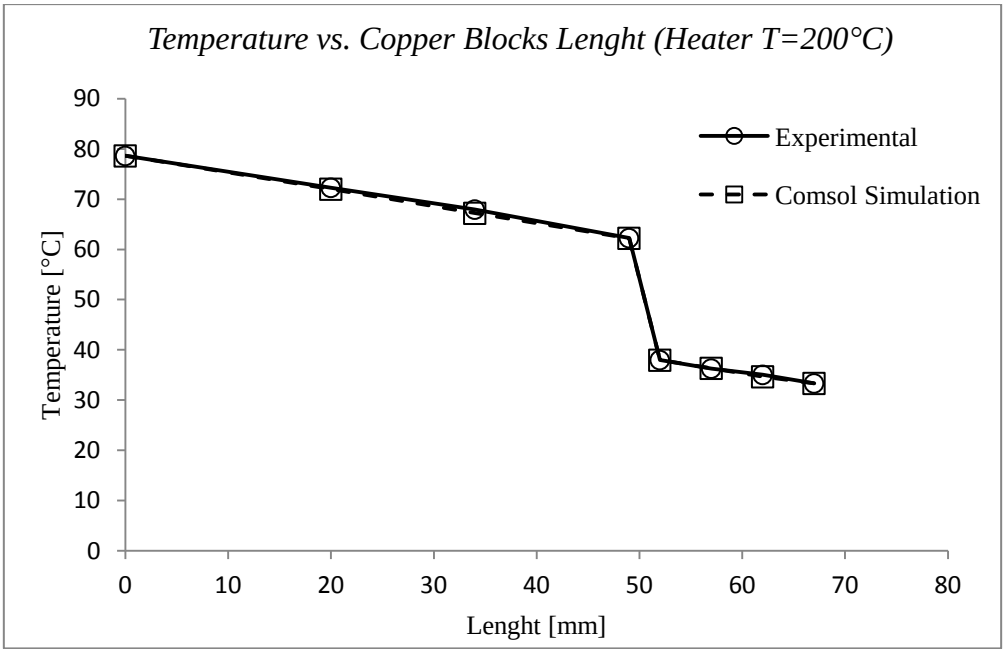

Figure 4.5

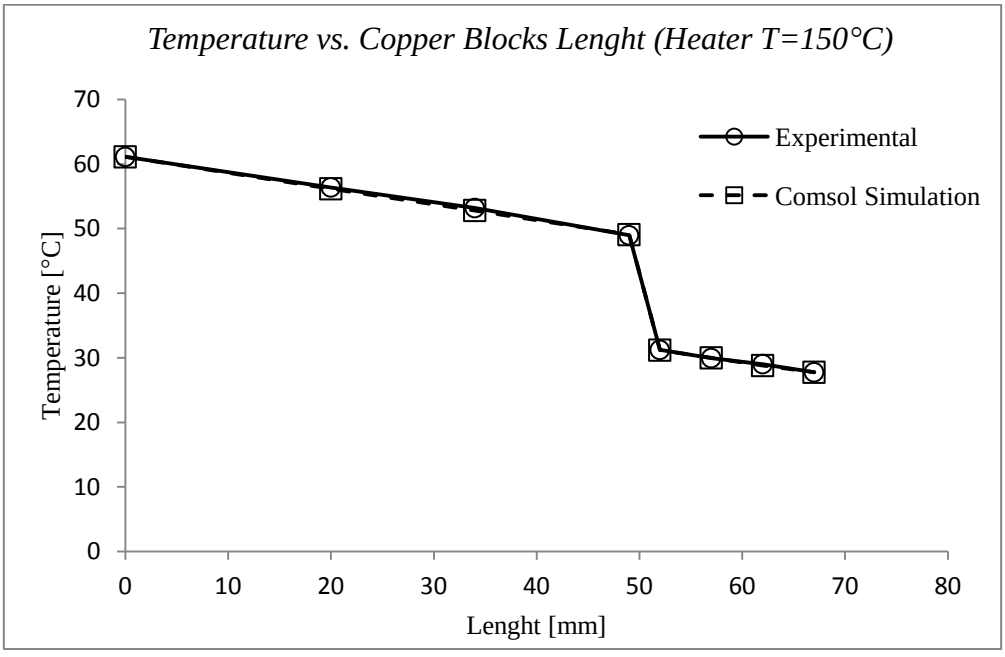

Figure 4.6

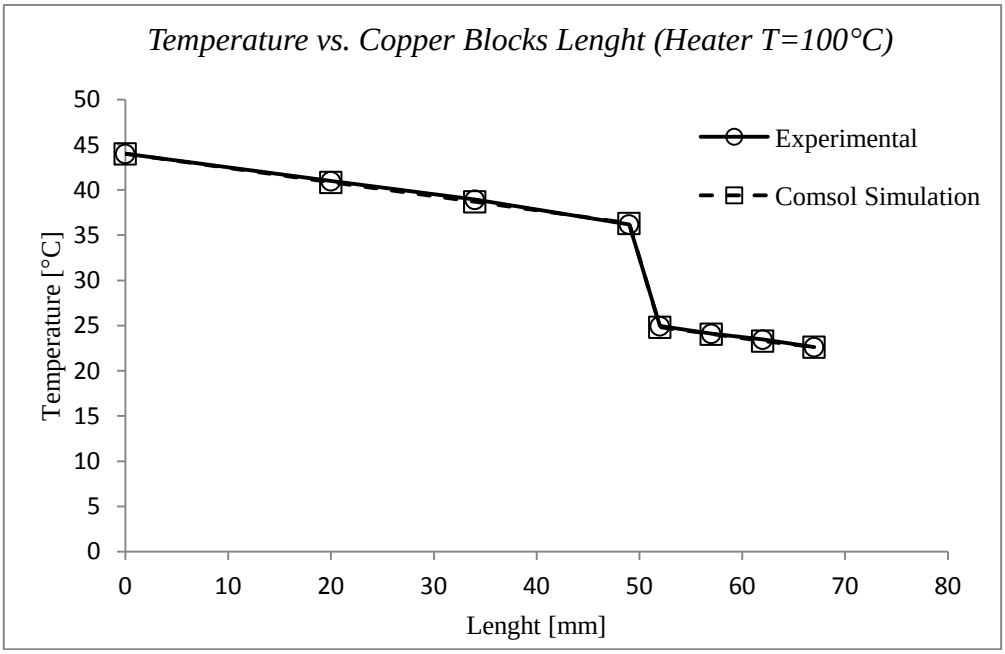

Figure 4.7

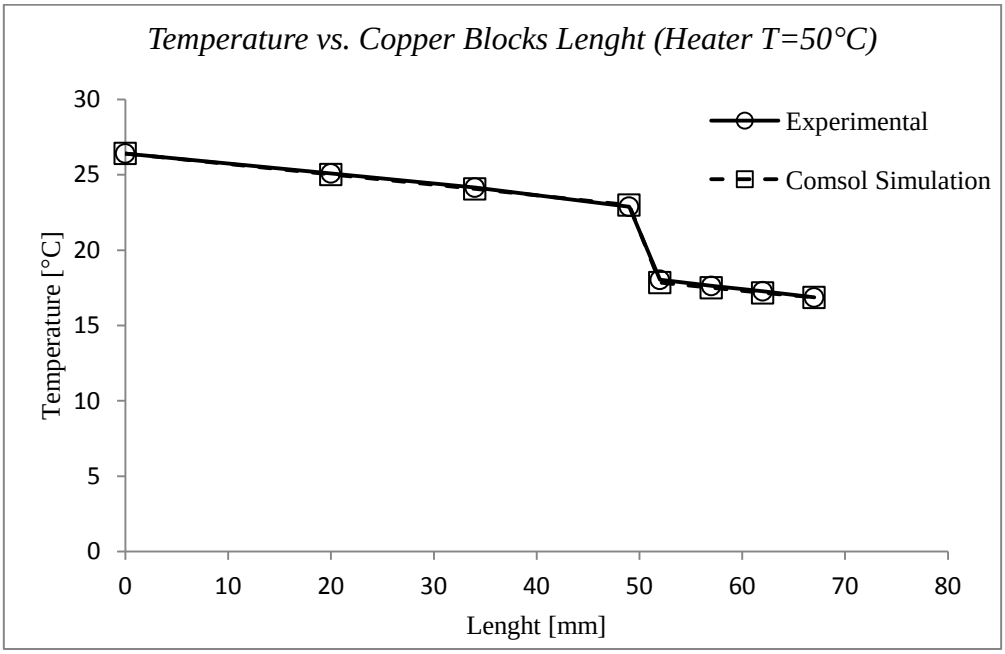

Figure 4.8

4.3.2 Temperature Comparisons for Insulated Copper Blocks

In the case of the insulated pillar, the temperatures values we are going to obtain with the module test system are higher than the case without insulation. Also in this case we can observe a 3D plot for the temperature distribution, referring to the first heater temperature step at 200°C. In *Figure 4.9* it is noticeable the thermal insulator that provides a inhibition

toward the convective cooling and the radiation contribution of copper that otherwise would affect the heat conduction along the pillar in a more evident way.

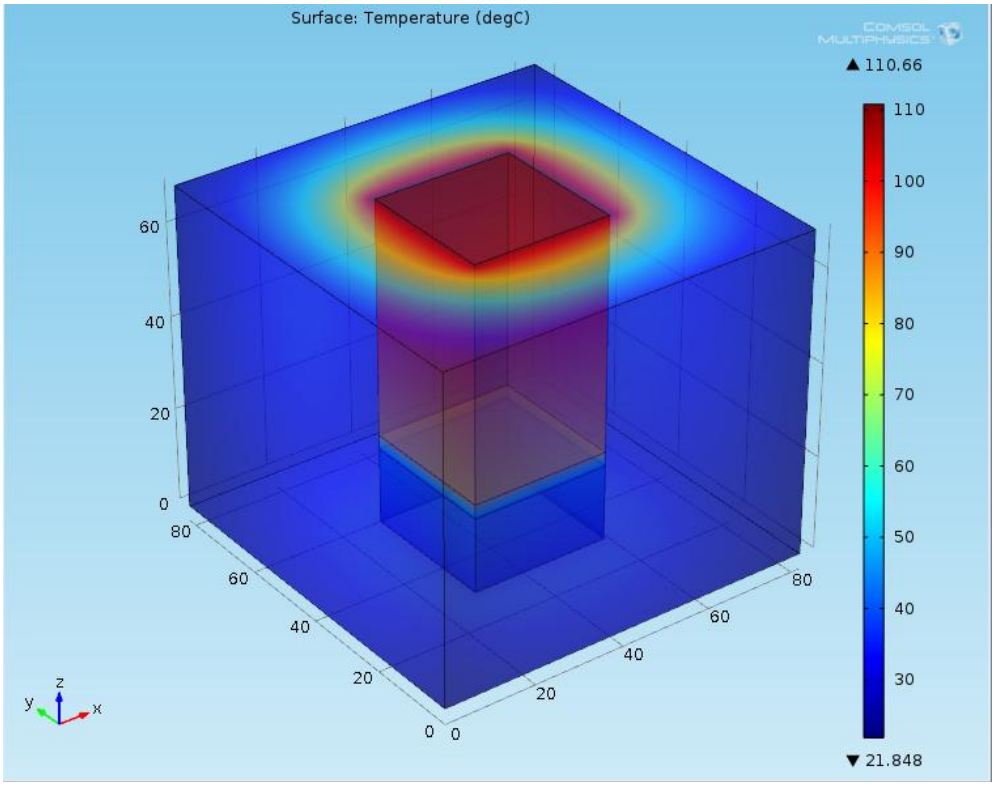

Figure 4.9

As showed in the case without insulation, in *Table 3* (a, b, c, d) are listed the temperature data comparisons between the experimental results and the computational model for the insulated copper blocks.

Table 3

Heater Temperature 200 °C		
Thermocouples	T exp [°C]	T Comsol [°C]
T1	110,7	110,7
T2	99,2	100,0
T3	91,9	92,7
T4	84,5	84,5
T5	41,5	42,9
T6	39,3	40,3
T7	37,0	37,7
T8	34,9	34,9

a)

Heater Temperature 150 °C		
Thermocouples	T exp [°C]	T Comsol [°C]
T1	85,6	85,6
T2	77,2	77,6
T3	72,0	72,2
T4	66,6	66,1
T5	33,8	35,0
T6	32,2	33,1
T7	30,5	31,1
T8	29,1	29,1

b)

Heater Temperature 100 °C		
Thermocouples	T exp [°C]	T Comsol [°C]
T1	60,1	60,1
T2	54,9	55,0
T3	51,6	51,5
T4	48,2	47,6
T5	26,6	27,4
T6	25,6	26,2
T7	24,4	24,9
T8	23,6	23,6

c)

Heater Temperature 50 °C		
Thermocouples	T exp [°C]	T Comsol [°C]
T1	33,5	33,5
T2	31,4	31,4
T3	30,0	29,9
T4	28,5	28,2
T5	19,4	19,7
T6	19,0	19,2
T7	18,4	18,7
T8	18,1	18,1

d)

Also in the insulated case, as it is shown in the tables above, what the theoretical model depicts it's a close similarity to the experimental values. This condition it's even more underlined considering *Figure 4.10, 4.11, 4.12, 4.13.*

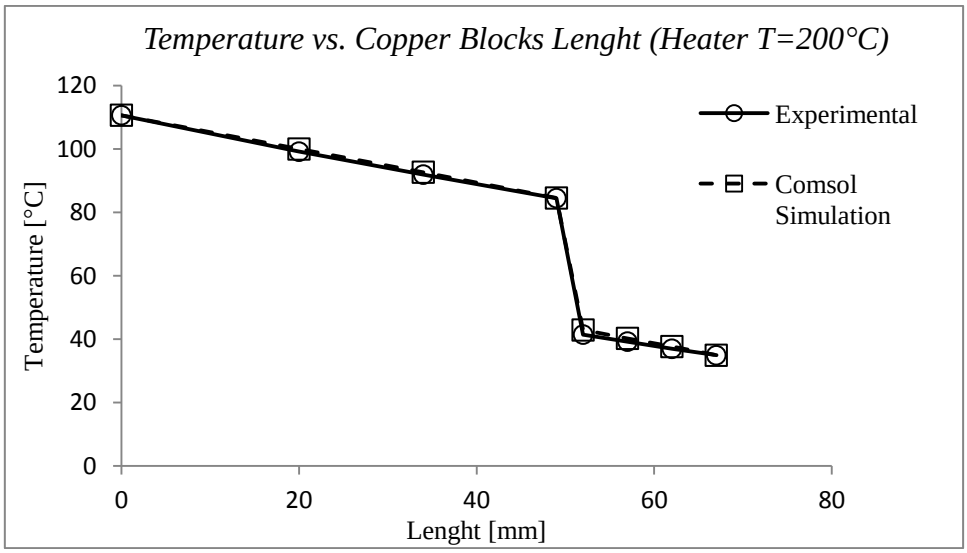

Figure 4.10

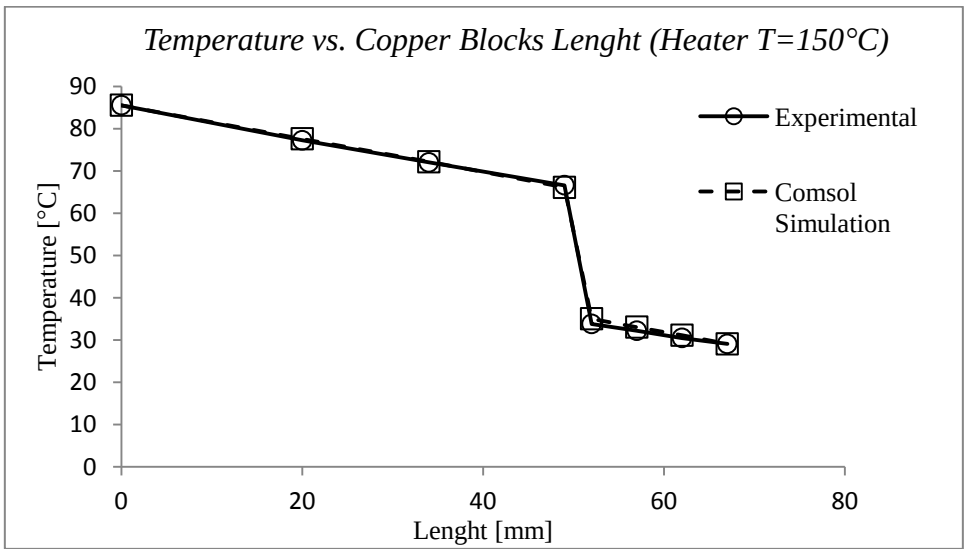

Figure 4.11

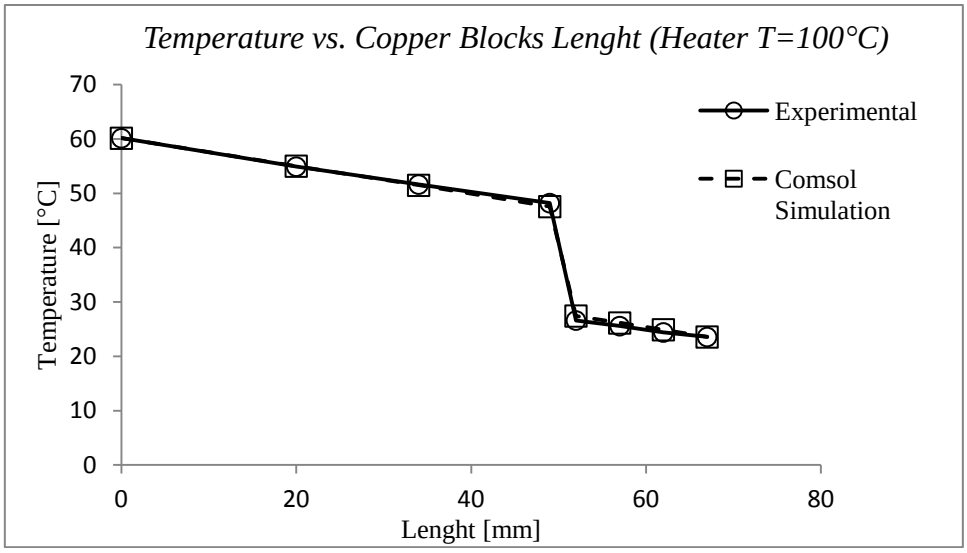

Figure 4.12

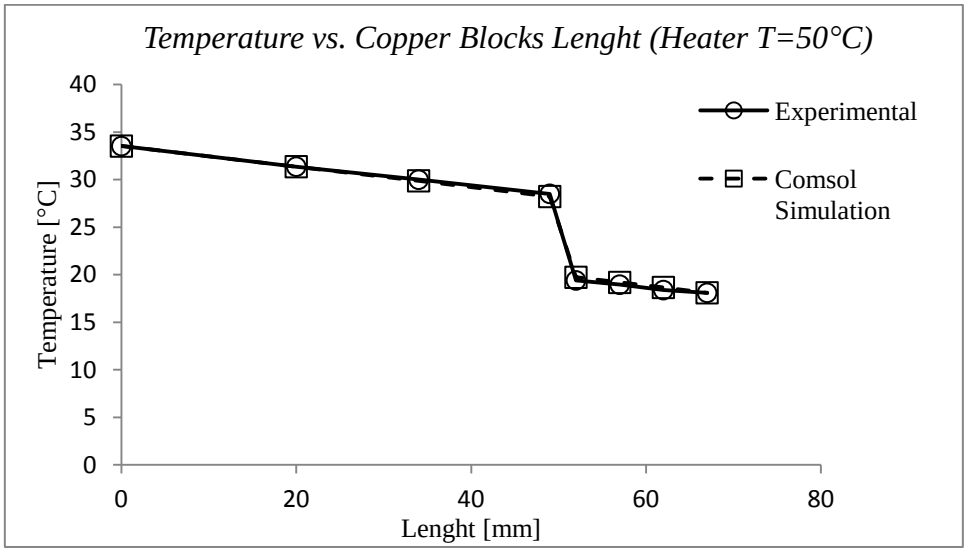

Figure 4.13

4.4 Heat Fluxes Comparisons

In the validation process that involves the data comparisons, the heat fluxes have an important role. After the acquisition of the temperature distributions for different steps of the heater conditions, it is thus possible to calculate the heat flows along the copper blocks and compare them with the numerical models. Through this way of procedure, when the TEG modules will be inserted in the pillar, it will be noticeable how the presence of a thermoelectric converter affect the heat conduction in the module test system. In our case the experimental heat flows calculations have been obtained using the Fourier Law (as showed in the 3.4 paragraph) while the Comsol software uses its own computational method. However, also in this measurement step, the heat flows calculated using the module

test system are quite similar to the one calculated through the simulation models. This can let us say that our measurement are reliable and they can be used in the following phase of thermoelectric module characterization.

4.4.1 Heat Fluxes Comparisons for Copper Blocks Without Insulation

In the case of the copper blocks under working condition without a surrounding insulation material, the comparisons between experimental and computational results are listed in the *Table 4* (a, b, c, d) below.

Table 4

Heater Temperature 200 °C		
Lenght [mm]	Heat Flow Exp [W/m²]	Heat Flow Comsol [W/m²]
20	139811,3	141964,8
34	138913,2	140813,9
49	138142,1	139741,5
56	137103,8	139530,5
61	136973,4	139455,5
66	136858,6	139448,8

a)

Heater Temperature 150 °C		
Lenght [mm]	Heat Flow Exp [W/m²]	Heat Flow Comsol [W/m²]
20	103916,7	104455,0
34	103237,5	103752,3
49	102652,8	103049,2
56	102479,2	102922,8
61	102468,9	102885,0
66	102448,2	102872,4

b)

Heater Temperature 100 °C		
Lenght [mm]	Heat Flow Exp [W/m²]	Heat Flow Comsol [W/m²]
20	66952,0	66852,8
34	66506,9	66489,7
49	66115,4	66130,9
56	66097,5	66076,0
61	66097,5	66061,9
66	66104,9	66057,3

c)

Heater Temperature 50 °C		
Lenght [mm]	Heat Flow Exp [W/m²]	Heat Flow Comsol [W/m²]
20	29577,0	29763,3
34	29477,6	29696,4
49	29345,1	29638,6
56	29316,8	29638,3
61	29314,8	29646,7
66	29299,1	29653,5

d)

From table a) to d) it is clear that the heat fluxes values are very similar for the Comsol model and the experimental results. Moreover, the heat flow comparisons can be plotted as shown in *Figure 4.14, 4.15, 4.16.*

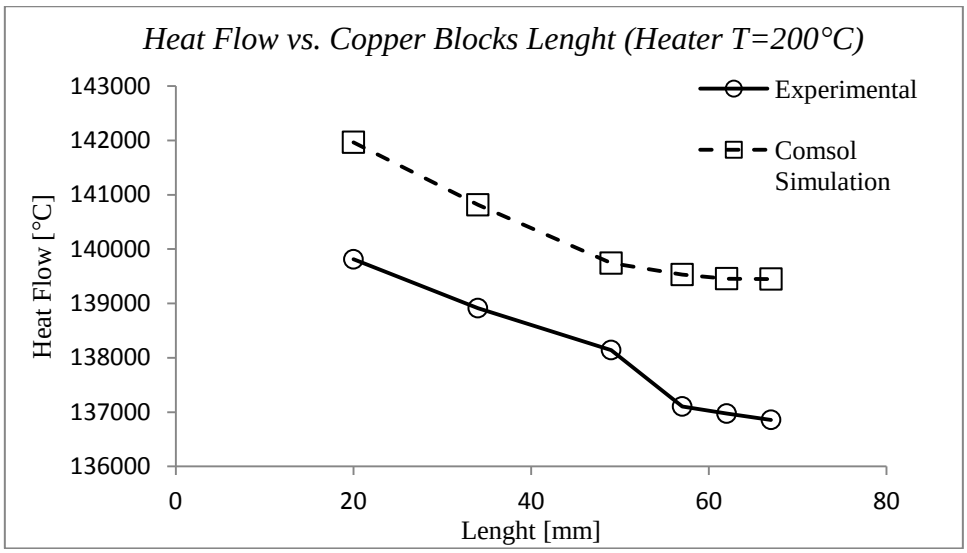

Figure 4.14

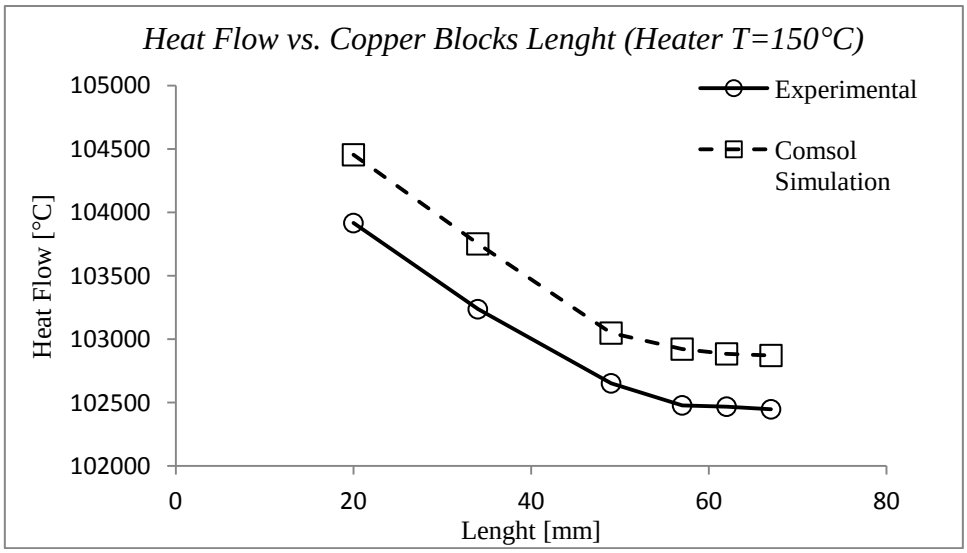

Figure 4.15

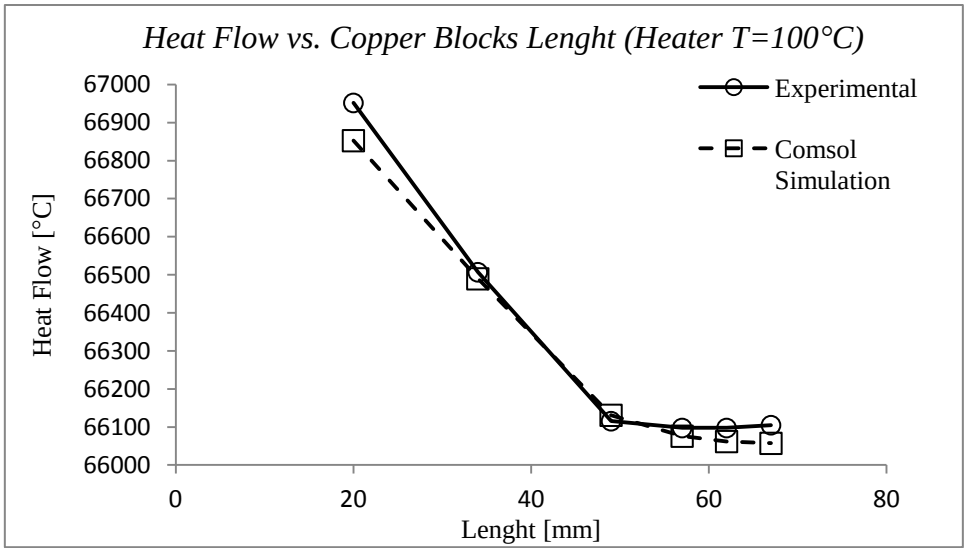

Figure 4.16

4.4.2 Heat Fluxes Comparisons for Insulated Copper Blocks

For the copper blocks surrounded by the insulation material, the compared results are listed in *Table 5* (a, b, c, d) below.

Table 5

Heater Temperature 200 °C		
Lenght [mm]	Heat Flow Exp [W/m²]	Heat Flow Comsol [W/m²]
20	224568,3	224258,3
34	224046,5	223801,2
49	223533,6	223088,1
56	223333,5	223155,8
61	223383,4	223223,3
66	223433,4	223247,3

a)

Heater Temperature 150 °C		
Lenght [mm]	Heat Flow Exp [W/m²]	Heat Flow Comsol [W/m²]
20	167636,0	167313,2
34	166574,3	166982,5
49	166424,8	166465,0
56	166407,5	166521,3
61	166426,1	166574,5
66	166463,3	166593,7

b)

Heater Temperature 100 °C		
Lenght [mm]	Heat Flow Exp [W/m²]	Heat Flow Comsol [W/m²]
20	108430,8	108374,8
34	108397,9	108174,6
49	108148,6	107855,2
56	107670,2	107897,9
61	107682,3	107935,5
66	107694,3	107949,4

c)

Heater Temperature 50 °C		
Lenght [mm]	Heat Flow Exp [W/m²]	Heat Flow Comsol [W/m²]
20	45642,4	45674,5
34	45652,6	45608,9
49	45498,0	45495,7
56	45492,1	45522,2
61	45497,2	45542,5
66	45497,2	45550,2

d)

Also in the insulated case we can see a close similarity between experimental and simulation data, as it is also possible to see in *Figure 4.17*, *Figure 4.18* and *Figure 4.19*.

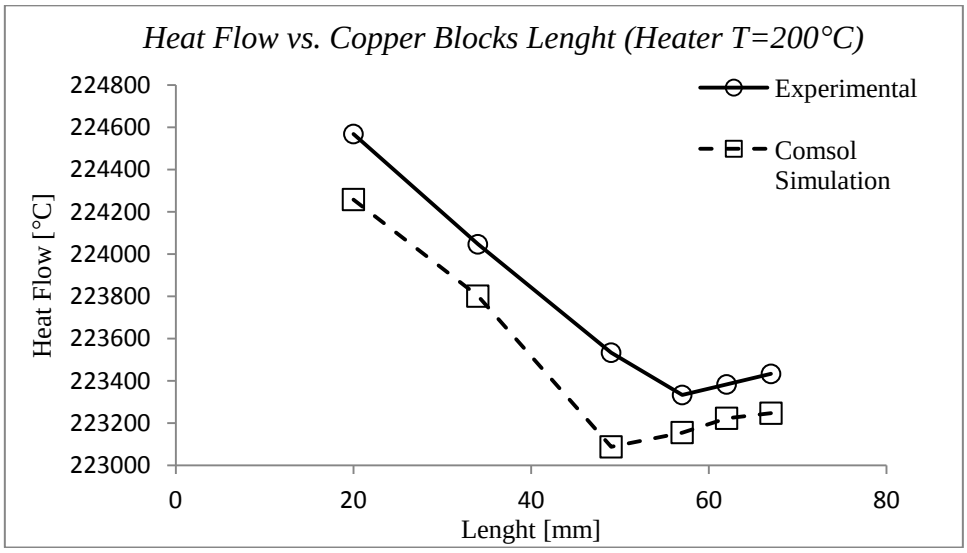

Figure 4.17

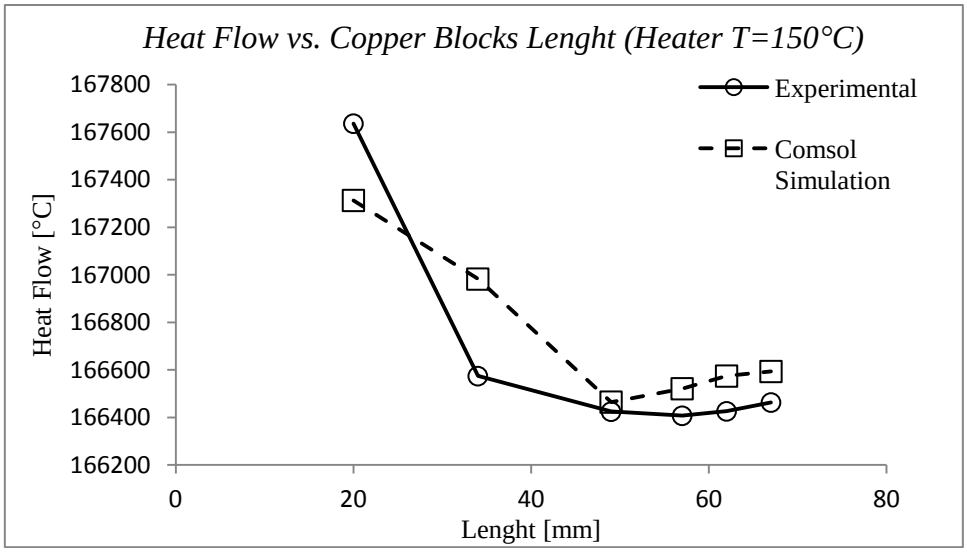

Figure 4.18

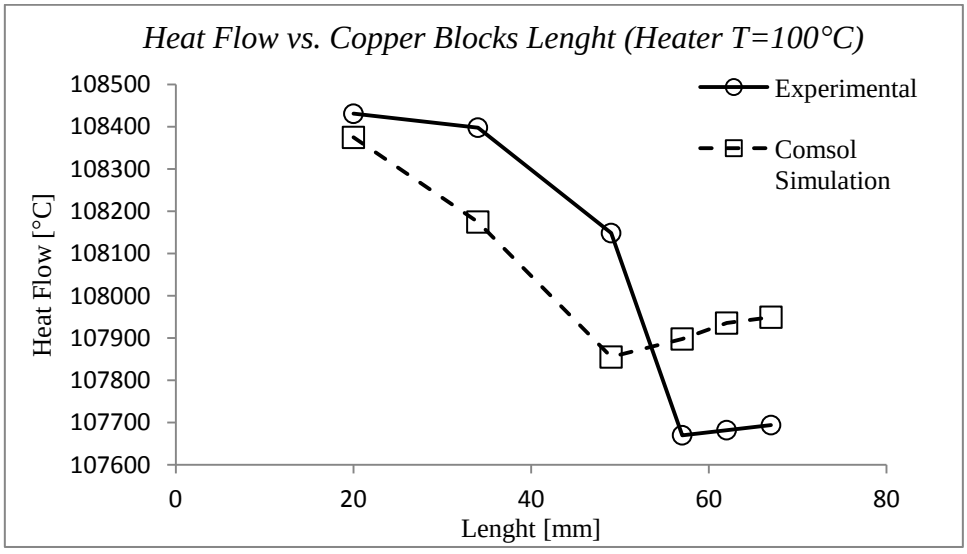

Figure 4.19

5

Thermoelectric Module Characterization

5.1 Introduction

In the previous chapters all the results and the measurements that have been carried forward were both a validation and a background support of the thermoelectric modules characterization.

In the Department of Energy Conversion and Storage of DTU, Technical University of Denmark, Riso Campus, it is available a module test system that is responsible for the acquisition of the output parameters of the TEGs. After the process that involves the test system setup and the analysis of the comparisons between the experimental and the simulation results, lastly thermoelectric converters will be inserted in the pillar were the copper blocks are positioned.

In the next paragraphs will be introduced what kind of commercial thermoelectric module has been used in order to extrapolate data that will be later used to obtain the efficiencies and the power outputs. Also in this case will be used the Comsol Multiphysics models implemented to have a mirror that helps the quantification of the reliability of the working conditions.

Besides efficiencies and power output values, will be also showed, in appropriate plots, all the other parameters that can be calculated starting from the module test system operations, such as current and voltage outputs, heat flows across the TEG and resistance loads involved.

In this chapter a single thermoelectric commercial module will be characterized, considering as well both the insulated and the not insulated cases, while results obtained

with other modules will be shown in the *Appendix* section. In this way it will be possible to show the procedure used for the characterization of one module that it will be the same also for the other commercial modules.

5.2 Thermoelectric Commercial Module for Power Generation

When the module test system is ready for the data acquisition process, it is possible to insert the thermoelectric module between the two copper blocks previously introduced. In this way the pillar that until now has been analyzed for its thermodynamic properties, is now complete in all its elements (upper weight, heater, upper copper block, thermoelectric module, bottom copper block, cooling plate). The procedure that involves the working conditions with the presence of the TEG is the same introduced in the previous chapter where the thermocouples inserted along the pillar were the main element for the temperature data acquisition.

In this case, besides the thermocouples, also the thermoelectric module has to be connected to the system in order to see the resistance loads that will be operating during the working conditions. Since the heat flow across the elements of the module test system is influenced by the contact between the different surfaces, thin graphite sheets are interposed between the copper blocks and the thermoelectric module external surfaces. In this way, considering also a good polishing of the copper, it is possible to improve the thermal contacts and provide a more efficient data acquisition.

Once the module is inserted in the system and the software has been provided with the input data, we can start the data acquisition.

In the Department of Energy Conversion and Storage of DTU, Technical University of Denmark, Riso Campus, different commercial modules were available to get used in the module test system. We are going to show the results for one out of a total of three commercial modules studied during the experimental process. The results for the two left modules can be seen in the *Appendix* section.

The TEG we are going to show the results about is a commercial one that comes from Marlow Industries an American company involved in the field of high quality standard thermoelectric converters, that was also involved in previous collaborations with the Department of Energy Conversion and Storage. It was thus available a reference datasheet were the output parameters of the Marlow commercial module are listed in order to get comparisons with the experimental data. The module, on the Marlow datasheet, is presented as a TG12-4L thermoelectric generator with the serial number 31144. In *Figure 5.1* and *Figure 5.2* are showed the Marlow TEG used in the experiments and its mechanical characteristics. It is possible to notice the wires (in blue and red colors respectively) that are in charge to connect the thermoelectric converter to the module test system. Moreover it is

evident the reduced geometrical size of the module that in the case of the height length is in the range of few millimeters. This is why is appropriate a good alignment of the copper block with the TEG in order to avoid conductive losses.

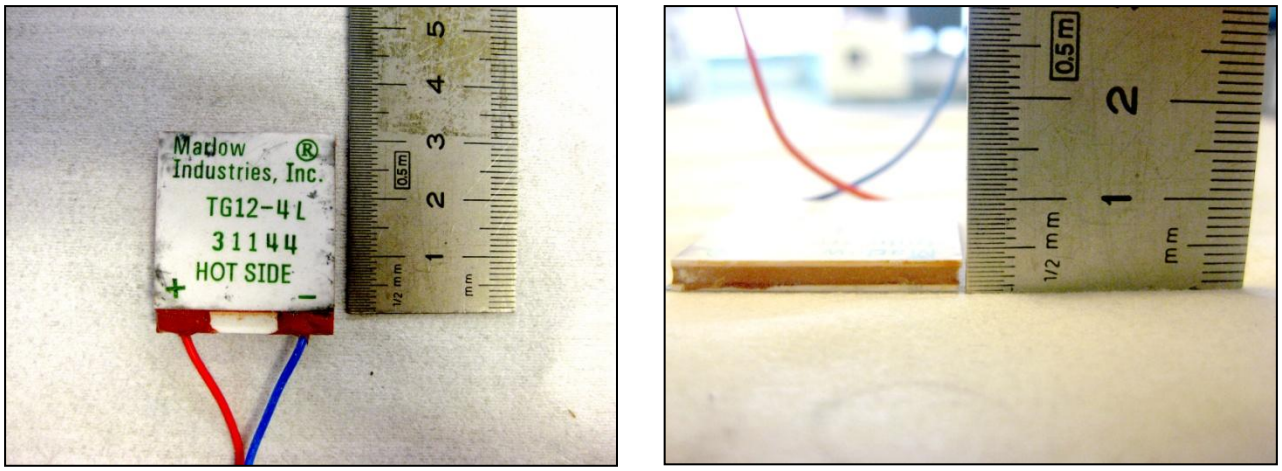

Figure 5.1

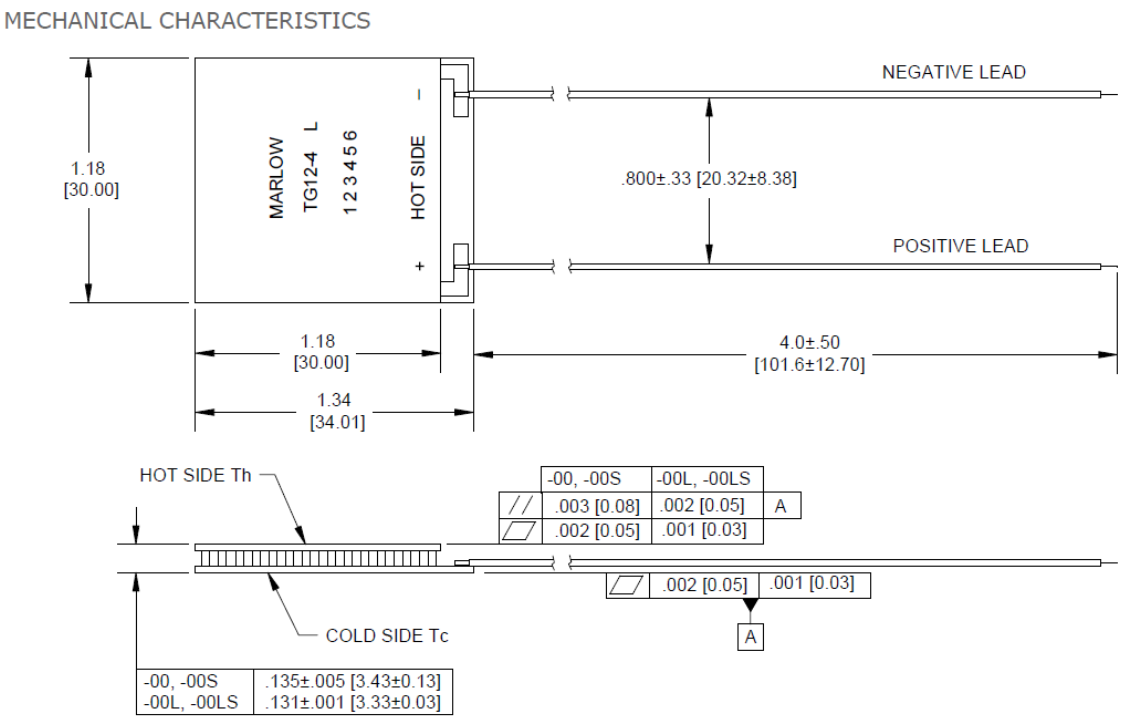

Figure 5.2

From the datasheet it is also possible to get a list of parameters such as efficiencies, power and current outputs, load resistances and heat flows that will be compared with the experimental results after the data acquisition process.

5.3 Marlow TG12-4L Module Characterization

During the working conditions, the thermoelectric module is able to release a current output when the difference of temperature between its two surfaces reaches certain values. In our case we considered, as also seen in the previous chapter, four steps of temperature imposed to the heater. The starting step is 50°C the final one is 200°C using steps of 50°C. We consider as well both cases with insulation and without insulation. The difference that the insulator brings to the data acquisition is an increasing temperature difference between the module surfaces that will result in increasing performances.

The Comsol Multiphysics models will be always take into consideration in order to compare the experimental results with what is expected from a theoretical point of view. Moreover, with the introduction of the TEG in the module test system, the changes that we have to import in the computational model are not so many. In fact, since it is important mainly to have a temperature mirror that allows to detect possible errors, it will be sufficient to change the thermal conductivity between the two copper blocks in order to simulate the presence of a solid block (the thermoelectric converter) that inhibits the heat flow. Thanks to this simulation, when the temperature trends will be reasonably close to the experimental results, the thermal conductivities resulting from the simulation will be used in the calculation of the heat flow that crosses the TEG under working conditions. This procedure thus allows an inverse process than the one used until now, in fact, since the module thermal conductivity is a parameter hard to calculate both with the hardware configuration we are using and during the normal working conditions, we take the simulation value that depicts the physical behavior of the pillar elements, and we use it in the experimental calculations.

5.3.1 Marlow Module without Insulation

The module test system is ready to start, so when the operator run the software the data acquisition begins. Consequently, the heater begins to raise the temperature, and the module starts to release an output current that is addressed to a resistance load. A rang of seven resistance steps has been taken into account in order to extrapolate I-V curves that depicts the power outputs as well. The resistance loads varies in step of 1 OHM from 0 OHM to 7 OHM. This range of resistance has been chosen since it covers the usual working load conditions for thermoelectric modules at low temperatures such as the one we are using in the experiments.

Between one temperature step and the following a waiting time of 30 min has been set to the heater as to permit a good stabilization of the thermodynamic conditions along the blocks, while a waiting time of 10 sec has been set to the software between the seven resistance loads steps involved in each different temperature data acquisition.

When all the steps imposed to the heater are over, the software gives a complete table where every values is listed (time, temperature, resistance loads, current, voltage). It this thus possible to begin, as to verify the reliability of the experiment, to the data comparison with the simulation models. In *Figure 5.3* and *Figure 5.4* are showed the comparisons for the heater temperature of 200°C.

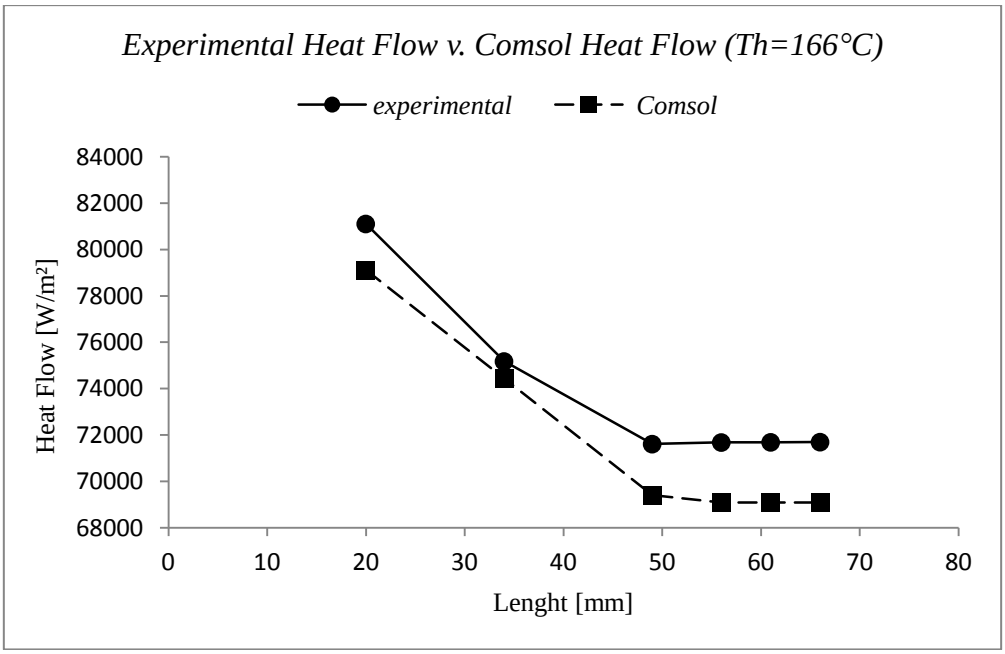

Figure 5.3

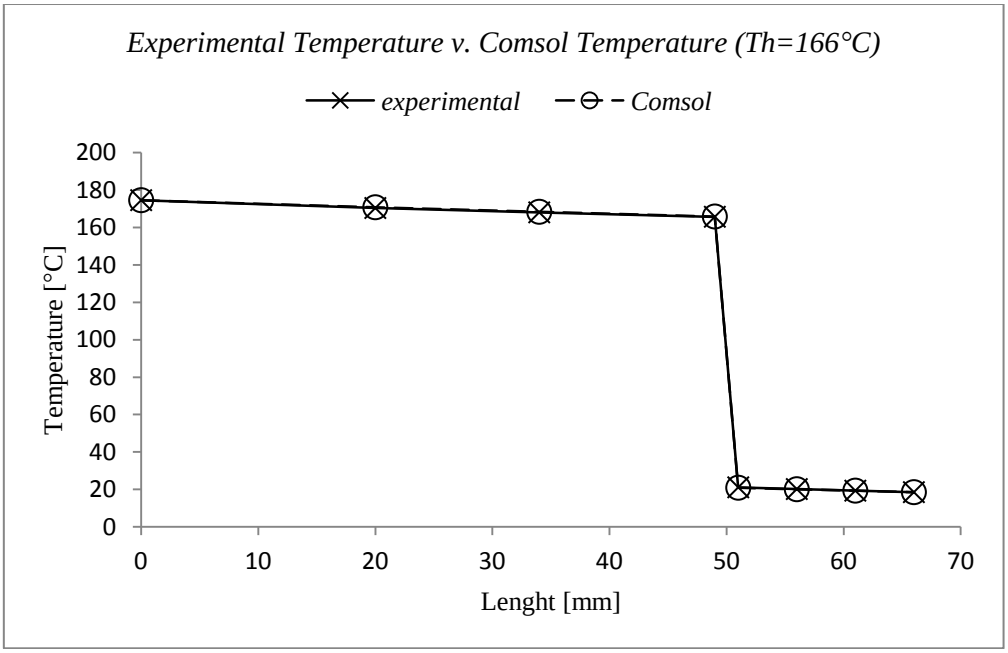

Figure 5.4

The *Th* abbreviation refers to the hot side temperature of the thermoelectric module, and, in this case, a 200°C temperature imposed to the heater, results to a 166°C temperature on the upper surface of the TEG. From the *Figure 5.3* and *Figure 5.4* it is possible to see that the Comsol models depicts in a realistic way what has been extrapolated from the experimental results. As a consequence we can proceed with the calculation of the other parameters since we are using a reliable process. In *Table 1* it is showed a summary of all the relevant parameters obtained from the module test system plus efficiencies and heat flow calculated in the post-processing.

Heater Temperature [°C]	200	150	100	50
Hot Side TEG Temperature [°C]	165,7	124,4	84,5	44,9
Cold Side TEG Temperature [°C]	21,1	19,7	17,4	15,2
Optimum Efficiency, η	3,53%	2,82%	1,82%	0,77%
Optimum Power [W]	2,65	1,53	0,63	0,12
Optimum Current [A]	0,71	0,57	0,39	0,17
Load resistance for Opt η [Ω]	5,27	4,70	4,23	3,99
Open Circuit Voltage, Voc [V]	7,07	5,10	3,17	1,33
Closed Circuit Current [A]	1,42	1,15	0,78	0,34
Heat Flow [W]	74,95	54,24	34,65	15,38

Table 1

From the table it is possible to see how the parameters change as the steps of temperature imposed by the heater decrease. The heat flow refers to the heat that crosses the thermoelectric module from the hot side to the cold side, and, in combination with the power output, it allows us to calculate the efficiencies of the commercial Marlow module that we are taking into account. In *Figure 5.5* it is shown an I-V curve plot for the higher temperature step. It is obvious that the maximum value of the power output is reached when the product

$$P = V \cdot I \quad [W]$$

reaches the maximum. Moreover, as it has been shown in the first chapter, the optimum current output value that gives the optimum efficiency, is reached when the internal resistance of the thermoelectric converter is equal to the resistance load imposed by the system. In this way, the *optimum* terms showed in *Table 1* refer to the peak values that can be reached by the module with that particular temperature difference.

The experimental data acquired with the module test system are then compared to the reference data that are available with the commercial Marlow module. In this way it is possible to check the compatibility of the system with the real working conditions of the module. In *Table 2* it is showed a summary of the datasheet values given by Marlow company for TG12-4L module under characterization.

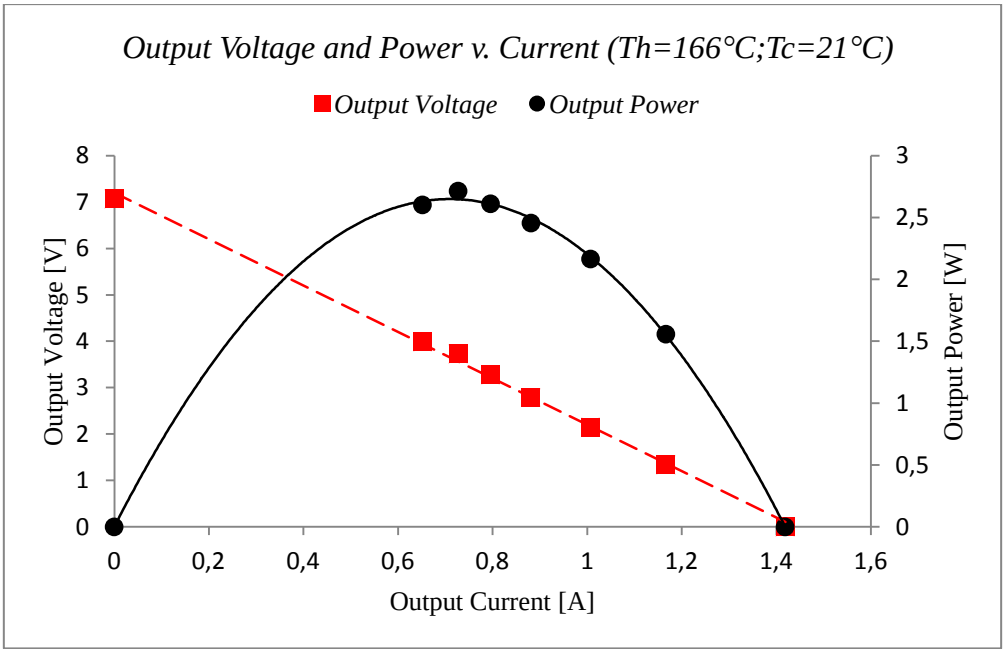

Figure 5.5

Hot Side TEG Temperature [°C]	230	170	110
Cold Side TEG Temperature [°C]	50	50	50
Optimum Efficiency, η	4,97%	4,08%	2,39%
Optimum Power [W]	4,05	2,12	0,61
Optimum Current [A]	0,77	0,58	0,33
Load resistance for Opt η [Ω]	6,83	6,32	5,72
Open Circuit Voltage, Voc [V]	9,45	6,5	3,28
Closed Circuit Current [A]	1,71	1,32	0,75
Heat Flow [W]	78,55	52,36	26,18

Table 2

From the datasheet table we can notice that the temperatures steps are slightly higher than the ones used in our characterization but however it is possible to use the reference values in order to see how much the experimental process of the thesis work differs from the results given from the company.

In the following *Figures 5.6, 5.7, 5.8,* and *5.9* are showed comparison plots that take into account different parameters distribution as the current output changes. Considering the heat flow distributions, it has been plotted vs the matched load output current that is the current that occurs when the load resistance imposed by the system is equal to the internal resistance of the module.

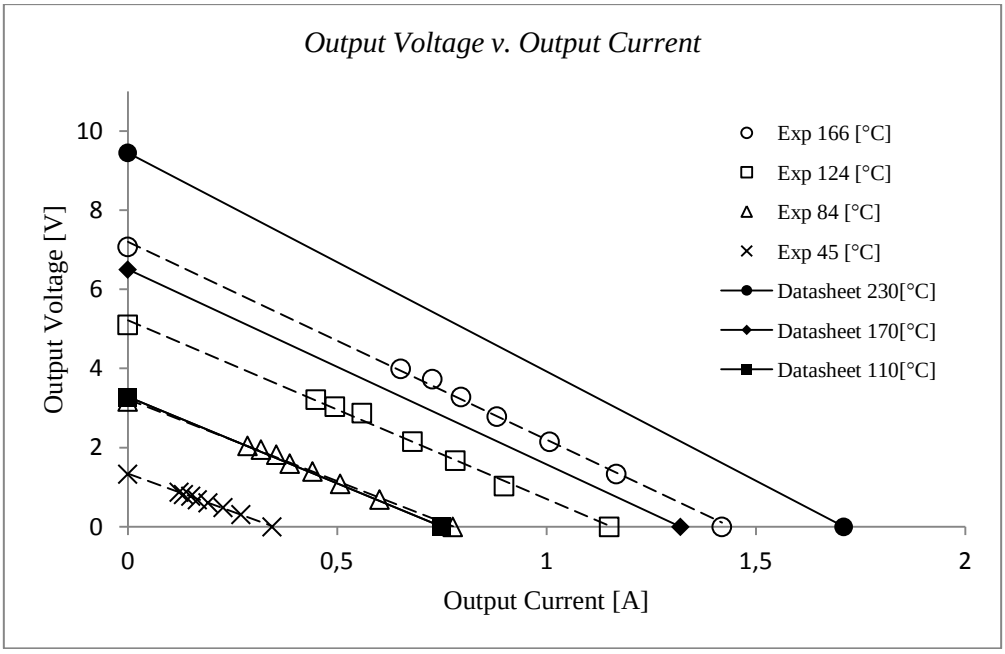

Figure 5.6

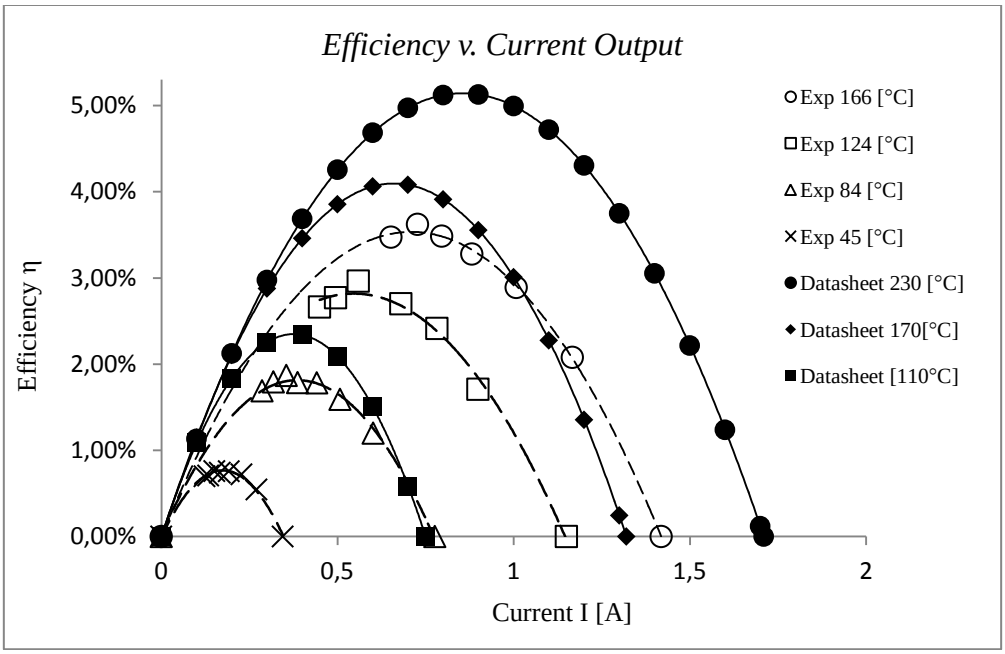

Figure 5.7

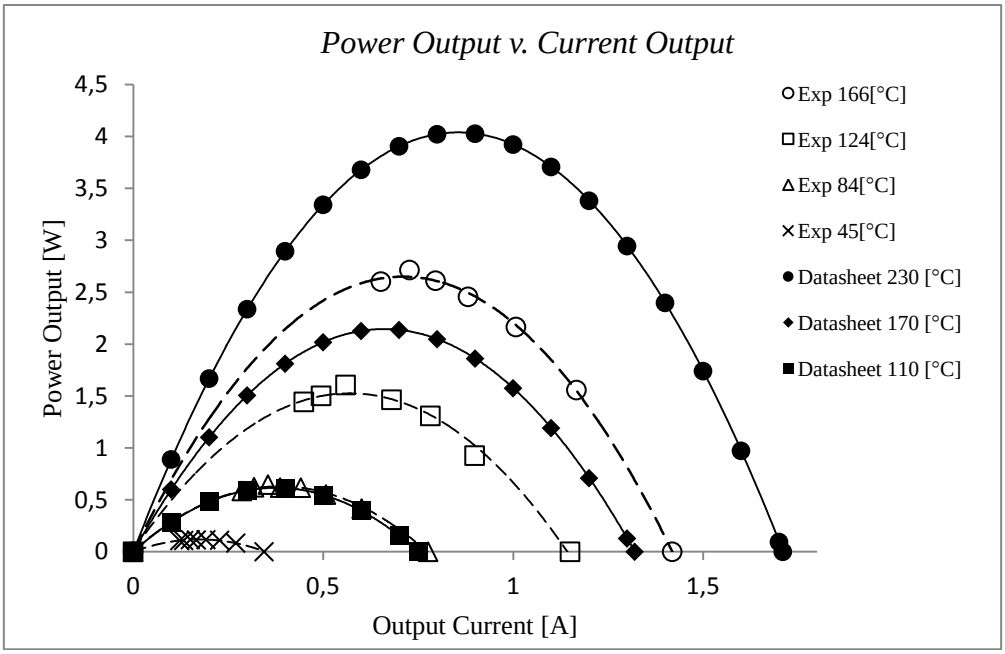

Figure 5.8

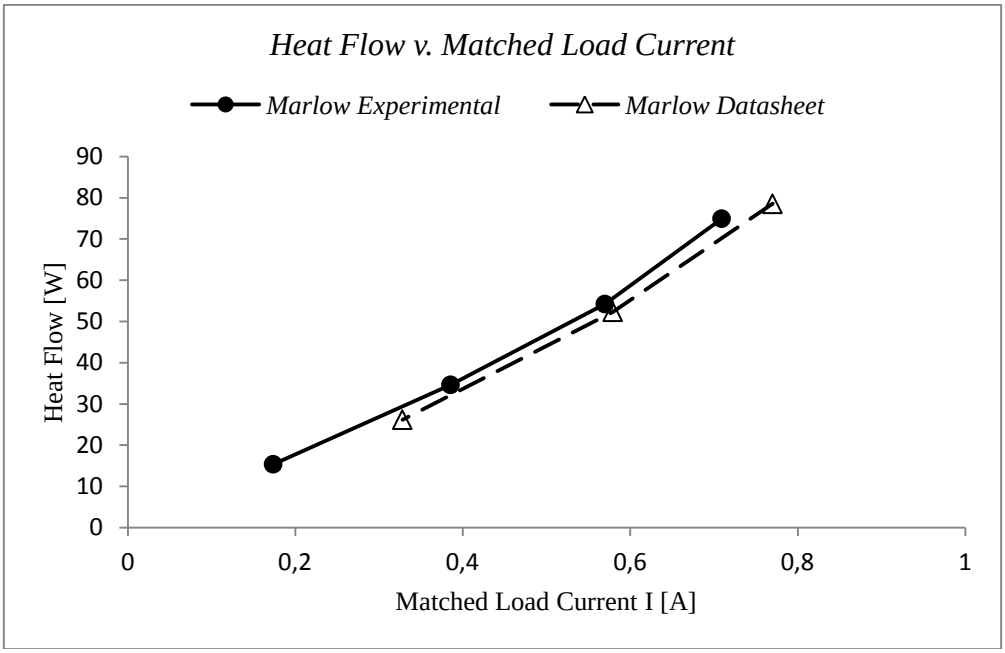

Figure 5.9

It is evident, from the figures above, that the reference data given by Marlow Company follow the same trend of the experimental data extrapolated from our characterization using the module test system. We can say that, both from the validation of the simulation models and from the comparisons with the company datasheet, the process used to characterize the thermoelectric commercial module, can be used systematically all the experiments that requires a study of the output parameters of a thermoelectric converter.

In the following plots showed in *Figure 5.10, 5.11, 5.12* are instead showed the trends of different output parameters as the temperature difference between the hot side and cold side

of the module changes. It has been also added a ΔT line that helps to understand in which range of temperature steps we are referring to.

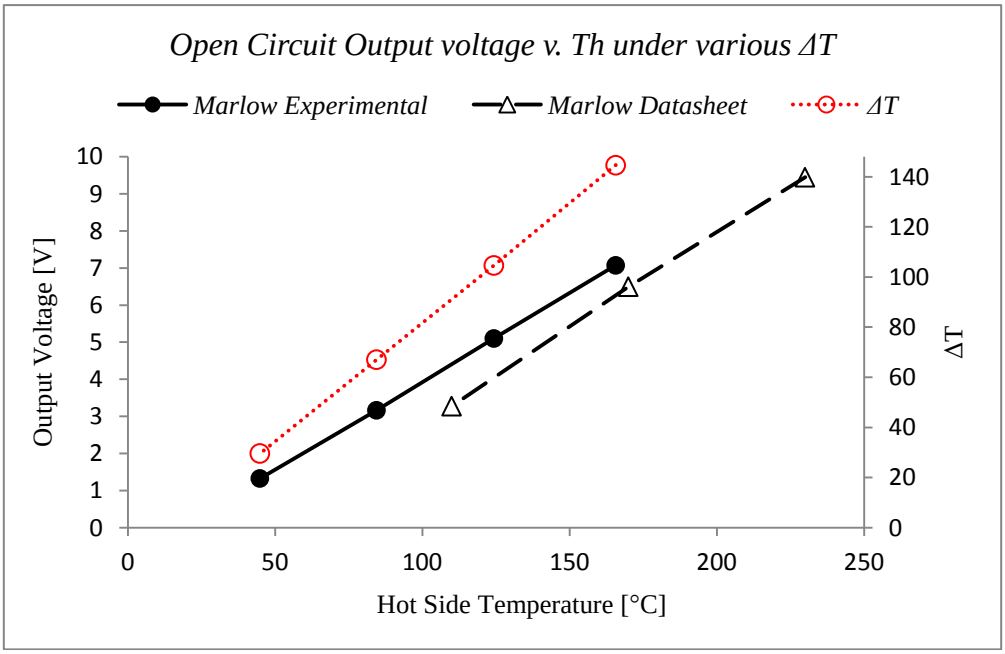

Figure 5.10

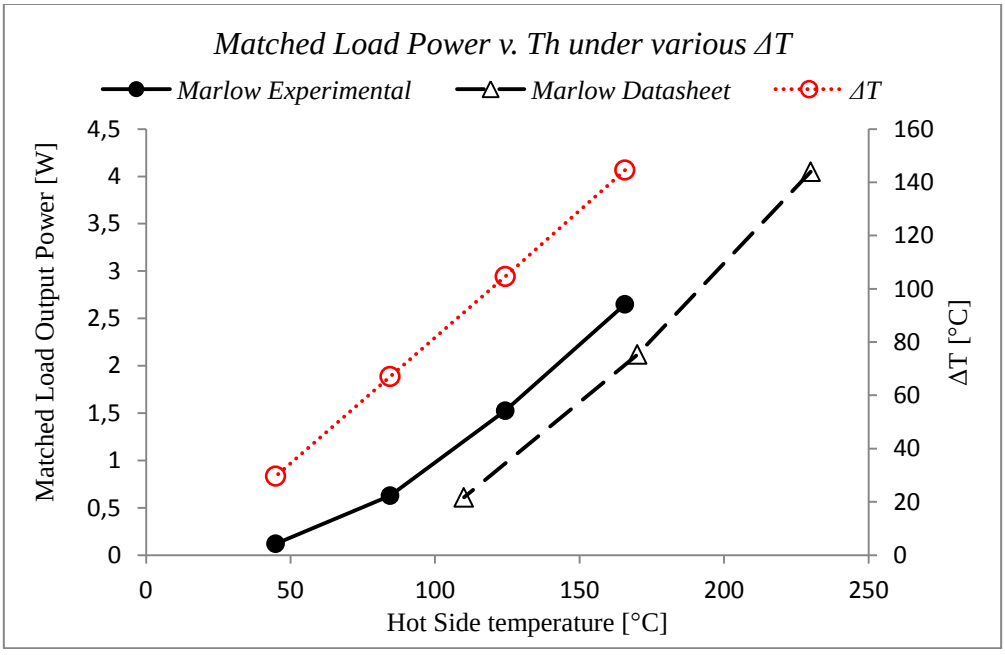

Figure 5.11

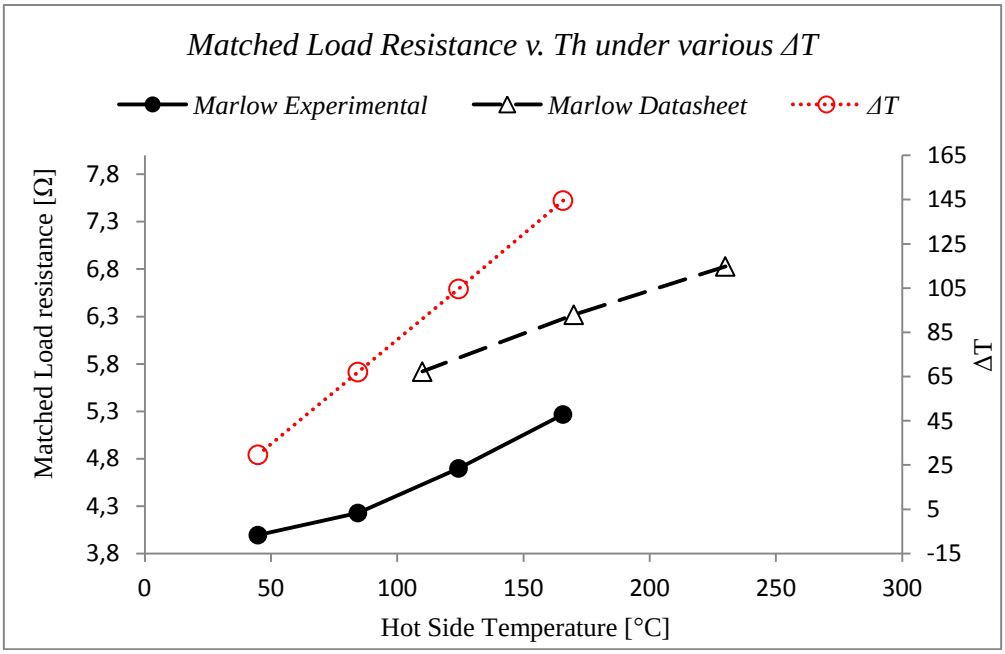

Figure 5.12

It is also possible to see how the power output changes as the resistance load increase (*Figure 5.13)*, and to have a better comprehension of the efficiency curve normalized to the optimum efficiency (*Figure 5.14*). In *Figure 5.14* it has been considered the highest temperature step of the heater (200°C) and also the resistance load and the voltage have been normalized to the matched resistance load and the open circuit voltage respectively.

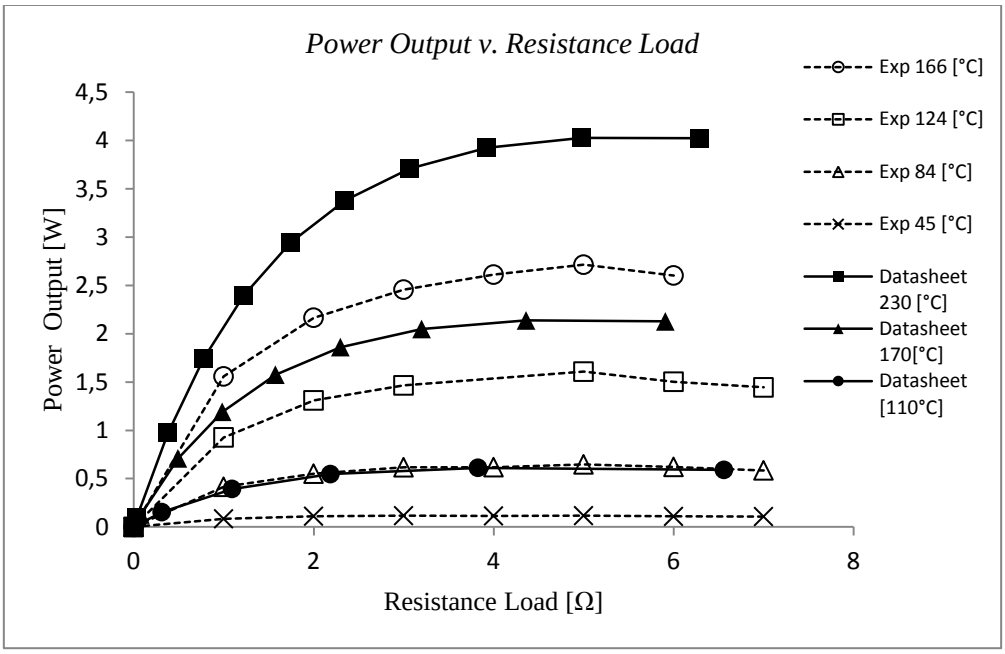

Figure 5.13

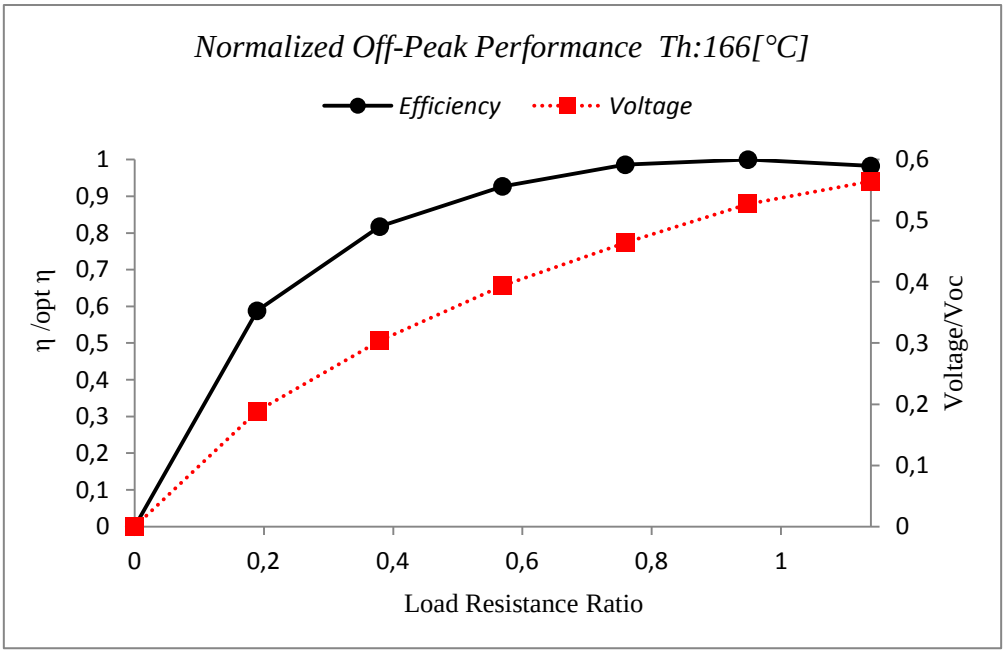

Figure 5.14

5.3.2 Marlow Module Insulated

The results from Marlow module in insulated working conditions are showed in *Table 3* below.

Heater Temperature [°C]	200	150	100	50
Hot Side TEG Temperature [°C]	179,9	134,9	89,8	46,0
Cold Side TEG Temperature [°C]	18,8	16,1	13,5	10,5
Optimum Efficiency, η	3,90%	3,25%	2,26%	1,06%
Optimum Power [W]	1,40	0,84	0,39	0,08
Optimum Current [A]	0,49	0,39	0,27	0,13
Load resistance for Opt η [Ω]	5,96	5,65	5,48	4,69
Open Circuit Voltage, Voc [V]	5,42	4,07	2,57	1,14
Closed Circuit Current [A]	0,95	0,75	0,52	0,26
Heat Flow [W]	35,15	25,91	16,66	7,75

Table 3

Using the insulation material it is evident how the temperature difference between the hot side and the cold side is different from the case without insulation. As a result, the efficiencies are higher in the insulated case.

If we also refer to the datasheet values we are able to obtain the same plots calculated for the case without insulation. The different output parameters vs the current output load are plotted in the following *Figure 5.15, 5.16, 5.17, 5.18.*

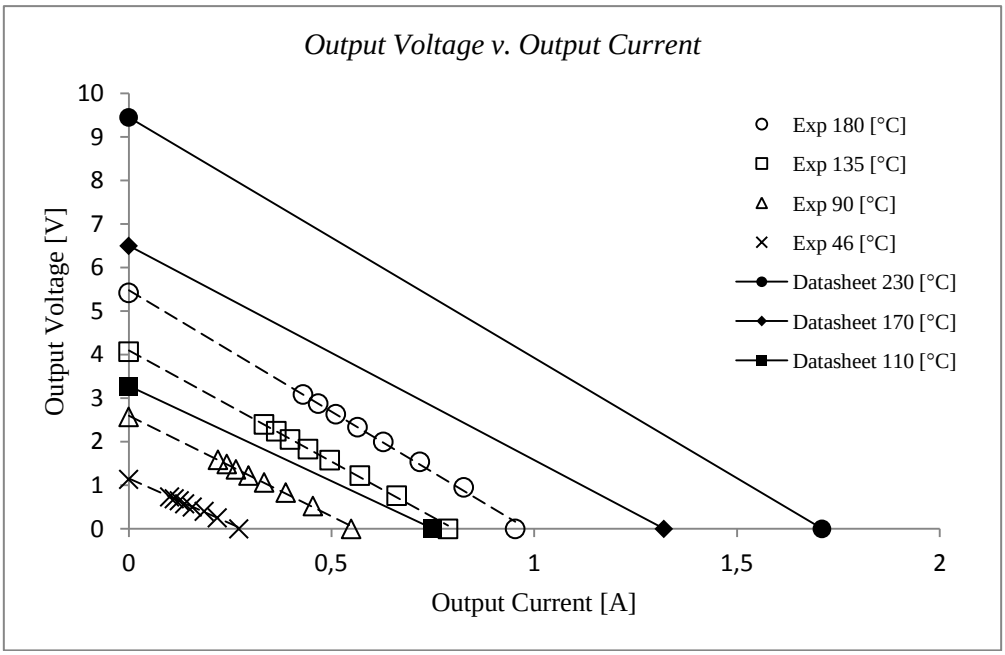

Figure 5.15

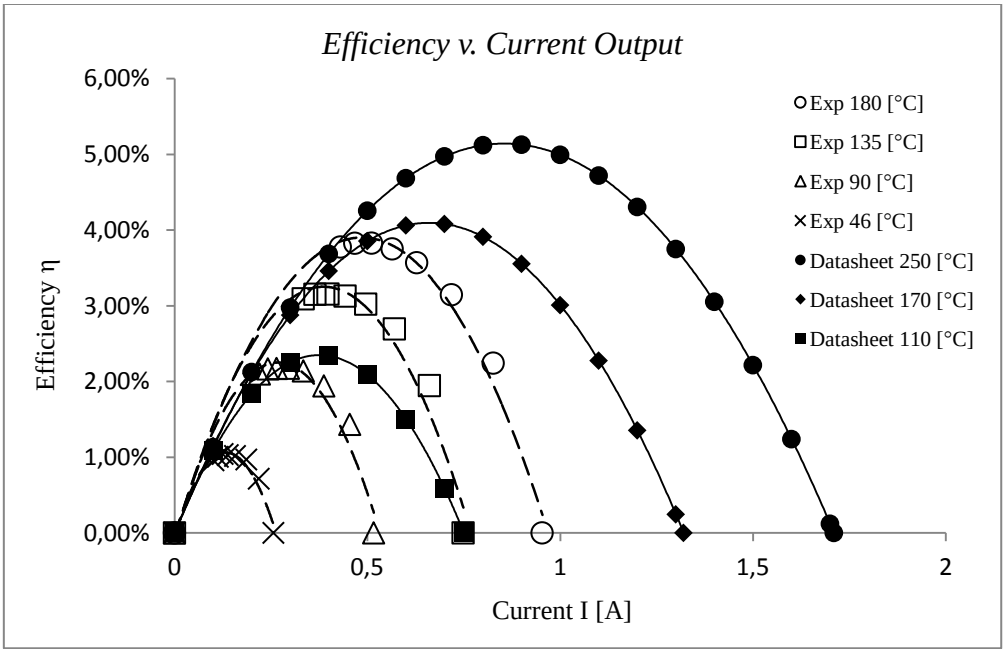

Figure 5.16

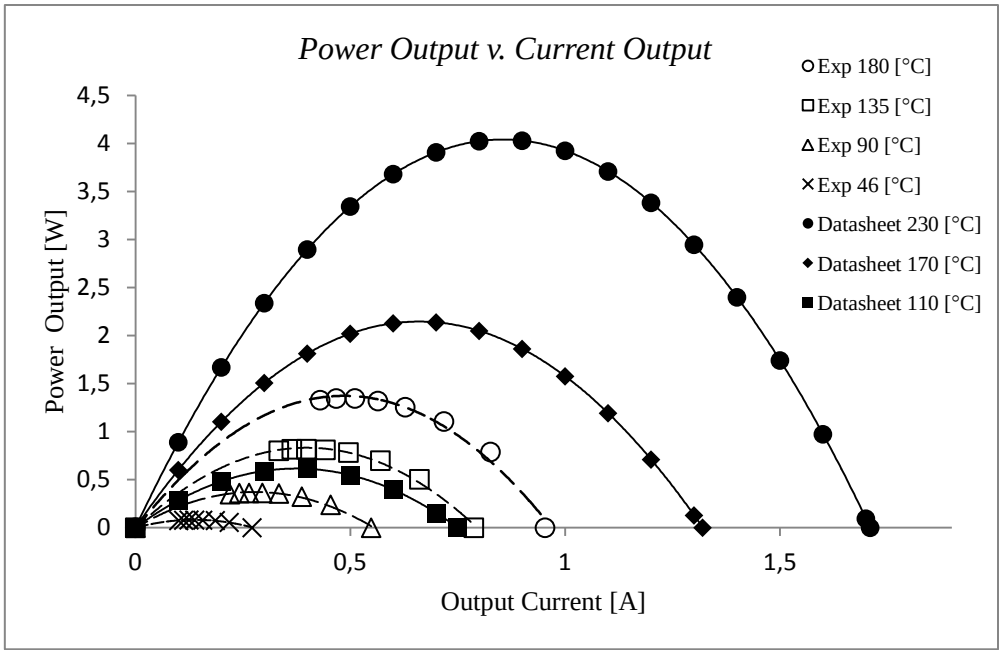

Figure 5.17

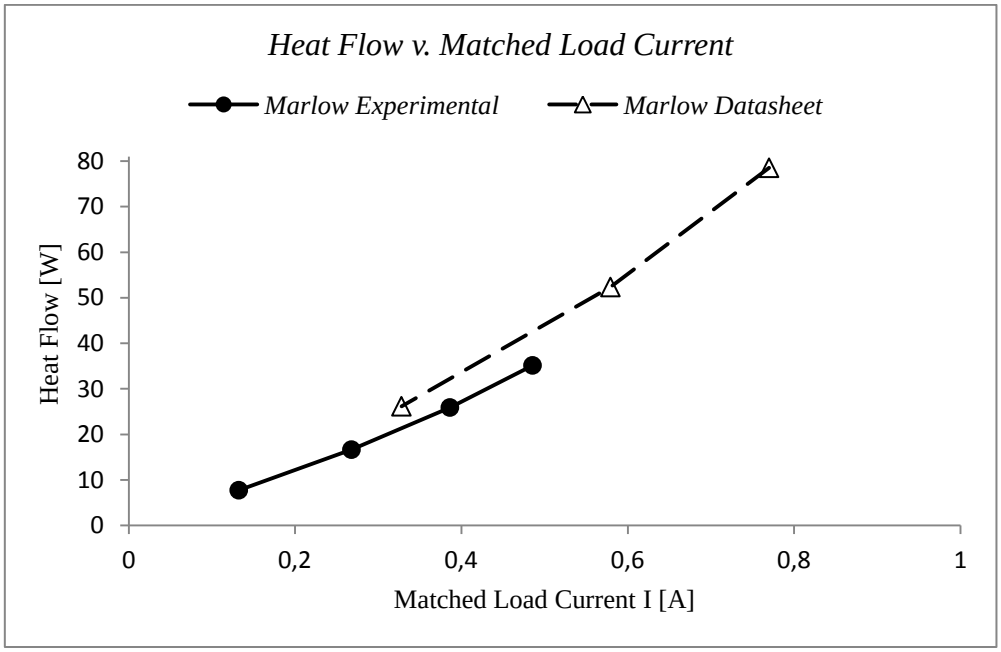

Figure 5.18

As it is possible to notice from the figures above, the reference values for the Marlow module (summarized in the previous *Table 2)* are close to the experimental ones. In the module test system we used for the experiments the temperature steps were lower than the one used by the commercial datasheet, but still it can be seen from the plots that the trends are quite similar to each other.

The temperature increase is directly proportional to a parallel increase of the module performances as it can be noticed especially in the efficiency plot as well as the power output plot.

In the *Figures 5.19, 5.20, 5.21, 5.22, 5.23* are also showed the output parameters of the thermoelectric converter under different steps of temperature differences.

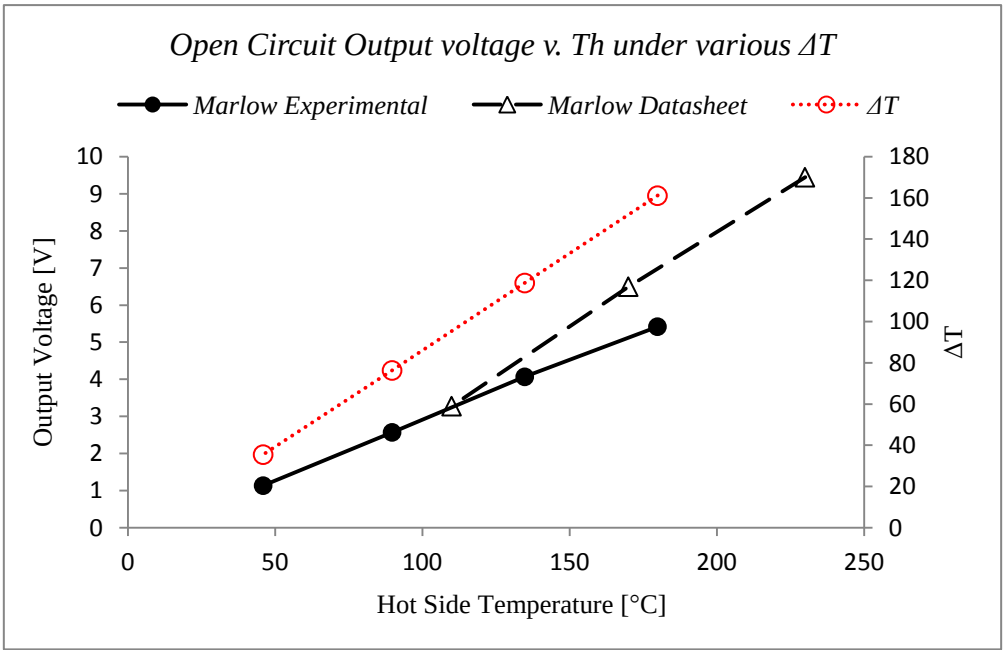

Figure 5.19

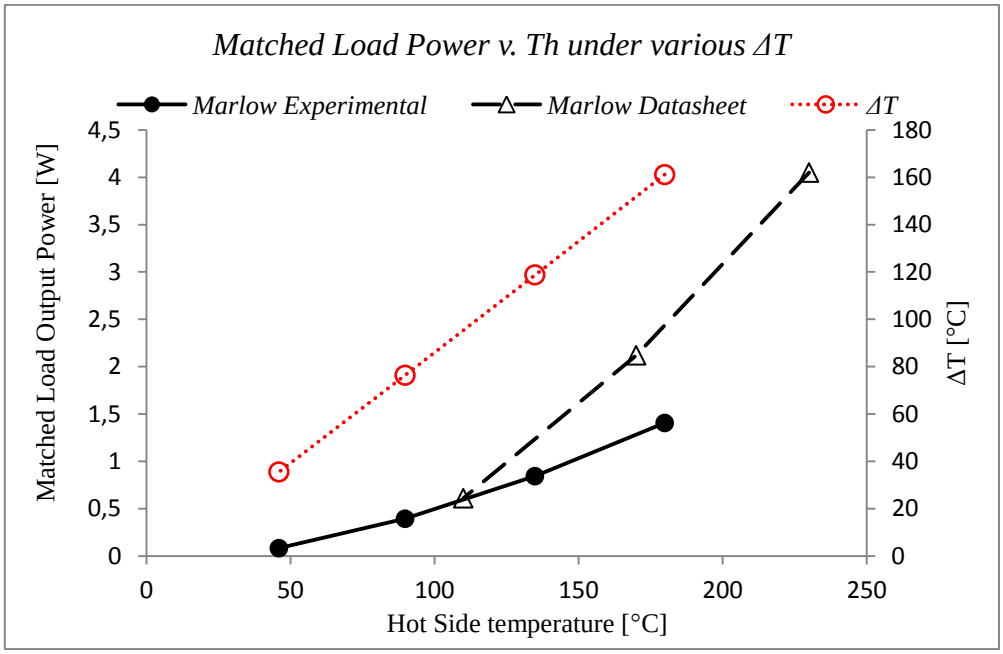

Figure 5.20

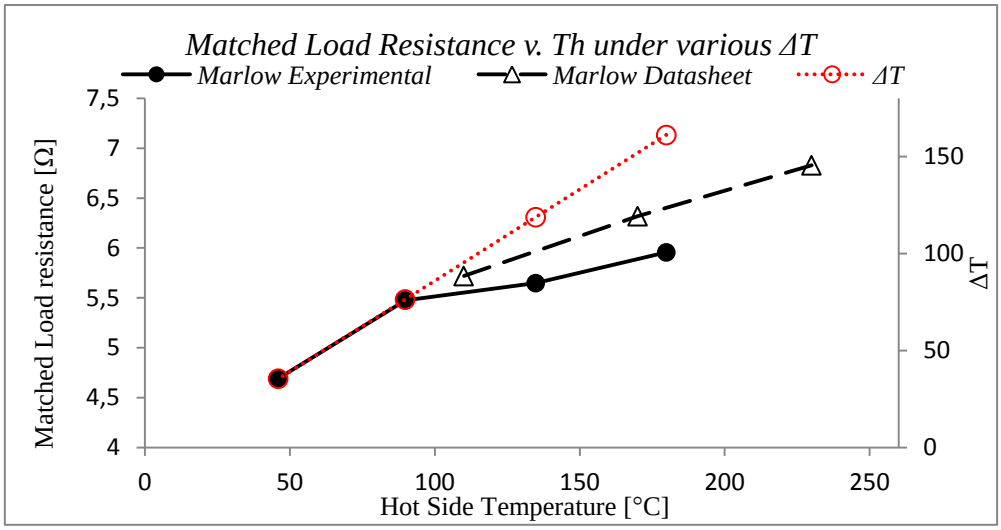

Figure 5.21

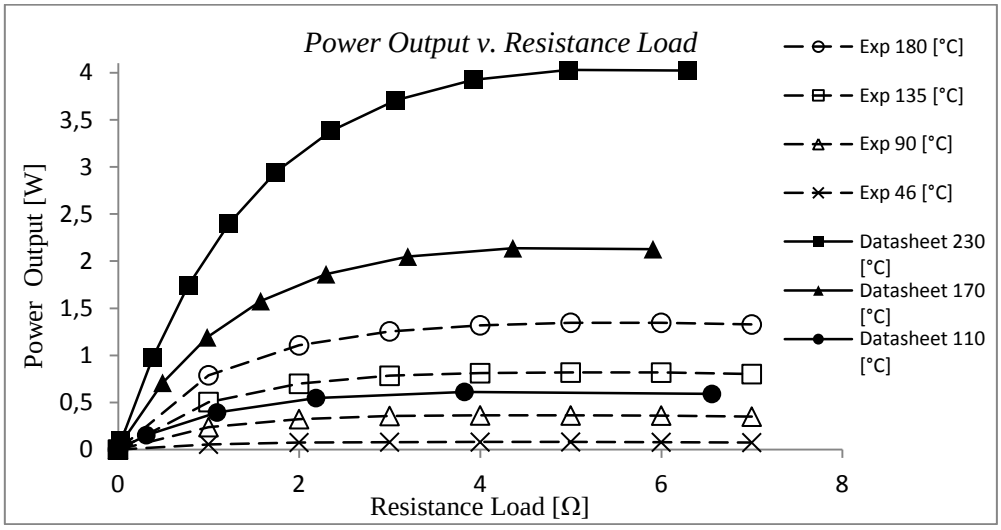

Figure 5.22

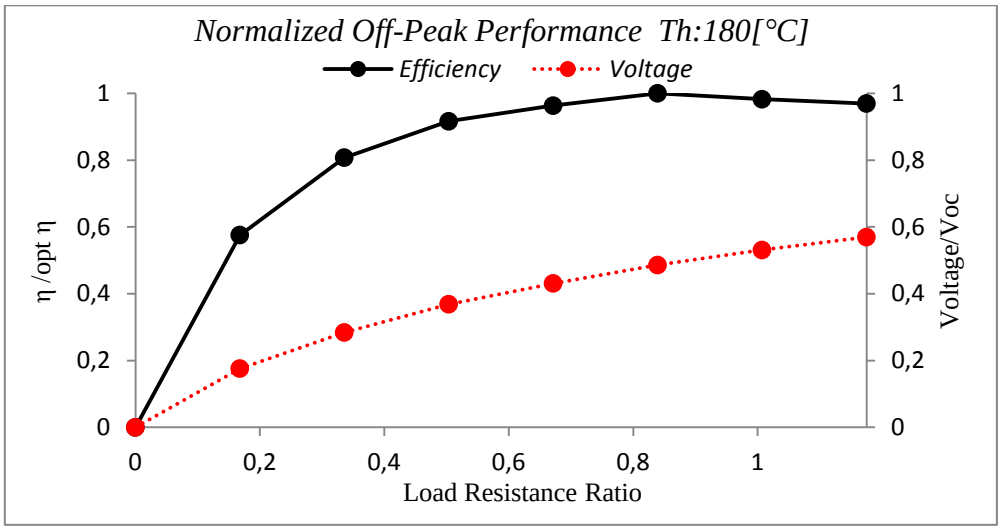

Figure 5.23

The same considerations for the case without insulation can be done also for the output parameters plots in this insulated case. In *Figure 5.22* has been chosen the highest values of the temperature imposed by the heater (200°C) that results in a hot side temperature of the module of 180°C.

5.3.3 Comparisons between Not Insulated and Insulated Experiments

Starting from the results showed in the previous paragraphs it is also possible to elaborate plots in which the difference between the insulated and not insulated case helps to understand what are the effects on the thermoelectric module performances.

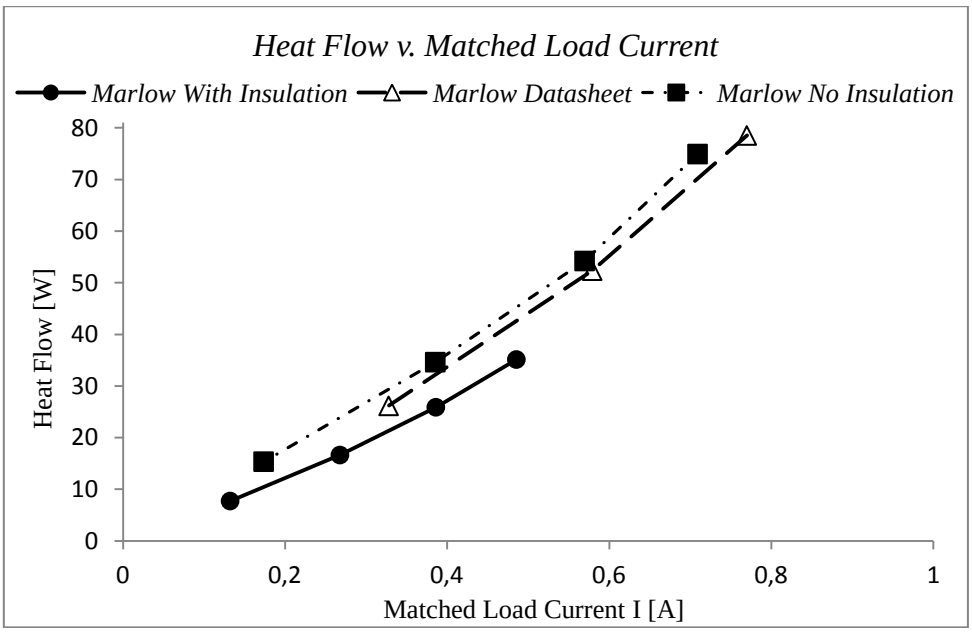

Figure 5.23

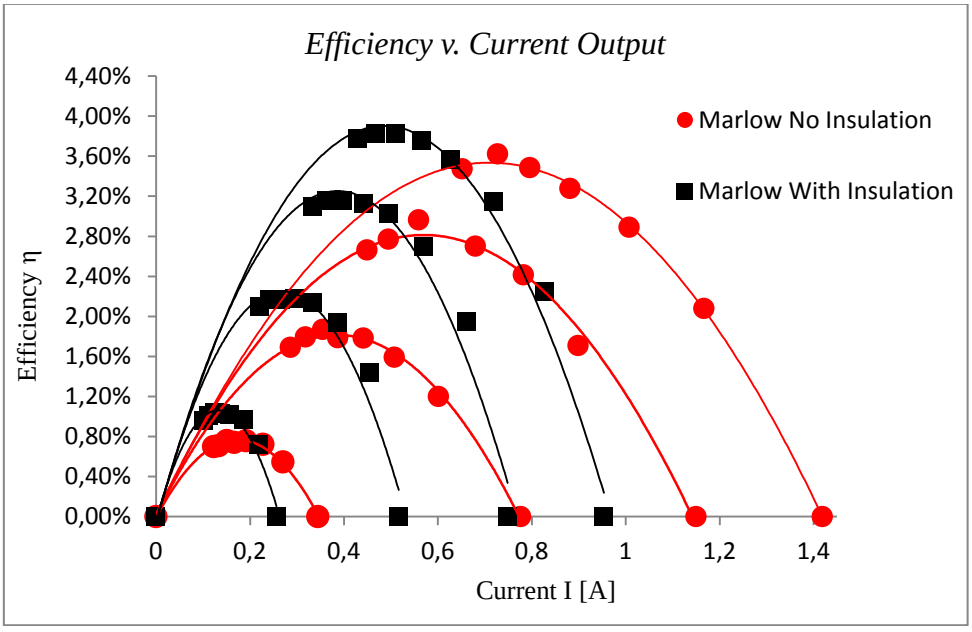

Figure 5.24

In the *Figure 5.23* and *5.24* it is shown the difference for the two cases (insulated and not insulated) regarding the heat flow distribution and the efficiency output. It can be seen how the insulator affect the performance of the module since it helps to get higher efficiencies values with the same elements thanks to the increased temperature difference between the hot side and the cold side of the module.

Conclusions

This thesis work was developed in order to understand both from a theoretical and experimental way the behavior of thermoelectric commercial modules under working conditions. The use of a module test system was necessary for the data acquisition process developed during the experiments.

However the characterization of a thermoelectric module was intended as the final step of a series of intermediate actions that were used as a support for the validation of the entire work. If the elements available for the experiments were all liable to a good understanding of their thermodynamic behavior, a simulation model implemented with Comsol Multiphysics software was necessary to validate the measurement process that has been carried forward along the thesis work.

Starting from a knowledge of the basic physical principles that drive thermoelectric effects it was then possible to consider the use of a module test system in order to characterize the commercial TEGs. The system used was available in the Department of Energy Conversion and Storage of DTU, Technical University of Denmark, Riso Campus, and it's been implemented by PANCO company. It was important, before running the system, to understand the actual situation of the improvements done in the field of module testing and to include in the development of the thesis work, an analysis of the PANCO system in all its main aspects.

Accordingly to a previous understanding of the theoretical aspects on one side and the hardware configuration on the other, it was successively possible to begin the experimental data acquisition at first without the TEG inserted in the system. In fact the first part of the data acquisition process was centered on the heat conduction analysis along the elements composing the module test system with the help of the numerical models implemented on Comsol Multiphysics. Thanks to this comparison it was possible to understand if the range of temperatures values detected by the thermocouples and the heat flow along the copper blocks were depicting what would have happened in a theoretical condition.

The most part of the thesis work was thus focused on a sort of "preparation" that was necessary to obtain reliable results in the thermoelectric modules characterization. As a sample for being tested in the system a commercial module provided by Marlow Ind. Company was chosen. In this way it was also possible to understand how much the experimental data differ from the one elaborated by the company itself.

The results acquired from the TEG working conditions were then elaborated in plots that helped to understand which are the main parameters involved in a thermoelectric effect analysis for power generation and how they interrelate with the current outputs and the temperature distributions.

Effective results have been obtained since the power outputs and the efficiencies were included in a range valid both for the typical performances of thermoelectric modules and for the reference data showed by the commercial module datasheet.

We thus demonstrated that the configuration of the module test system, the software setup, the numerical models and the data acquisition process, are all a part of an experimental pattern that can be used systematically and reliably on other commercial modules that needs a verification of their performances.

Appendix

Section I

The thesis work experimental process has been carried forward using more than one commercial TEG to be characterized in the module test system. In the 5th chapter the analysis of the Marlow module TG14-4L was showed in order to complete all the previous steps that were necessary to validate the experimental results.

Once the process has been established and the first commercial module drove to a performances evaluation that could be systematically repeated, other two modules were characterize using Panco module test system.

The two further thermoelectric module characterized are the Teg Power Company module and the ZhiYuan International LTD Thermoelectric Module. Neither of them was provided with a datasheet, so the characterization of the two modules was focused on their performances evaluation in order to provide to the companies reliable results useful for future comparisons with pre-existent commercial modules.

As already showed for the Marlow commercial module, in this section will be introduced plots referring to the output parameters of the commercial modules as well as temperature distributions compared with the numerical simulations results.

Both the Teg Power module and the ZhiYuan International LTD module have been characterized in insulated conditions.

Teg Power Module

Heater Temperature [°C]	200	150	100	50
Hot Side Temperature [°C]	167,3	125,9	83,9	45,0
Cold Side Temperature [°C]	20,7	18,7	16,6	15,0
Optimum Efficiency, η	2,70%	2,02%	1,26%	0,55%
Optimum Power [W]	0,75	0,41	0,16	0,03
Optimum Current [A]	0,50	0,38	0,25	0,11
Load resistance for Opt η [Ω]	3,00	2,89	2,67	2,65
Open Circuit Voltage, Voc [V]	2,73	2,16	1,30	0,57
Closed Circuit Current [A]	0,99	0,75	0,49	0,22
Heat Flow [W]	27,99	20,46	12,85	5,73

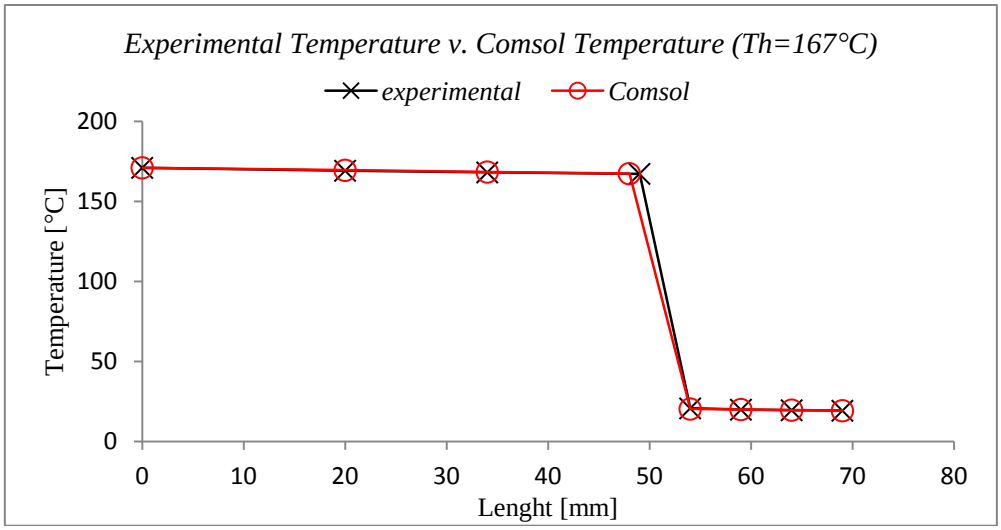
Experimental Temperature v. Comsol Temperature (Th=167°C)
experimental
Comsol
Temperature [°C]
200
150
100
50
0
0
10
20
30
40
50
60
70
80
Lenght [mm]

2

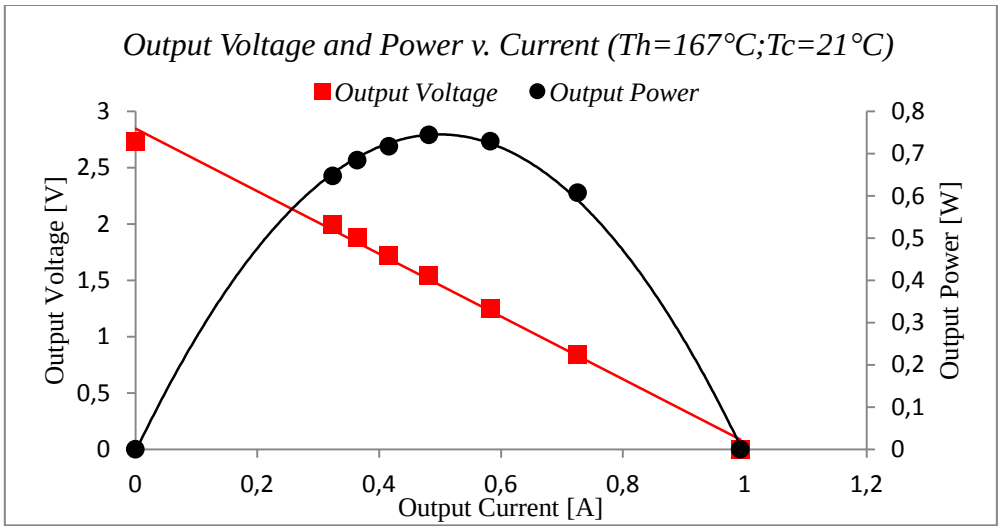
Output Voltage and Power v. Current (Th=167°C;Tc=21°C)
Output Voltage
Output Power
Output Voltage [V]
3
2,5
2
1,5
1
0,5
0
Output Power [W]
0,8
0,7
0,6
0,5
0,4
0,3
0,2
0,1
0
0
0,2
0,4
0,6
0,8
1
1,2
Output Current [A]

3

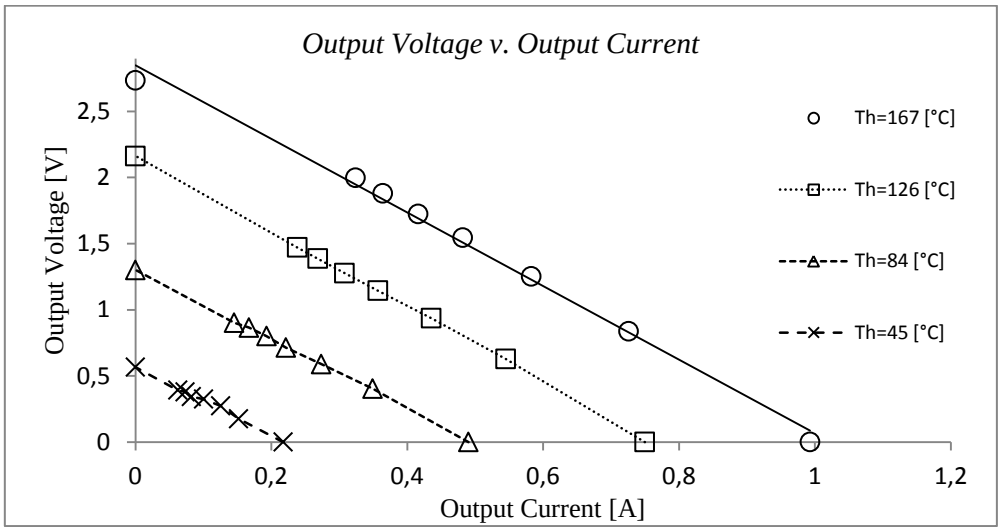
Output Voltage v. Output Current
Output Voltage [V]
2,5
2
1,5
1
0,5
0
Th=167 [°C]
Th=126 [°C]
Th=84 [°C]
Th=45 [°C]
0
0,2
0,4
0,6
0,8
1
1,2
Output Current [A]

4

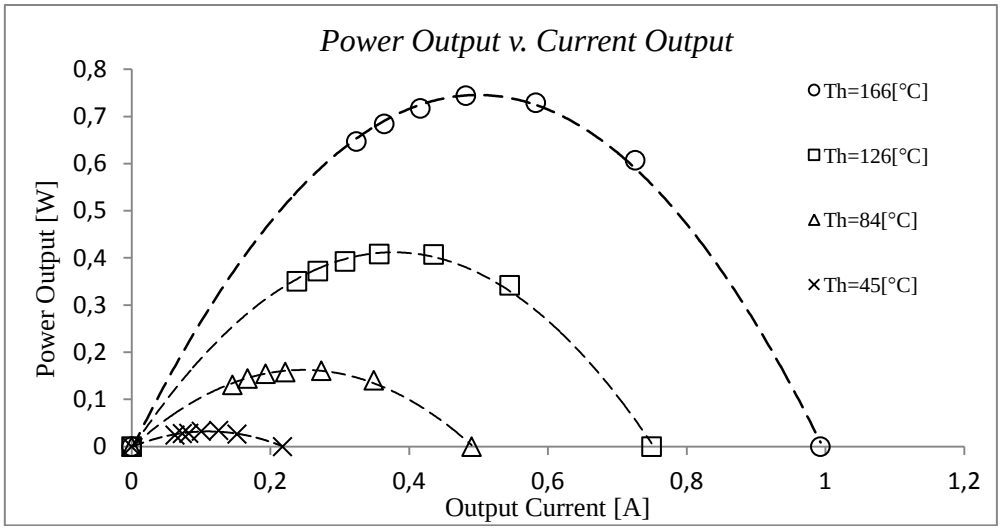
Power Output v. Current Output
Power Output [W]
0,8
0,7
0,6
0,5
0,4
0,3
0,2
0,1
0
0
0,2
0,4
0,6
0,8
1
1,2
Output Current [A]
Th=166[°C]
Th=126[°C]
Th=84[°C]
Th=45[°C]

5

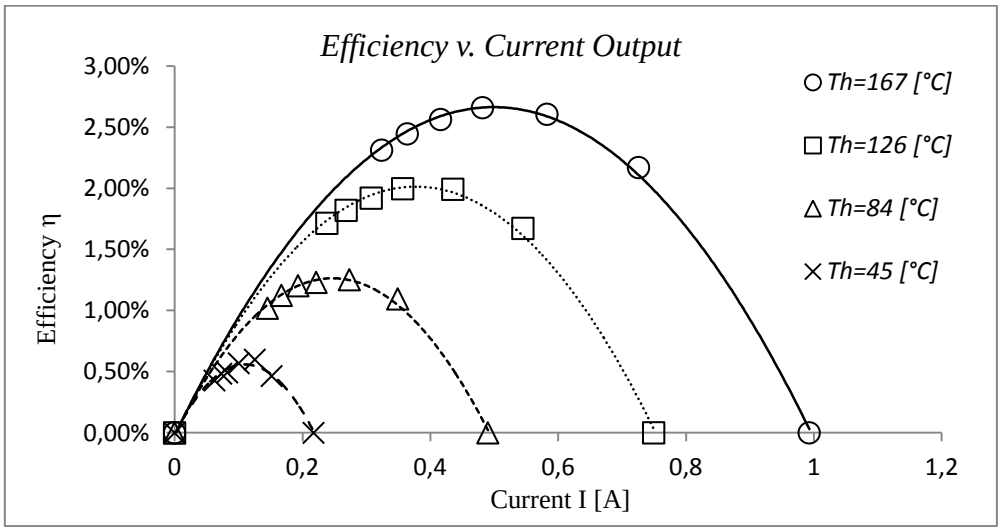
Efficiency v. Current Output
Efficiency η
3,00%
2,50%
2,00%
1,50%
1,00%
0,50%
0,00%
0
0,2
0,4
0,6
0,8
1
1,2
Current I [A]
Th=167 [°C]
Th=126 [°C]
Th=84 [°C]
Th=45 [°C]

6

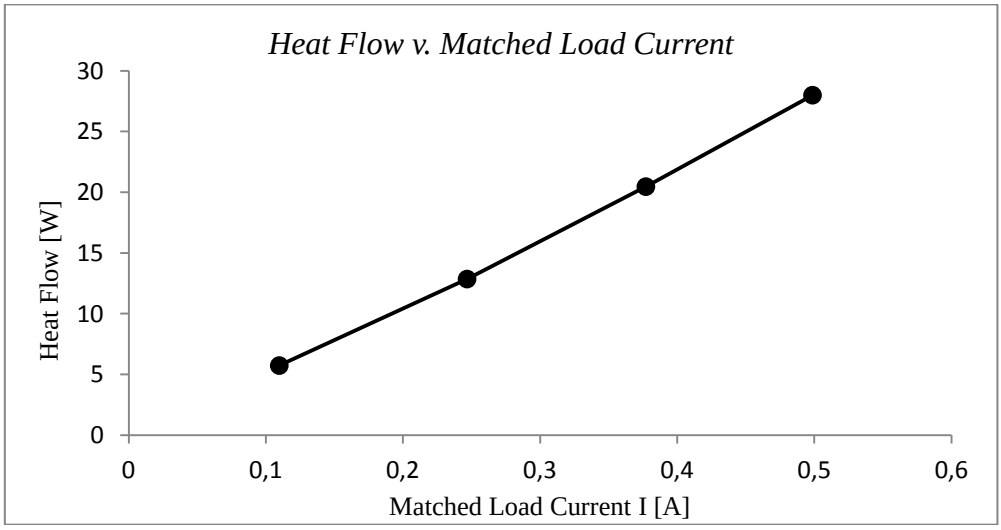
Heat Flow v. Matched Load Current
Heat Flow [W]
30
25
20
15
10
5
0
0
0,1
0,2
0,3
0,4
0,5
0,6
Matched Load Current I [A]

7

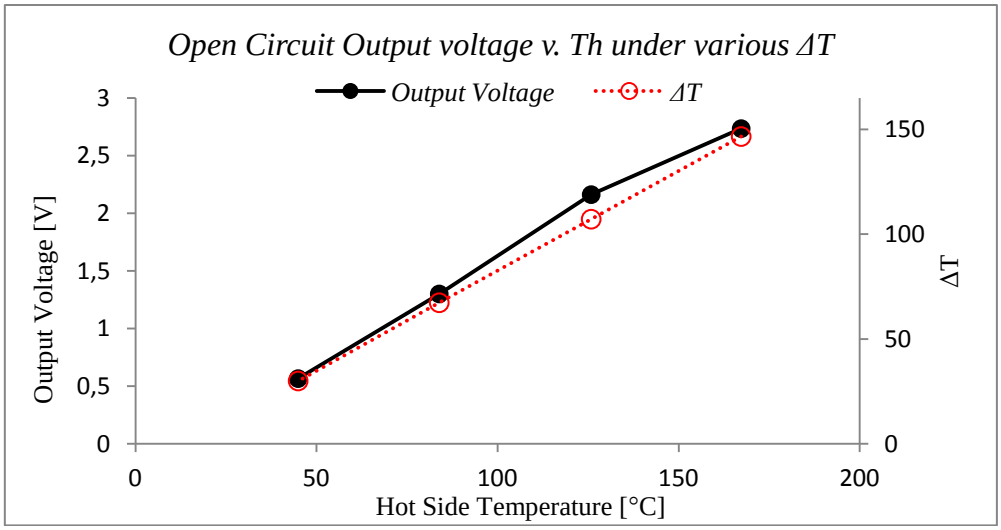
Open Circuit Output voltage v. Th under various ΔT
Output Voltage
ΔT
Output Voltage [V]
ΔT
Hot Side Temperature [°C]
0
0,5
1
1,5
2
2,5
3
0
50
100
150
200

8

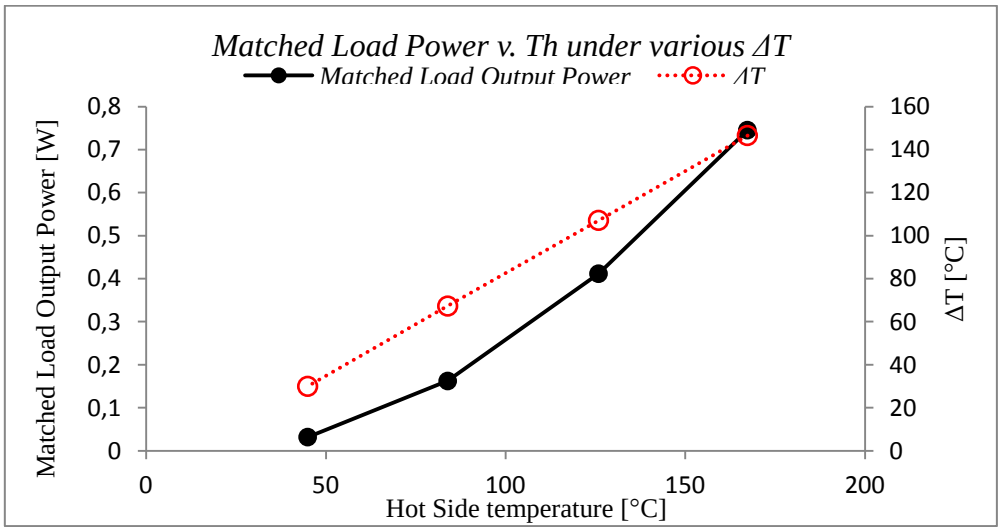
Matched Load Power v. Th under various ΔT
Matched Load Output Power
ΔT
Matched Load Output Power [W]
ΔT [°C]
Hot Side temperature [°C]
0
0,1
0,2
0,3
0,4
0,5
0,6
0,7
0,8
0
20
40
60
80
100
120
140
160
0
50
100
150
200

9

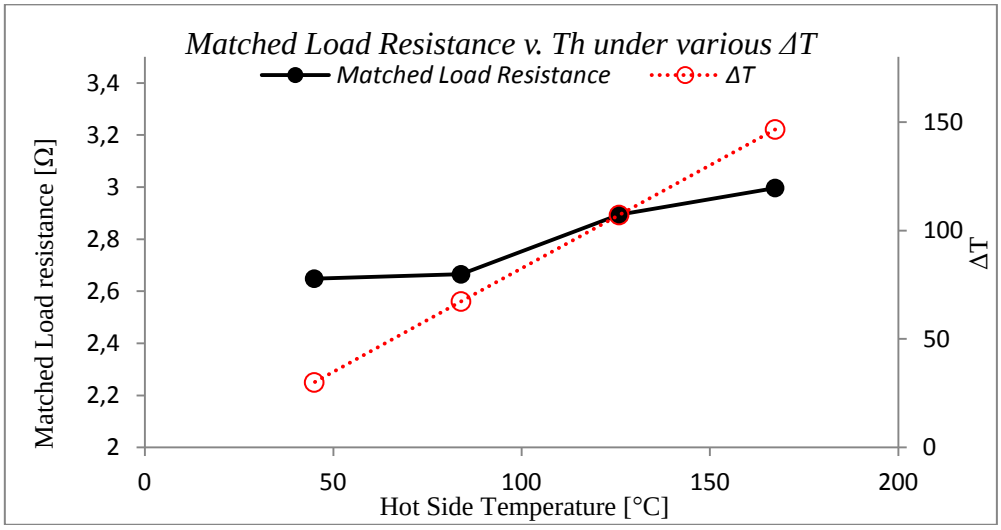
Matched Load Resistance v. Th under various ΔT
Matched Load Resistance
ΔT
Matched Load resistance [Ω]
ΔT
Hot Side Temperature [°C]
2
2,2
2,4
2,6
2,8
3
3,2
3,4
0
50
100
150
200

10

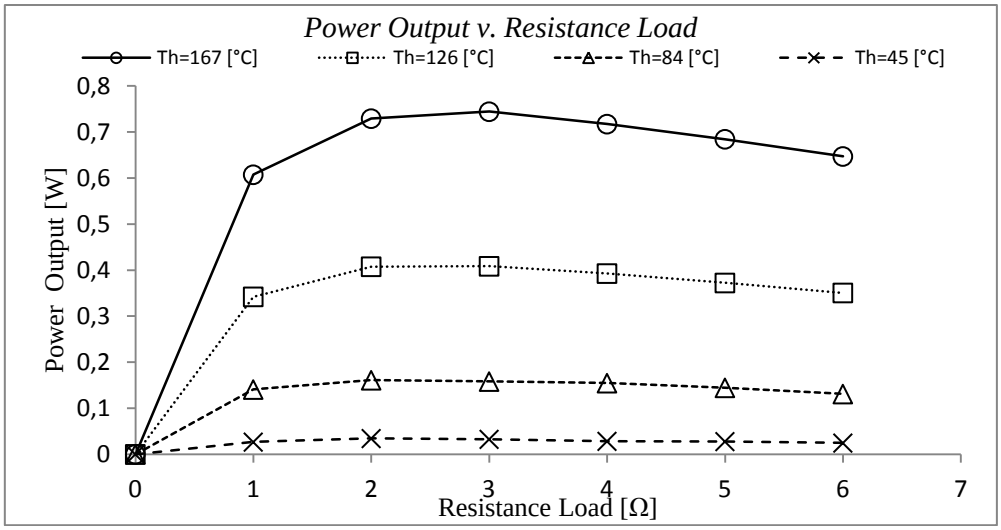

11

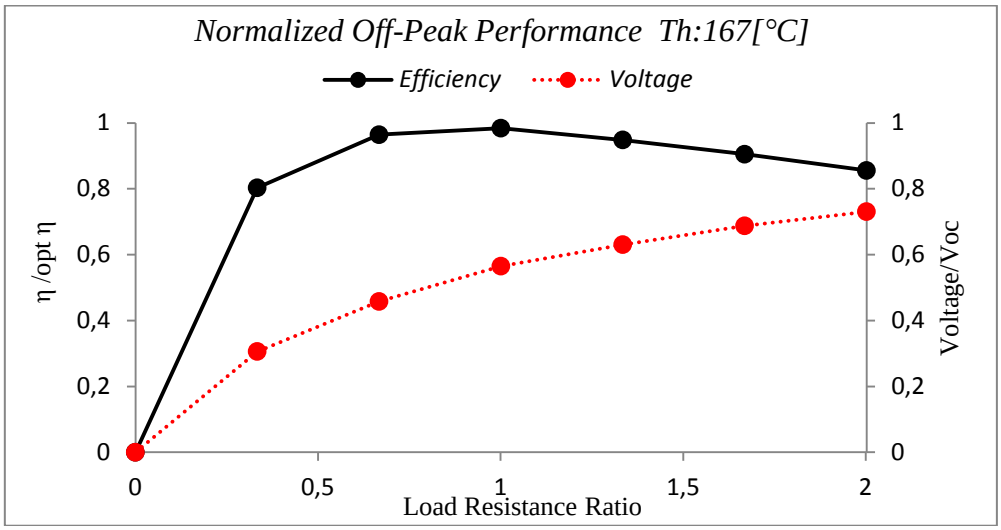

12

ZhiYuan International LTD module

Heater Temperature [°C]	200	150	100	50
Hot Side Temperature [°C]	152	114,6	76,7	41,4
Cold Side Temperature [°C]	23,5	21,0	18,5	15,8
Optimum Efficiency, η	2,26%	1,72%	1,09%	0,43%
Optimum Power [W]	0,79	0,44	0,17	0,03
Optimum Current [A]	1,51	1,16	0,73	0,32
Load resistance for Opt η [Ω]	0,35	0,33	0,32	0,31
Open Circuit Voltage, Voc [V]	1,01	0,73	0,44	0,18
Closed Circuit Current [A]	3,02	2,32	1,46	0,63
Heat Flow [W]	35,06	25,52	15,88	6,97

13

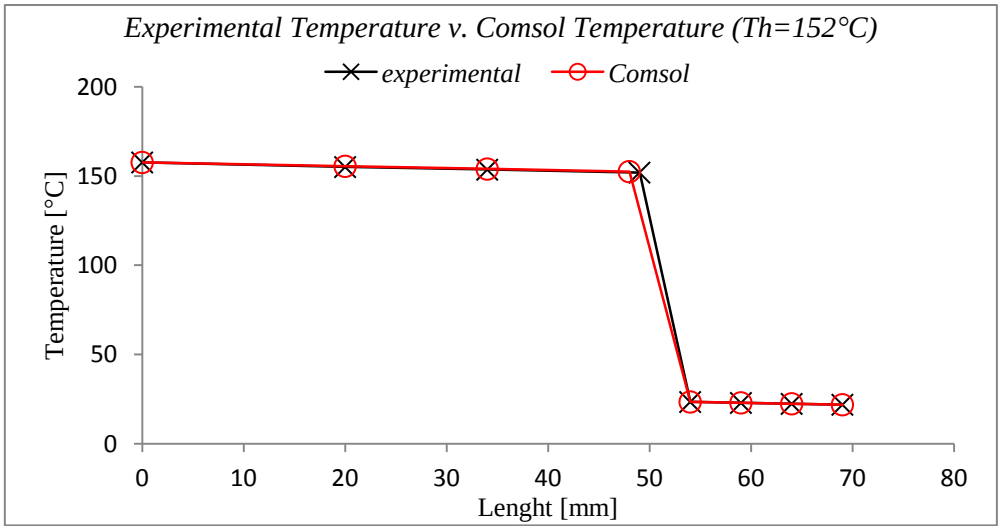
Experimental Temperature v. Comsol Temperature (Th=152°C)
experimental
Comsol
Temperature [°C]
200
150
100
50
0
0
10
20
30
40
50
60
70
80
Lenght [mm]

14

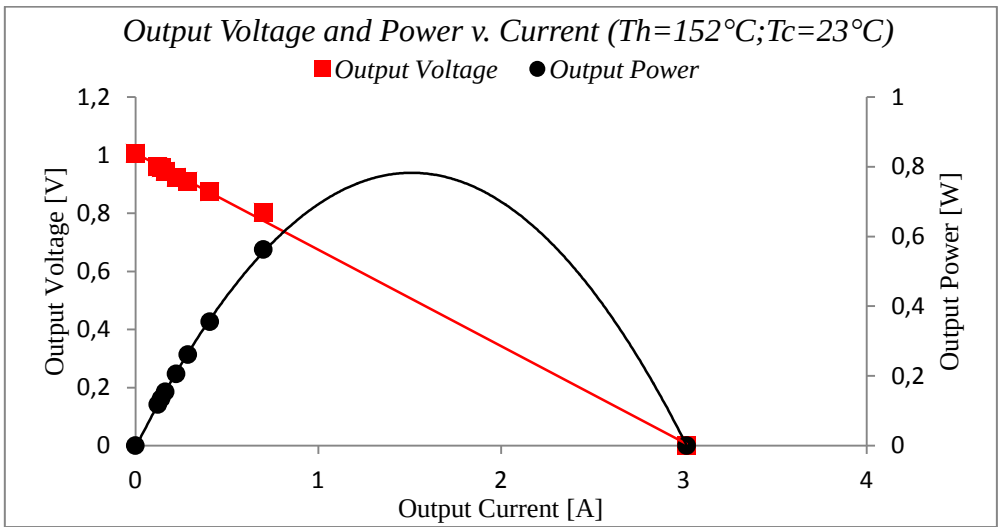
Output Voltage and Power v. Current (Th=152°C;Tc=23°C)
Output Voltage
Output Power
Output Voltage [V]
1,2
1
0,8
0,6
0,4
0,2
0
Output Power [W]
1
0,8
0,6
0,4
0,2
0
0
1
2
3
4
Output Current [A]

15

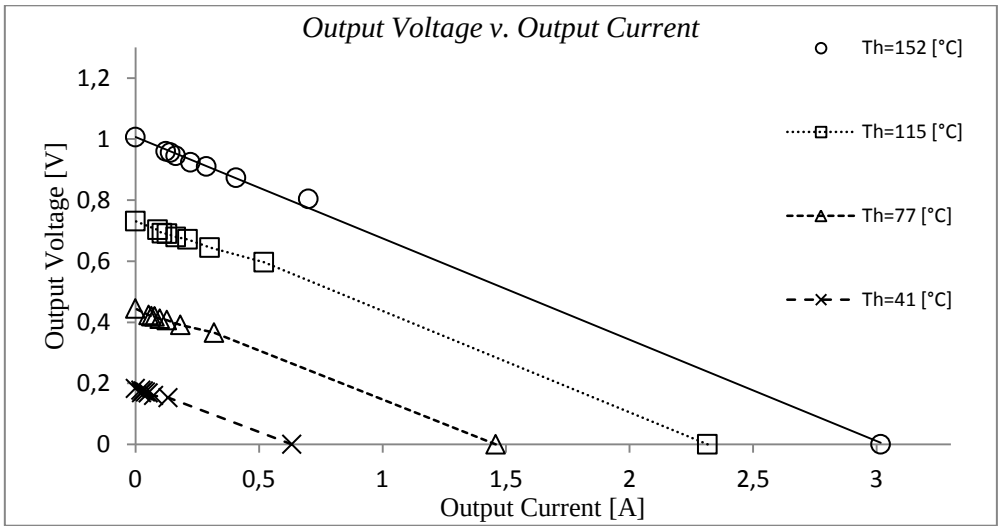
Output Voltage v. Output Current
Th=152 [°C]
Th=115 [°C]
Th=77 [°C]
Th=41 [°C]
Output Voltage [V]
1,2
1
0,8
0,6
0,4
0,2
0
0
0,5
1
1,5
2
2,5
3
Output Current [A]

16

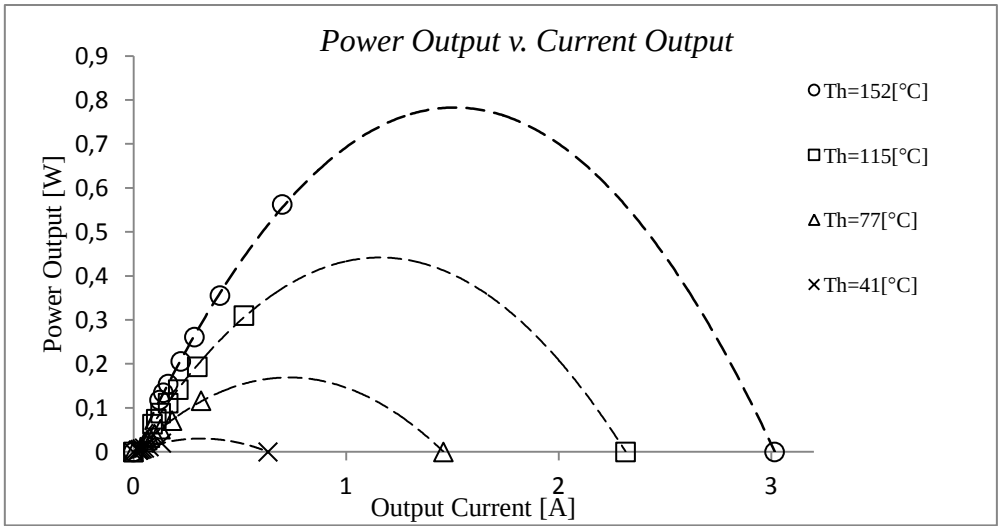
Power Output v. Current Output
Power Output [W]
0,9
0,8
0,7
0,6
0,5
0,4
0,3
0,2
0,1
0
0
1
2
3
Output Current [A]
Th=152[°C]
Th=115[°C]
Th=77[°C]
Th=41[°C]

17

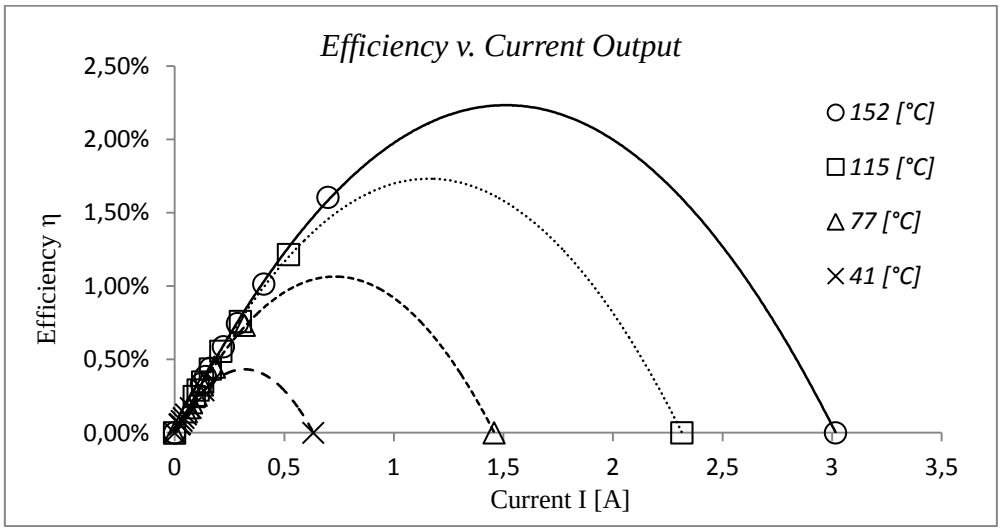
Efficiency v. Current Output
Efficiency η
2,50%
2,00%
1,50%
1,00%
0,50%
0,00%
0
0,5
1
1,5
2
2,5
3
3,5
Current I [A]
152 [°C]
115 [°C]
77 [°C]
41 [°C]

18

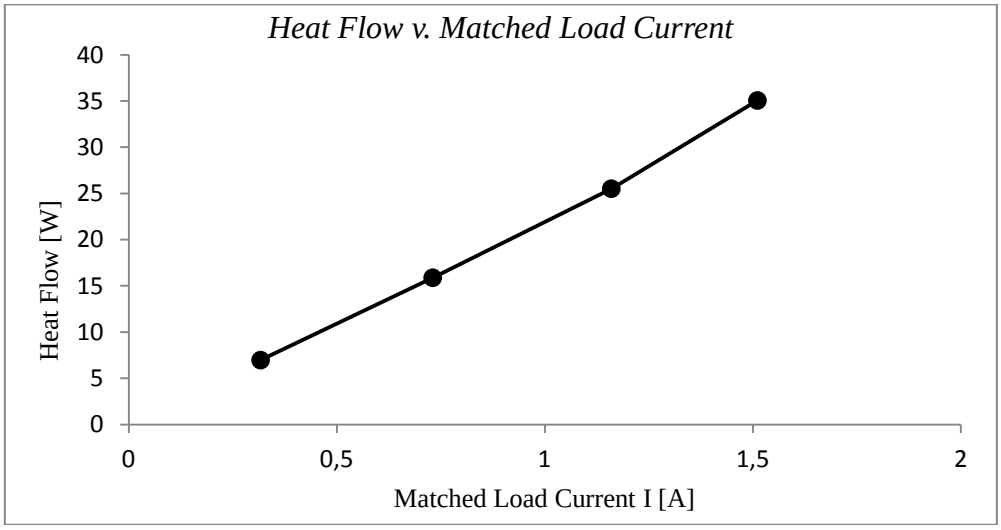
Heat Flow v. Matched Load Current
Heat Flow [W]
40
35
30
25
20
15
10
5
0
0
0,5
1
1,5
2
Matched Load Current I [A]

19

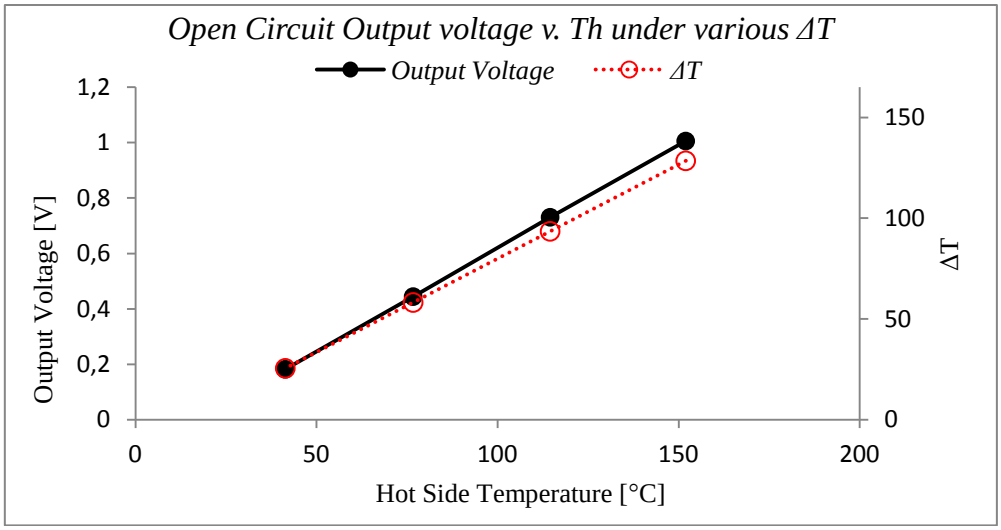
Open Circuit Output voltage v. Th under various ΔT
Output Voltage
ΔT
Output Voltage [V]
ΔT
Hot Side Temperature [°C]
1,2
1
0,8
0,6
0,4
0,2
0
150
100
50
0
0
50
100
150
200

20

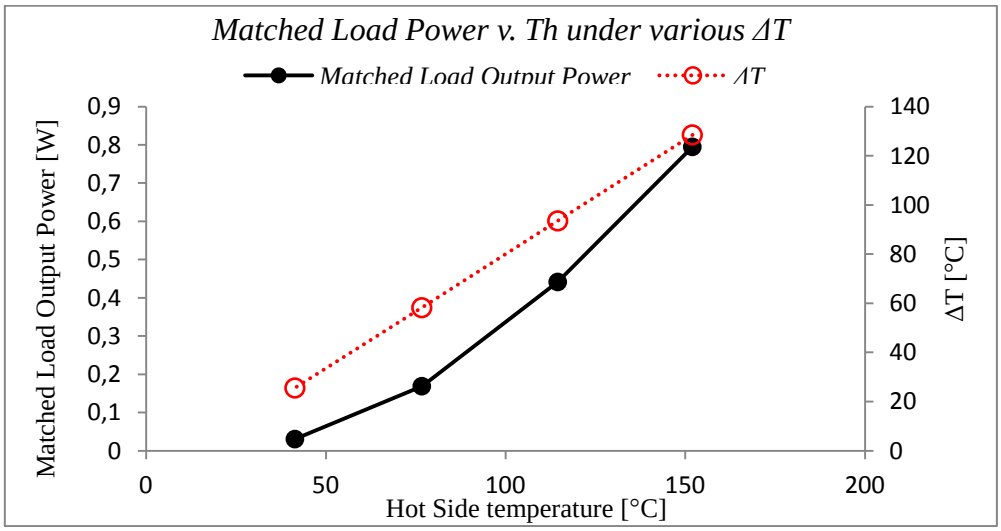
Matched Load Power v. Th under various ΔT
Matched Load Output Power
ΔT
Matched Load Output Power [W]
ΔT [°C]
Hot Side temperature [°C]
0,9
0,8
0,7
0,6
0,5
0,4
0,3
0,2
0,1
0
140
120
100
80
60
40
20
0
0
50
100
150
200

21

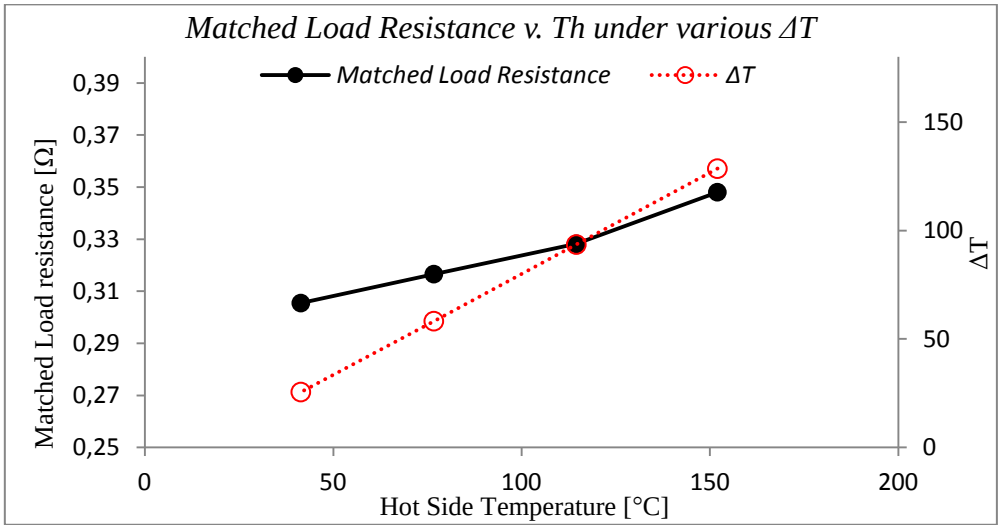
Matched Load Resistance v. Th under various ΔT
Matched Load Resistance
ΔT
Matched Load resistance [Ω]
ΔT
Hot Side Temperature [°C]
0,39
0,37
0,35
0,33
0,31
0,29
0,27
0,25
150
100
50
0
0
50
100
150
200

22

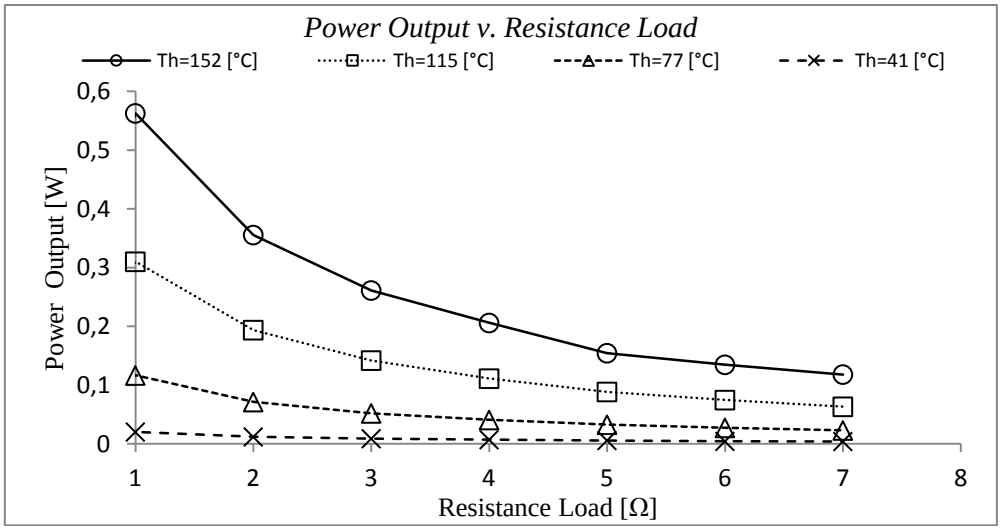

23

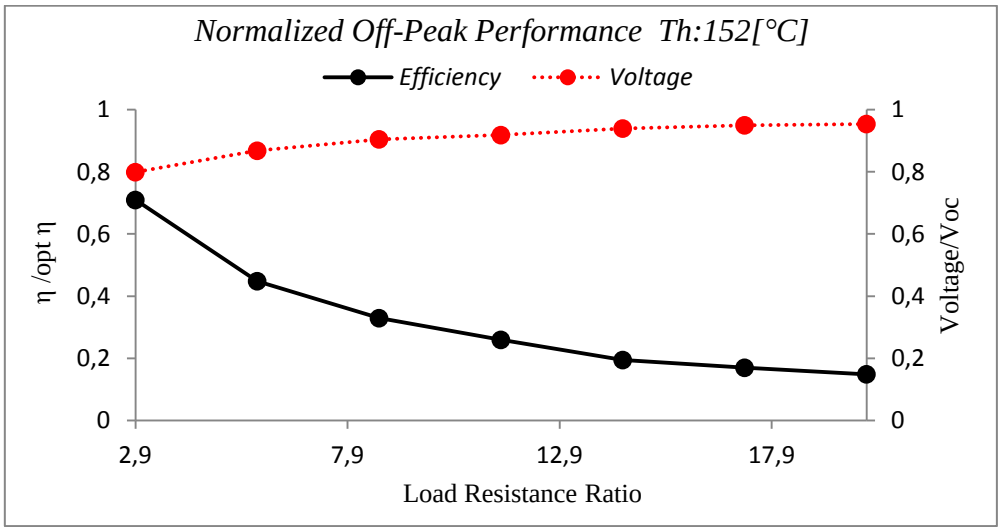

24

Section II

After the characterization of three different thermoelectric modules, it is possible to analyze a plot that involves all the efficiencies calculated from the experimental results. For different ranges of temperature and different current outputs, it can be observed how the efficiency curves changes referring to the different TEGs.

Marlow module has resulted the converter with the highest values of efficiencies considering the same steps of temperature imposed by the heater for each module. It is also showed the difference between the Marlow module efficiency performances in the insulated case and in the case without insulation.

Although ZhiYuan International LTD module covers a higher range of current output values than the other modules, it can be noticed that its efficiencies remain still lower than the Marlow modules for the same temperature steps.

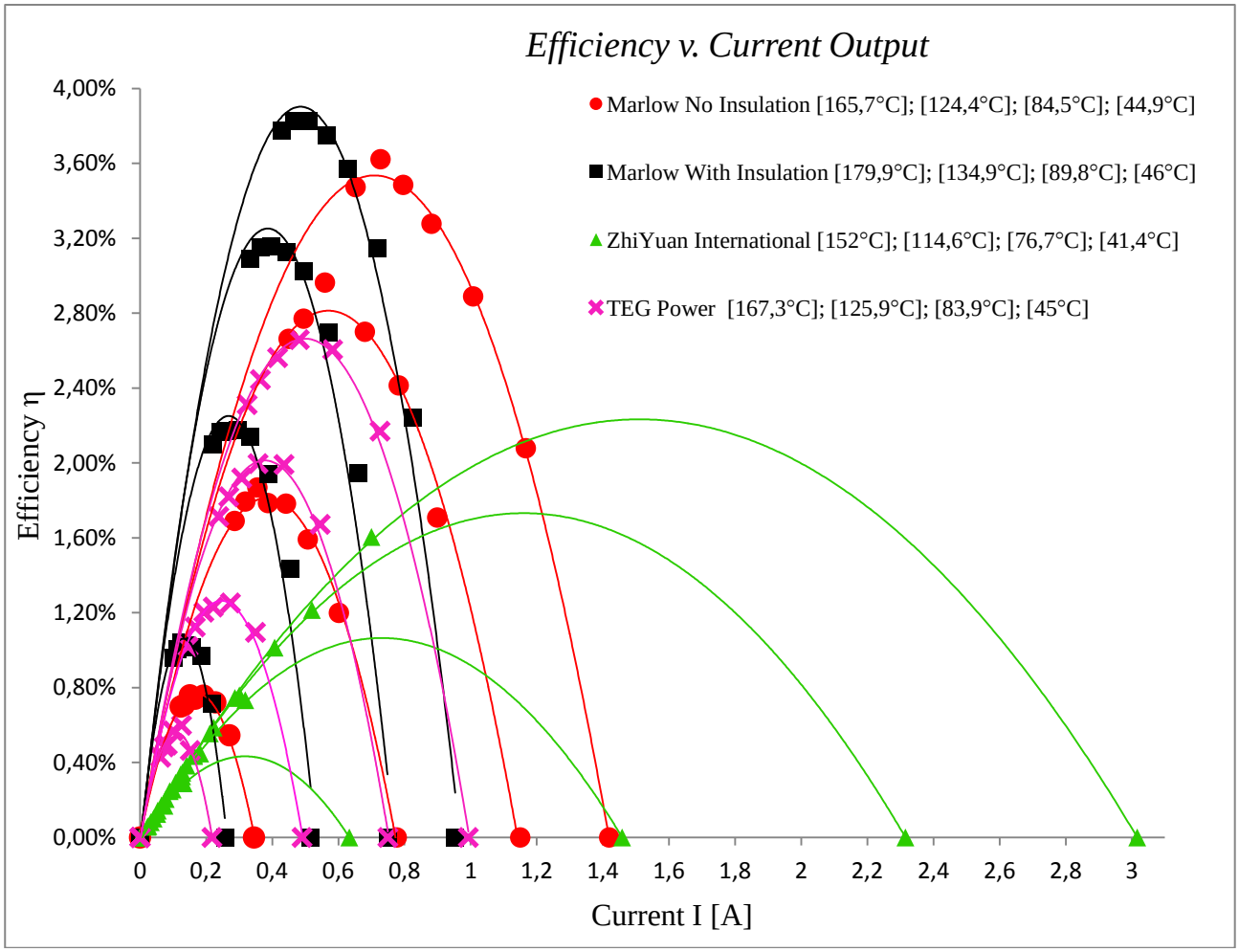
Efficiency v. Current Output
Marlow No Insulation [165,7°C]; [124,4°C]; [84,5°C]; [44,9°C]
Marlow With Insulation [179,9°C]; [134,9°C]; [89,8°C]; [46°C]
ZhiYuan International [152°C]; [114,6°C]; [76,7°C]; [41,4°C]
TEG Power [167,3°C]; [125,9°C]; [83,9°C]; [45°C]
Efficiency η
4,00%
3,60%
3,20%
2,80%
2,40%
2,00%
1,60%
1,20%
0,80%
0,40%
0,00%
0
0,2
0,4
0,6
0,8
1
1,2
1,4
1,6
1,8
2
2,2
2,4
2,6
2,8
3
Current I [A]

25

Bibliography

D.M. Rowe,(ed.), *Thermoelectrics Handbook, Macro to Nano*, CRC Press, Taylor and Francis Group, Boca Raton, FL, 2006, (Chapter 1, Chapter 11, Appendix I)

H.J. Goldsmid, *Introduction to Thermoelectricity*, Springer Series in Material Sciences, Editors: R. Hull, R.M. Osgood Jr., J. Parisi, H. Warlimont, Springer Heidelberg Dordrecht, London, New York, 2010, (Chapter 1)

Terry M. Tritt, *Thermoelectric Phenomena, Materials, and Applications,* Annual Review of Materials Research, 2011, Volume 41: 433-48

Terry M. Tritt, M.A. Subramanian, (guest ed.), *Thermoelectric Materials, Phenomena, and Applications: A Bird's Eye View,* MRS Bulletin, MRS, 506 Keystone Drive, Warrendale, PA, March 2006, Volume 31

C.A. Gould, N.Y.A. Shammas, S. Grainger, I. Taylor, *A Comprehensive Review of Thermoelectric Technology, Micro-Electrical and Power Generation Properties,* proc. 26th International Conference on Microelectronics (MIEL 2008), Nis, Serbia, 11-14 May 2008.

J.P. Carmo, J.Antunes, M.F. Silva, J.F. Ribeiro, L.M. Goncalves, J.H. Correia, *Characterization of Thermoelectric Generators by Measuring the Load- Dependance Behavior*, University of Minho, Dept. Industrial Electronics, Campus Azurem, 4800-058 Guimaraes, Portugal, Measurement, Elsevier Ltd., Volume 44: 2194-2199, 2011

E. Sandoz-Rosado, R.J. Stevens, *Experimental Characterization of Thermoelectric Modules and Comparison with Theoretical Models for Power Generation*, Mechanical Engineering, Rochester Institute of Technology, Rochester, NY, USA, Journal of Electronic Materials, 2009, Volume 38, No. 7

L. Rauscher, S. Fujimoto, H.T. Kaibe, S. Sano, *Efficiency Determination and General Characterization of Thermoelectric Generators Using an Absolute Measurement of the Heat Flow*, Komatsu LTD, Technology Research Center, Research Division, 1200 Manda, Hiratsuka, Kanagawa, Japan, Institute of Physics Publishing, Meas. Sci. Techolog. 16, 2005, 1054-1060

G.J. Sneider, T.S. Ursell, *Thermoelectric Efficiency and Compatibility*, Jet Propulsion Laboratory, California Institute of Technology, 4800, Oak Grove Drive, Pasadena, California, USA, Physical Review Letters, 2003, Volume 91, Number 14

R. Bonin, D. Boero, M. Chiaberge, A. Tonoli, *Design and Characterization of Small Thermoelectric Generators for Environmental Monitoring Devices*, Elsevier Ltd., Energy Conversion and Management, 2013, No. 73, 340-349

A.Y. Faraji, A. Akbarzadeh, *Design of a Compact, Portable Test System for Thermoelectric Power Generator Modules,* Journal of Electronic Materials, 2013, Vol. 42, No. 7

R. Aishka, S. Dislitas, *Computer Controlled Test System for Measuring the Parameters of the Real Thermoelectric Module*, Elsevier Ltd., Journal of Energy Conversion and Management, 2011, No. 52, 27-36

R. Aishka, S. Dislitas, G. Omer, *A New Method and Computer-Controlled System for Measuring the Time Constant of Real Thermoelectric Modules,* Elsevier Ltd., Journal of Energy Conversion and Management, 2012, No. 53, 314-321

R. Aishka, K. Aishka, *New Method for Investigation of Parameters of Real Thermoelectric Modules,* Elsevier Ltd., Journal of Energy Conversion and Management, 2010, No. 51, 338-345

G. Liang, J. Zhou, X. Huang, *Analytical Model of Parallel Thermoelectric Generator,* Elsevier Ltd., Journal of Applied Energy, 2011, No. 88, 5193-5199

B. Ciylan, S. Yilmaz, *Design of a Thermoelectric Module Test System Using a Novel Test Method,* Elsevier Ltd., International Journal of Thermal Sciences, 2007, No. 46, 717-725

M. Akoshima, T. Baba, *Thermal Diffusivity Measurements of Candidate reference Materials by the Laser Flash Method*, International Journal of Thermophysics, 2005, Vol. 26, No. 1

J. Zajas, P. Heiselberg, *Determination of the Local Thermal Conductivity of Functionally Graded Materials by a Laser Flash Method,* Elsevier Ltd., International Journal of heat and Mass Transfer, 2013, No. 60, 542-548

M. Akoshima, T. Baba, *Study on a Thermal-Diffusivity Standard for Laser Flash Method Measurements,* International Journal of Thermophysics, 2006, Vol. 27, No. 4

TEGeta Manual, *Measurement of Efficiency and Specifications of Thermoelectric Power Generators,* PANCO GmbH, Kaerlicher Str. 7, D-56218 Muelheim-Kaerlich